Uncovering a Novel Role of the Apoptotic Initiator Caspase, Caspase-2

by

Erika Lee Segear Johnson

Department of Pharmacology and Cancer Biology
Duke University

Date:_____

Approved:

_____
Sally Kornbluth, Supervisor

_____
Christopher Newgard

_____
Jeffrey Rathmell

_____
Gerard Blobe

_____
Blanche Capel

Dissertation submitted in partial fulfillment of
the requirements for the degree of Doctor
of Philosophy in the Department of
Pharmacology and Cancer Biology in the Graduate School
of Duke University

2014

ABSTRACT

Uncovering a Novel Role of the Apoptotic Initiator Caspase, Caspase-2

by

Erika Lee Segear Johnson

Department of Pharmacology and Cancer Biology
Duke University

Date:_____

Approved:

_____
Sally Kornbluth, Supervisor

_____
Christopher Newgard

_____
Jeffrey Rathmell

_____
Gerard Blobe

_____
Blanche Capel

An abstract of a dissertation submitted in partial
fulfillment of the requirements for the degree
of Doctor of Philosophy in the Department of
Pharmacology and Cancer Biology in the Graduate School of
Duke University

2014

Abstract

With the prevalence of obesity and metabolic syndrome rising sharply world-wide, it has become increasingly important to define the molecular mechanisms underlying the pathogenesis and progression of diseases associated with lipid-induced cytotoxicity. Cardiovascular disease, type-2 diabetes mellitus, and nonalchoholic fatty liver disease (NAFLD) have all recently gained recognition as diseases that are exacerbated by lipoapoptosis. In this dissertation, we demonstrate a novel role for caspase-2 as an initiator of lipoapoptosis. Using an unbiased metabolomics approach, we discovered that the activation of caspase-2, the initiator of apoptosis in *Xenopus* egg extracts, is associated with an accumulation of long-chain fatty acid (LCFA) metabolites. Metabolic treatments that block the buildup of LCFAs potently inhibit caspase-2, while add-back of a saturated LCFA restores caspase activation in the extract setting. Extending these findings to mammalian cells, we show that caspase-2 is engaged and activated in response to treatment with the saturated LCFA, palmitate. Down-regulation of caspase-2 significantly impairs cell death induced by saturated LCFAs, revealing a conserved, critical role for caspase-2 in mediating LCFA-induced lipoapoptosis.

Since lipoapoptosis has been implicated as a key driver of the progression of NAFLD, we aimed to determine the therapeutic significance of our findings by

evaluating the importance of caspase-2 in an *in vivo* model of this disease. We subjected wild-type and caspase-2 knockout mice to a diet which induces severe liver steatosis and the development of nonalcoholic steatohepatitis (NASH), the most advanced stage of NAFLD characterized by liver fibrosis. Interestingly, we observed an increase in caspase-2 protein levels in the livers of wild-type mice fed a NASH-inducing diet. These findings were of particular importance, since caspase-2 expression was also significantly elevated in patients diagnosed with NASH. Most importantly, we demonstrated that caspase-2 knockout mice are protected from apoptosis and fibrosis when fed a NASH-inducing diet, suggesting that caspase-2 is a major regulator of hepatocyte lipoapoptosis. Together, these findings reveal a previously unknown role for caspase-2 as an initiator of lipoapoptosis and suggest that caspase-2 may be an attractive therapeutic target for inhibiting pathological lipid-induced apoptosis.

Dedication

To my family:

To my daughter, Porter, who has enhanced everything in my life- you are an amazing little lady and I can't wait for everything that is to come.

To my sister, Timre, who has set the standard to which I measure my life's achievements- following in your footsteps has been difficult, as you have always set the bar high. Thank you for inspiring me to be as great as you are.

To my sister, Justine, who has been my closest friend and ally on the road of life- on the outside you are so strong and tough, but inside you really understand what matters in life. Thank you for always being there for me and for showing me that family is what is most important.

To my sister, Randi, who has a great passion for life and is always optimistic- you can always make me laugh and I love being around your carefree spirit. Thank you for always reminding me to enjoy and appreciate the little things in life.

To my sister, Sierra, who has an amazing mind and an even better personality- you have always amazed me with your brilliance and your confidence to be your own person. Thank you for inspiring me to be myself and to love the person that I am.

To my brother, John, who has never ceased to amaze me with his love of life and his insatiable thirst for knowledge- I am constantly surprised by you. Thank you for reminding me that nothing in life is predictable- except for the love of a brother.

To my late grandmother, Mare, who always reminded me that biology is "hard"- I miss you every day. Thank you for your inspiration and love always.

To my parents, who have always loved and supported me in everything I have done in life. You are both perfect examples of how if you work hard and believe in yourself then anything is possible. Thank you for always inspiring me to be the best person I can be and for giving me the most amazing family.

And, to my husband, Timothy, who had my heart at first sight. You have always pushed me to pursue my dreams and have been a great support for me when, at times, my dreams felt more like nightmares. You truly are the love of my life, and I know I can accomplish anything with you by my side. Thank you for never giving up on me and for all of your love and support over the past 10 years.

Contents

Abstract iv

List of Tables xiv

List of Figures xv

List of Abbreviations xvii

1. Introduction 1

1.1 Apoptosis 1

1.1.1 Apoptosis signaling cascade 2

1.1.1.1 Extrinsic pathway 4

1.1.1.2 Intrinsic pathway 6

1.2 Caspase-2 8

1.2.1 Caspase-2 structure 10

1.2.2 Caspase-2 localization 11

1.2.3 Caspase-2 mechanism of activation 14

1.2.3.1 Potential activation platforms 15

1.2.3.2 Proximity-induced autocatalytic processing 17

1.2.4 Caspase-2 activating stimuli 19

1.2.5 Caspase-2 regulation 23

1.2.5.1 Transcriptional and translational regulation 24

1.2.5.2 Post-translational modification 25

1.2.6 Caspase-2 substrates 27

1.2.7 Studying apoptosis in *Xenopus laevis* cell-free egg extract 31
1.3 Metabolism 33
1.3.1 Cellular metabolism 34
1.3.2 Glucose metabolism 36
1.3.2.1 Glycolysis 36
1.3.2.2 The tricarboxylic acid cycle 37
1.3.2.3 Oxidative phosphorylation 38
1.3.3 Lipid metabolism 39
1.3.3.1 Fatty acid synthesis 41
1.3.3.2 Beta-oxidation 42
1.4 Obesity and apoptosis 42
1.4.1 Lipotoxicity and lipoapoptosis 43
1.4.2 Lipoapoptosis as a critical mediator of nonalcoholic fatty liver disease 45
2. Materials and Methods 48
2.1 Xenopus techniques 48
2.1.1 *Xenopus* egg extract 48
2.1.2 Caspase Assay 48
2.1.3 *In vitro* translated caspase-2 protein synthesis 49
2.1.4 Analysis of *in vitro* translated caspase-2 protein processing 50
2.1.5 Fatty acid preparation and supplementation 50
2.1.6 NAD+/NADH nucleotide analysis 51
2.1.7 Oxygen consumption analysis 51

2.2 Metabolomic profiling (performed in collaboration with Dr. Chris Newgard) 52
2.2.1 Sample preparation 52
2.2.2 Amino acid and acylcarnitine analysis 52
2.2.3 Organic acid analysis 53
2.3 Mammalian cell techniques 53
2.3.1 Cell culture 53
2.3.2 siRNA transfection 54
2.3.3 Fatty acid preparation and treatments 55
2.3.4 Caspase assay 55
2.3.5 Western blot analysis 55
2.3.6 Gel filtration chromatography 56
2.3.7 Bimolecular fluorescence complementation 57
2.3.8 Propidium ioidide staining 58
2.4 Mouse model techniques (performed in collaboration with Dr. Anna Mae Diehl) 58
2.4.1 Murine models 58
2.4.2 Hepatocyte isolation 59
2.4.3 Histopathological Analysis 60
2.4.4 TUNEL staining 60
2.4.5 Fibrosis staining 60
2.5 Reagents 61
2.5.1 Antibodies 61

2.5.2 Additional Reagents 61

2.6 Statistics 61

3. Metabolic stress-induced activation of caspase-2 in *Xenopus laevis* egg extracts 62

3.1 Introduction 62

3.2 Results 65

3.2.1 Amino acid metabolism and the accumulation of succinate precede caspase activation in *Xenopus* egg extract 66

3.2.2 The absence of mitochondrial respiration in incubated extract results in the accumulation of long-chain acylcarnitines and a decrease in the NAD+/NADH ratio 69

3.2.3 Inhibition of amino acid transamination by aminooxyacetate blocks caspase activation 71

3.2.4 Metabolic treatments that block caspase activation also prevent the accumulation of long-chain fatty acid metabolites 73

3.2.5 Supplementation of the extract with glucose-6-phosphate blocks long-chain fatty acid metabolite accumulation 75

3.2.6 Palmitate accelerates caspase activation and overrides the protective effect of AOA 77

3.3 Discussion 79

3.3.1 Potential mechanism of extract metabolism 80

3.3.2 Inhibition of extract metabolism and long-chain fatty acid stress 81

3.3.3 The extract as a model of metabolic stress 82

4. Caspase-2 as an initiator of lipid-induced cell death in mammalian cells 84

4.1 Introduction 84

4.2 Results 85

4.2.1 Caspase-2 plays a central role in mediating lipotoxicity in 293T cells 85

4.2.2 Caspase-2 mediates saturated fatty acid-induced lipoapoptosis via acyl-CoA cytotoxicity 89

4.2.3 Caspase-2 is required for LCFA-induced apoptosis in hepatocytes 92

4.3 Discussion 95

4.3.1 Caspase-2 initiates saturated LCFA-induced lipoapoptosis in 293T cells 95

4.3.2 Implications for hepatocyte lipoapoptosis and NAFLD/NASH 97

5. Caspase-2 as a regulator of hepatocyte lipoapoptosis in a mouse model of nonalcoholic fatty liver disease 99

5.1 Introduction 99

5.2 Results 102

5.2.1 Caspase-2 KO hepatocytes are protected from palmitate- induced apoptosis *in vitro* 102

5.2.2 Caspase-2 is significantly upregulated in patients with NASH and in mice fed an MCD diet 103

5.2.3 Caspase-2 KO mice are protected from MCD diet-induced apoptosis and fibrosis 105

5.3 Discussion 108

5.3.1 Caspase-2 expression is significantly increased in hepatocytes in NASH 108

5.3.2 Potential mechanism for caspase-2 activation in NASH 110

5.3.3 Caspase-2 is a favorable therapeutic target in preventing apoptosis and fibrosis in NASH progression 111

6. Conclusion and perspectives 113

6.1 Lipid accumulations promote the activation of caspase-2 in Xenopus egg extract 113

6.2 Caspase-2 regulates lipoapoptosis in mammalian cells 117

6.3 The loss of caspase-2 protects against lipoapoptosis and fibrosis in a mouse model of NASH 121

6.4 Concluding Remarks 123

References 125

Biography 144

List of Tables

Table 1.1: Examples of stimuli that have been reported to activate caspase-2.....20

Table 3.2: Putative caspase-2 substrates and cleavage sites.....29

List of Figures

Figure 1.1: The apoptotic signaling cascade 3

Figure 1.2: The extrinsic apoptotic pathway 5

Figure 1.3: The intrinsic apoptotic pathway 8

Figure 1.4: Mechanism of caspase-2 processing 18

Figure 1.5: Metabolic regulation of caspase-2 by phosphorylation 26

Figure 1.6: Cellular metabolic pathways 35

Figure 1.7: Progression of NAFLD 47

Figure 3.1: Amino acid metabolism and the accumulation of succinate precede caspase activation in *Xenopus* egg extract. 68

Figure 3.2: The absence of mitochondrial respiration results in the accumulation of long-chain acylcarnitines and a decrease in the NAD+/NADH ratio 70

Figure 3.3: The inhibition of amino acid transamination by aminooxyacetate blocks caspase activation 72

Figure 3.4: Metabolic treatments that block caspase activation also prevent the accumulation of long-chain fatty acid metabolites 74

Figure 3.5: Supplementation of the extract with glucose-6-phosphate blocks long-chain fatty acid metabolite accumulation 76

Figure 3.6: Palmitate accelerates caspase activation and overrides the protective effect of AOA 78

Figure 4.1: Caspase-2 plays a central role in mediating lipotoxicity in 293T cells 87

Figure 4.2 Caspase-2 mediates saturated fatty acid-induced lipoapoptosis via acyl-CoA cytotoxicity 92

Figure 4.3: Caspase-2 is required for LCFA-induced apoptosis in hepatocytes 94

Figure 5.1: Caspase-2 KO hepatocytes are protected from palmitate-induced apoptosis *in vitro* 102

Figure 5.2: Caspase-2 is significantly upregulated in patients with NASH and in mice fed an MCD diet 104

Figure 5.3: Caspase-2 KO mice are protected from MCD diet-induced apoptosis 106

Figure 5.4: Caspase-2 KO hepatocytes are protected from MCD diet-induced fibrosis . 107

List of Abbreviations

TNF	Tissue necrosis factor
FADD	Fas-associated death domain
DISC	Death-inducing signaling complex
MOMP	Mitochondrial outer membrane permeabilization
Apaf-1	Apoptotic protease activating factor
Nedd-2	Neural precursor cells-expressed, developmentally downregulated
Ich-1	Interleukin-1 converting enzyme/*C. elegans* cell death gene (ICE/CED-3) homolog 1
KO	Knockout
CARD	Caspase recruitment domain
ER	Endoplasmic reticulum
NLS	Nuclear localization signal
DD	Death domain
RAIDD	(RIP)-associated ICH-1/CED-3 homologous protein with a death domain
PIDD	p53-induced protein with a death domain
RIP1	Receptor-interacting serine/threonine-protein kinase 1
TRAF2	TNF receptor associated factor 2
IRE1α	Inositol requiring enzyme 1 alpha

CaMKII	Calcium/calmodulin-dependent protein kinase type II
CoA	Coenzyme A
Cdk1	Cyclin dependent kinase-1
PKCK2	Protein kinase casein kinase 2
HDAC4	Histone deacetylase 4
NADPH	Nicotinamide adenine dinucleotide phosphate
TCA	Tricarboxylic acid
NAD+	Nicotinamide adenine dinucleotide
NADH	Reduced nicotinamide adenine dinucleotide
FAD+	Flavin adenine dinucleotide
$FADH_2$	Reduced flavin adenine dinucleotide
G6P	Glucose-6-phosphate
PPP	Pentose phosphate pathway
ROS	Reactive oxygen species
VLDL	Very-low-density-lipoprotein
FASN	Fatty acid synthase
LCFA	Long-chain fatty acid
NAFLD	Nonalcohlic fatty liver disease
NASH	Nonalcoholic steatphepatitis
AST	Aspartate aminotransferase

ALT	Alanine aminotransferase
HSC	Hepatic stellate cell
β-HCG	β-human chorionic gonadotropin
BSA	Bovine serum albumin
AA	Amino acid
AC	Acylcarnitine
OA	Organic acid
GC/MS	Gas chromatography/mass spectrometry
ATCC	American Type Culture Collection
DMEM	Dulbecco's Modified Eagle Medium
FBS	Fetal bovine serum
BiFC	Bimolecular fluorescence complementation
Dox	Doxycycline
PI	Propidium iodide
MCD	Methionine choline-deficient
HRP	Horseradish peroxidase
DAB	Diaminobenzidine
TUNEL	Terminal deoxynucleotidyl transferase-mediated dUTP nick-end labeling
Sirt1	Sirtuin 1
ETC	Electron transport chain

AOA	Aminooxyacetate
Bcl-xL	B cell lymphoma XL
HMW	High molecular weight
TRE	Tetracycline-response element
NAC	N-acetyl cysteine
T2DM	Type-2 diabetes mellitus
LPC	Lysophosphatidylcholine
ATM	Ataxia telangiectasia mutated
GFP	Green fluorescent protein

1. Introduction

1.1 Apoptosis

Apoptosis is a form of programmed cell death that is activated in response to pro-death stimuli. Characterized by rapid cellular fragmentation and phagocytosis, apoptosis eliminates damaged or unneeded cells, while preserving the integrity of the surrounding tissue. This energy-consuming process is defined by distinct molecular and morphological characteristics, including chromatin condensation, DNA fragmentation, membrane phosphatidylserine externalization, and plasma membrane blebbing. Importantly, the intracellular contents of the dying cell are never exposed to the extracellular environment, but rather are excreted from the dying cell through membrane-enclosed apoptotic vesicles. These vesicles, which pinch off from the dying cell as it blebs, are engulfed and disposed of by neighboring phagocytes and thus, do not elicit a host immune or inflammatory response.

Apoptosis is critical for proper tissue development and homeostasis. Under normal physiologic conditions, apoptosis of damaged or unneeded cells must be precisely balanced by cellular regeneration in order to maintain tissue structure and function. Disruption of the apoptotic program can result in either excessive cell death or inappropriate cell survival. Excessive cell death can lead to immunodeficiency or the development of chronic degenerative diseases, while inappropriate cell survival can manifest as cancer or autoimmunity. Regardless of the disturbance, improper apoptotic

signaling can significantly compromise tissue function and thus, insight into the molecular mediators of this highly regulated process could be useful in conditions requiring therapeutic intervention.

1.1.1 Apoptosis signaling cascade

The apoptotic signaling cascade is mediated by a group of cysteine proteases known as caspases. Synthesized as inactive zymogens, caspases can become activated following cellular insult through either oligomerization and/or proteolytic processing. Following their activation, caspases use a cysteine residue in their active site to cleave protein substrates at aspartic acid residues. Cleavage of substrates can promote apoptosis in two ways: through the direct dismantling of the cell, or by promoting a feed-forward activation of the apoptotic signaling cascade. Activation of this cascade is accomplished by either initiating additional pro-death signaling molecules or inhibiting antagonistic pro-survival pathways.

Caspase proenzymes are classified as either initiator or executioner caspases based on their role in the apoptotic program. Initiator caspases (e.g., caspases-2,-8, and -9), which are important in upstream signaling, become activated through the binding of adaptor proteins to their prodomains. This binding facilitates their oligomerization into high molecular weight protein complexes, which triggers their dimerization and processing into active enzymes. Once active, initiator caspases activate executioner caspases (e.g., caspases-3 and -7) via proteolytic cleavage. Executioner caspases then go

on to cleave protein substrates, leading to an organized dismantling of the cell and ultimately cell death (Figure 1.1).

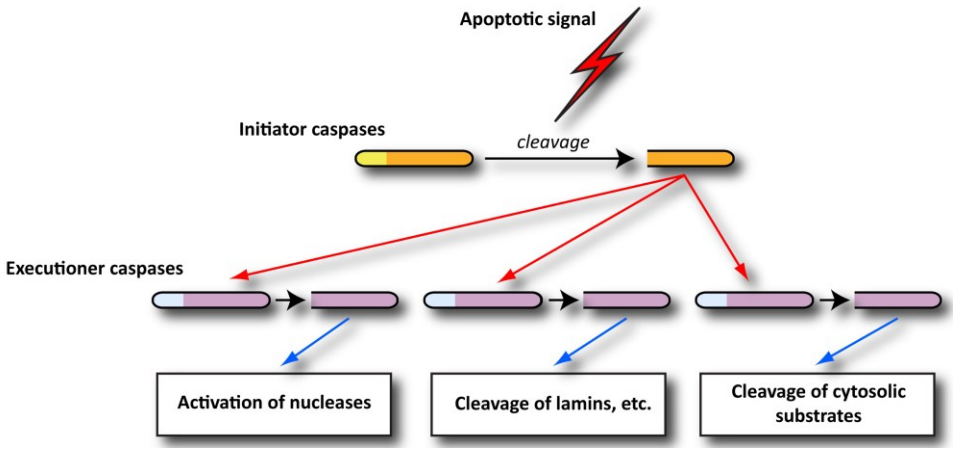

Figure 1.1: The apoptotic signaling cascade

Figure 1.1: The apoptotic signaling cascade is initiated in response to pro-death stimuli. Apoptotic signaling results in the activation of initiator caspases, which oligomerize and undergo auto-catalytic cleavage to form mature, active enzymes. Initiator caspases then go on to cleave and activate executioner caspases. Executioner caspases cleave multiple cytosolic substrates, trigger the activation of nucleases, and breakdown structural components of the cells (i.e., lamins), leading to an organized dismantling of the cell and ultimately cell death.

Surprisingly, little is known about how caspase-mediated cleavage of substrates promotes the characteristic morphological changes observed during apoptosis, including chromatin condensation, membrane phosphatidylserine externalization, and apoptotic body formation. To date, over 700 caspase cleavage sites have been identified in more than 550 unique substrates, all of which have been experimentally validated (Fridman et al., 2013). Despite our lack of clarity regarding cellular disassembly

processes, it is clear that the activation of caspases serves to amplify a pro-death signal, pushing the cell towards death via a complex network of signaling events.

Apoptotic signaling pathways are initiated by either extracellular or intracellular stress signals. Extracellular initiation, more commonly referred to as the extrinsic apoptotic pathway, results from the engagement of plasma membrane death receptors. These receptors, which become activated upon pro-death ligand binding, initiate downstream executioner caspase activation and apoptosis. Conversely, intracellular stress cues result in activation of the intrinsic apoptotic pathway. This pathway, which signals through the mitochondria, promotes the release of the mitochondrial respiratory chain protein, cytochrome *c*. Cytosolic cytochrome *c*, in combination with other pro-apoptotic proteins, triggers the activation of executioner caspases (Waterhouse and Green, 1999). The similarities and differences between these two apoptotic pathways are discussed in detail below.

1.1.1.1 Extrinsic pathway

Activation of the extrinsic apoptotic pathway is regulated by pro-death ligand binding to extracellular death receptors, which triggers trimerization and activation of intracellular pro-apoptotic signaling (Figure 1.2). For example, the family of tissue necrosis factor (TNF) receptors, which includes both TNF and Fas receptors, function as initiators of death. Interaction of these receptors with their extracellular ligands, TNF and FasL respectively, results in clustering of the receptors at the plasma membrane

(Ogasawara et al., 1993; Suda et al., 1993; Tartaglia et al., 1993; Trauth et al., 1989). In the case of Fas, binding of FasL to the receptor triggers a clustering event, which results in the recruitment of the intracellular Fas-associated death domain (FADD) protein, forming what is known as the death-inducing signaling complex (DISC) (Muzio et al., 1996).

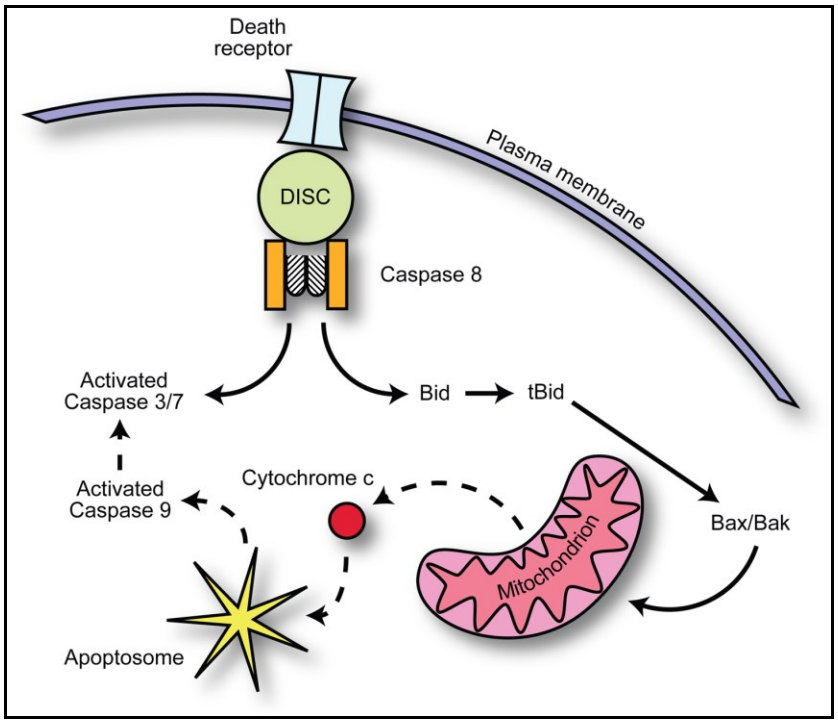

Figure 2.2: The extrinsic apoptotic pathway

Figure 1.2: The extrinsic apoptotic pathway is initiated at the plasma membrane by the binding of a ligand to its extracellular death receptor. Ligand binding recruits the death-induced signaling complex (DISC), which binds and activates the initiator caspase, caspase-8. Once active, caspase-8 can directly cleave effector caspases (caspase-3/-7) and/or the BH3-only protein Bid. Cleavage of Bid forms truncated Bid (tBid), which can activate mitochondrial permeabilization by promoting the oligomerization of Bax and Bak. Mitochondrial permeabilization results in cytochrome *c* release, formation of the apoptosome, and activation of the initiator caspase, caspase-9. Caspase-9 can then directly cleave and activate the executioner caspase, caspase-3.

DISC formation provides a platform for the recruitment and proximity-induced activation of caspase-8 (Kischkel et al., 1995). Once active, caspase-8 can trigger the activation of the executioner caspases in either one of two ways; directly through cleavage of caspases-3 and -7 or indirectly through cleavage of the BH3-only protein Bid, which promotes mitochondrial permeabilization (the mechanistic signaling pathway is discussed further in the next section) (Li et al., 1998; Luo et al., 1998; Scaffidi et al., 1998). Interestingly, while the intrinsic apoptotic cascade relies entirely on mitochondrial signaling, the extrinsic pathway may or may not require mitochondrial feedback for amplification of cell death. Regardless of whether the pathway utilizes mitochondrial cytochrome *c* release in the cell death process, classical apoptotic morphology is still observed; suggesting that activation of executioner caspases is truly what drives the cellular characteristics observed in apoptosis.

1.1.1.2 Intrinsic pathway

A variety of intracellular stresses have been shown to initiate the intrinsic apoptotic pathway, including hypoxia, oxidative stress, and DNA damage. The activation of the intrinsic pathway is regulated by members of the Bcl-2 family of proteins, whereby pro-apoptotic BH3-only proteins (i.e., Bid, Bad, etc.) sequester anti-apoptotic Bcl-2 proteins (i.e., Bcl-xL) away from Bax and Bak, allowing them to oligomerize. The oligomerization of Bax and Bak induces mitochondrial outer membrane permeabilization (MOMP) through the formation of Bax/Bak pore and

enables the release of cytochrome *c* from the intermitochondrial space into the cytosol (Danial and Korsmeyer, 2004). Once cytosolic, cytochrome *c* forms a multimeric complex with the apoptotic protease activating factor (Apaf-1), resulting in recruitment and activation of caspase-9 (Kluck et al., 1997; Liu et al., 1996; Ow et al., 2008). This complex, termed the apoptosome, cleaves and activates the executioner caspases, caspase-3 and -7, which then dismantle the cell through substrate cleavage (Inoue et al., 2009; Li et al., 1997b).

Importantly, caspase-2 has been shown to function as an initiator caspase in the intrinsic apoptotic pathway, signaling upstream of the mitochondria to promote cytochrome *c* release (Figure 1.3) (Ho et al., 2008; Imre et al., 2012; Tu et al., 2006a). The prevailing model is that caspase-2, once activated, cleaves the BH3-only protein Bid to generate truncated Bid (tBid). tBid then activates Bax to promote cytochrome *c* release (Bonzon et al., 2006; Guo et al., 2002). Amplification of the intrinsic apoptotic pathway relies heavily on MOMP, since activation of the executioner caspase, caspase-3, can feedback to promote cleavage and direct activation of caspase-2 to further propagate apoptotic signaling (Li et al., 1997a; Swanton et al., 1999).

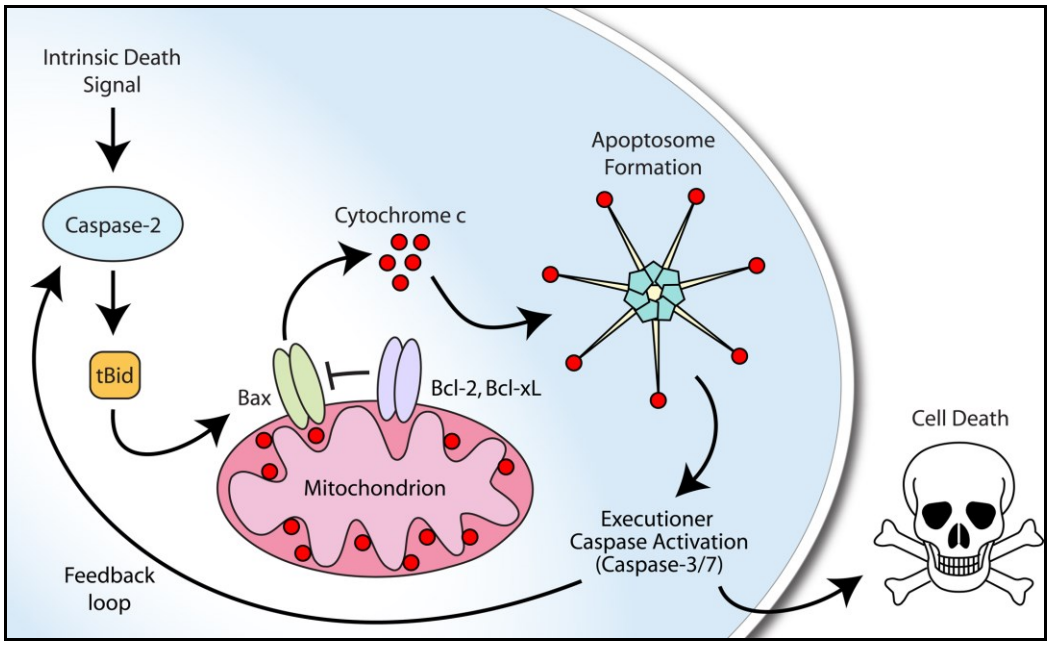

Figure 3.3: The intrinsic apoptotic pathway

Figure 1.3: The intrinsic apoptotic pathway is activated in response to intracellular stress and results in the activation of the initiator caspase, caspase-2. Caspase-2 cleaves the BH3-only protein Bid, forming truncated Bid or tBid. tBid can activate mitochondrial permeabilization through modulation of bcl-2 proteins at the mitochondria, including the pro-apoptotic proteins, Bax and Bak. Anti-apoptotic bcl-2 family members (Bcl-2, Bcl-xL) antagonize the oligomerization and activation of Bax/Bak, controlling mitochondrial cytochrome *c* release. Once cytosolic, cytochrome *c* can induce the oligomerization of Apaf-1, forming a large, heptameric complex, known as the apoptosome. The apoptosome recruits and activates the initiator caspase, caspase-9, which can directly cleave and active the executioner caspases, caspase-3 and -7. Executioner caspases can cleave a number of cellular substrates leading to cell death or they can cleave caspase-2 in a positive feedback loop to promote amplification of the apoptotic signaling cascade.

1.2 Caspase-2

Caspase-2 is the most apical initiator caspase involved in the intrinsic apoptotic cascade. Since its initial discovery more than twenty years ago, caspase-2 has been identified in the literature by a number of names, including Nedd-2 (neural precursor

cells-expressed, developmentally downregulated) and ICH-1 (interleukin-1 converting enzyme/*C. elegans* cell death gene (ICE/CED-3) homolog 1) (Kumar et al., 1994; Kumar et al., 1992; Wang et al., 1994; Yuan et al., 1993). Interestingly, caspase-2 is the most evolutionarily conserved of all the caspases, suggesting that the structure and function of this enzyme are so important that it needed to be greatly maintained, despite the evolution of species.

Highly conserved proteins are often thought to be required for basic cellular function, such that the loss of the protein would be developmentally detrimental to the survival of the organism. Despite sharing 43% amino acid identity with its *C. elegans* homolog, CED-3, caspase-2 is not required for proper embryonic development. For example, caspase-2 knockout (KO) mice are developmentally normal, showing only a mild apoptotic phenotype in female germ cells (Bergeron et al., 1998). This phenotype is due to a loss of apoptosis that occurs during normal ovary development. Briefly, the female ovary undergoes a substantial clonal expansion of oocytes during normal embryonic development. Since the ovary simply cannot sustain such a large number of germ cells, nearly 1/2 to 2/3 of the oocytes produced undergo apoptosis late in gestation (Ratts et al., 1995; Tilly et al., 1997). Oocytes from caspase-2 KO mice fail to undergo this elimination process and thus, female mice are born with an excess number of oocytes (Bergeron et al., 1998).

In addition to this mild germ cell phenotype, recent data has revealed that caspase-2 KO mice also suffer from an enhanced aging phenotype. Notably, the loss of caspase-2 is associated with a shortened maximum lifespan, impaired hair growth, increased bone loss, and reduced body fat content (Zhang et al., 2007). All of these traits are commonly observed in the setting of premature aging and suggest that caspase-2 may play a role in protecting animals from aging. Remarkably, this study was the first to link caspase-2 to an age-related phenotype and suggests that additional studies should be performed to determine how a pro-apoptotic gene could influence such a complex biological process (Zhang et al., 2007).

1.2.1 Caspase-2 structure

The structure of caspase-2 is similar to other initiator caspases in that it contains a large amino-terminal prodomain, followed by a large subunit and small subunit. The prodomain of caspase-2 serves as a binding site for protein-protein interactions, while the large and small subunits combine to form the active enzyme. The prodomain of caspase-2 contains a caspase recruitment domain (CARD) motif, which is used to bind other CARD-containing proteins in a homotypic interaction. The CARD domain of caspase-2 is believed to facilitate its activation by triggering dimerization with CARD-containing adaptor proteins (Kumar et al., 1997; Kumar et al., 1994; Wang et al., 1994). This activation process is similar to other well-characterized initiator caspases, including caspase-8 and -9, which are believed to exist as monomers in solution, becoming

dimerized only after ligand binding and engagement (Renatus et al., 2001; Talanian et al., 1996).

Interestingly, the crystal structure of human caspase-2 suggests that the proenzyme can also exist in solution as a stable dimer. Caspase-2 proenzymes were observed to bind *in vitro* in the absence of adaptor protein regulation, forming a covalent disulfide bond across the dimer interface that helps to both stabilize the protein pair and promote enzyme activation (Baliga et al., 2004; Schweizer et al., 2003). Although formation of this disulfide bond can increase the catalytic efficiency of the enzyme, additional *in vitro* studies have revealed that the formation of this bond is dispensable for caspase-2 activation (Baliga et al., 2004). It is still yet to be determined whether caspase-2 proteins can dimerize independently of adaptor protein regulation *in vivo* and thus, the prevailing mechanism of caspase-2 activation is via adaptor-protein mediated dimerization (Note: The mechanism of caspase-2 activation will be discussed in greater detail in section 1.2.2).

1.2.2 Caspase-2 localization

Caspase-2 differs from other caspase family proteins in its unique subcellular distribution. For example, while the majority of caspases have been shown to be primarily cytoplasmic, caspase-2 can be found in nearly every cellular compartment, including the cytoplasm, nucleus, Golgi complex, endoplasmic reticulum (ER), and the mitochondria (Cheung et al., 2006; Mancini et al., 2000; Susin et al., 1999; van Loo et al.,

2002; Zhivotovsky et al., 1999). The nuclear localization of caspase-2 is regulated by the nuclear localization signal (NLS) located within its prodomain (Colussi et al., 1998). The NLS interacts with the nuclear import proteins, α/β-importin, to facilitate its transport into the nucleus (Baliga et al., 2003; Colussi et al., 1998; Shikama et al., 2001). The functional relevance of caspase-2 nuclear localization is not well understood and the mechanism of its nuclear export is still unknown.

The localization of caspase-2 at ER membranes has been demonstrated by both immunofluorescence and membrane fractionation studies (Cheung et al., 2006). Interestingly, studies visualizing the activation of caspase-2 have shown that it can be activated in a perinuclear membrane region, similar to the ER (Bouchier-Hayes et al., 2009). These findings are of particular importance, as caspase-2 has recently gained recognition as an initiator of ER stress-induced apoptosis in a number of cellular settings (Gu et al., 2008; Penna et al., 2012; Uchibayashi et al., 2011; Upton et al., 2012). It is tempting to hypothesize that caspase-2 is localized to the ER in order to activate ER-stress-induced apoptosis. Although this idea is an attractive one, it appears that there may be more to the story, as at least one recent publication has provided evidence that caspase-2 can play a role in the modulation of ER stress (Nemcova-Furstova et al., 2013). This paper demonstrated that the loss of caspase-2 could dampen the ER stress response elicited by saturated fatty acids in pancreatic islet β-cells (Nemcova-Furstova et al.,

2013). Thus, regardless of its influence on apoptotic signaling, subcellular distribution of caspase-2 at the ER may ready the enzyme for ER stress-induced activation.

Since membrane and protein trafficking can occur simultaneously between the ER and the Golgi complex, it is perhaps not surprising that caspase-2 has also been shown to localize to the Golgi (Mancini et al., 2000; O'Reilly et al., 2002). This subcellular fraction of caspase-2 has been shown to play a role in Golgi complex disassembly during apoptotic cell death by cleaving the structural support protein, golgin-160 (Mancini et al., 2000). Although other caspases have been shown to cleave golgin-160, caspase-2 is the only one that has been shown to be localized at the Golgi complex in healthy, living cells (Mancini et al., 2000; O'Reilly et al., 2002).

Although caspase-2 was initially shown to be localized to the mitochondria, subsequent studies have had difficulty replicating these findings. The original publication provided evidence that the proenzyme form of caspase-2 could be localized to the mitochondrial intermembrane space (Susin et al., 1999). It was suggested that caspase-2 is released to the cytoplasm following MOMP and that this would enable its interaction with cytoplasmic adaptor proteins and facilitate its activation (Susin et al., 1999). Numerous follow-up studies have failed to observe such an event, including a detailed mitochondrial fractionation study which assessed the release of several well-established mitochondrial molecules (i.e., cytochrome *c*, SMAC/DIABLO) following apoptotic initiation (van Loo et al., 2002). Due to this fact, the mitochondrial localization

of caspase-2 is the most controversial of its putative subcellular localization sites and most of the studies published to date favor the idea that caspase-2 is not a mitochondrially-localized factor (van Loo et al., 2002).

1.2.3 Caspase-2 mechanism of activation

Similar to other well-characterized initiator caspases, including caspase-8 and caspase -9, caspase-2 is activated by proximity-induced dimerization. Dimerization is the key event required to activate caspase-2. Although not required for catalytic activity, auto-processing of the enzyme at aspartic acid residue 333, promotes enzyme stabilization and enhancement of its activity (Baliga et al., 2004; Butt et al., 1998; Read et al., 2002). As discussed in the previous section, caspase-2 can exist in solution as a dimer. However, dimerization of caspase-2 proenzymes in the absence of adaptor protein regulation has failed to be demonstrated *in vivo*. Thus, the prevailing mechanism is that caspase-2 is activated via the binding of adaptor proteins to its prodomain. This binding, which facilitates its oligomerization into a high molecular weight complex, triggers its dimerization and auto-catalytic processing into an active enzyme. Once activated, caspase-2 cleaves and activates the pro-apoptotic Bcl-2 family member, Bid, which in turn promotes Bax translocation to the mitochondria and cytochrome *c* release (Bonzon et al., 2006; Guo et al., 2002).

Although canonically, caspase-2 is believed to be activated by proximity-induced dimerization, a second potential mechanism of caspase-2 activation has been described,

whereby caspase-3 mediates the cleavage and activation of caspase-2 (Li et al., 1997a; Swanton et al., 1999). This secondary mechanism of activation is often thought to function as a feed-forward activation of the apoptotic signaling cascade, promoting further activation of caspases in order to enhance cell death. This feed-forward circuitry has been shown to be required for cell death, since the low levels of caspase-3 activated by a single cell death pathway are not sufficient for apoptotic execution (Swanton et al., 1999).

1.2.3.1 Potential activation platforms

As mentioned previously, caspase-2 is believed to be activated through the binding of adaptor protein complexes to its prodomain. The most well-characterized activation complex for caspase-2 has been termed the "PIDDosome" and it is composed of the CARD and death domain (DD)-containing protein, RAIDD, and the p53-inducible DD-containing protein, PIDD (Tinel and Tschopp, 2004). This complex, which has been shown to be responsive to DNA damage, is activated by the p53 mediated upregulation of PIDD expression (Lin et al., 2000).

The structural assembly of the PIDDosome has been well studied, with crystallography studies showing that five PIDD and seven RAIDD molecules comprise the core of this complex, in a structure similar to the caspase-9 activating platform, the apoptosome (Park et al., 2007a). Despite such comprehensive structural work, the significance of this platform has been challenged by genetic experiments showing that

PIDD is dispensable for the activation of caspase-2 *in vivo* (Kim et al., 2009; Manzl et al., 2009). Interestingly, RAIDD has been shown to be required for caspase-2 activation, even in settings where PIDD has been shown to be dispensable, suggesting that RAIDD may play a more central role in mediating caspase-2 oligomerization (Ribe et al., 2012). Nevertheless, these studies imply that alternative modes of caspase-2 activation must exist beyond the PIDDosome.

One such alternative mechanism for caspase-2 activation is the DISC, an extrinsic apoptotic signaling complex that functions to activate caspase-8 in response to extracellular death stimuli. Multiple studies have demonstrated that the proenzyme form of caspase-2 can be recruited to and activated by the DISC in response to DNA damage (DNA damage upregulates the expression of the CD95 death receptor, promoting clustering at the plasma membrane) (Lavrik et al., 2006; Olsson et al., 2009). Activation of caspase-2 by this platform is dependent upon caspase-8, such that the two enzymes must interact to facilitate cleavage of caspase-2 by caspase-8 (Olsson et al., 2009). While these observations provide an alternative activation platform for caspase-2, it is not known whether this platform can be triggered in the absence of DNA damage, which would make it a more general signaling platform, capable of initiating cell death in response to a variety of intracellular stressors.

Two additional caspase-2-containing complexes have been cited in the literature, one of which includes its interaction with the serine/threonine-protein kinase 1 (RIP1)

and the TNF receptor associated factor 2 (TRAF2). This complex, which has been implicated in the activation of pro-survival signaling pathways, such as NF-κB and p38 MAPK, does not require the catalytic activity of caspase-2 to elicit these responses (Lamkanfi et al., 2005). Unfortunately, the formation of this complex has only been demonstrated in overexpression settings or upon prolonged incubation of lysates at 37°C, and thus the physiological relevance of this complex is still undefined. Another putative caspase-2-containg complex was shown to consist of RAIDD, RIP1, TRADD, and the TNF-R1. Although over-expression studies have demonstrated that caspase-2 can form a complex with these proteins, evidence for endogenous complex formation still remains elusive (Ahmad et al., 1997). Therefore, since little evidence has been presented to suggest that either of these complexes can form in response to physiological stimuli, their involvement in caspase-2 activation remains strictly speculative.

1.2.3.2 Proximity-induced autocatalytic processing

As mentioned briefly, caspase-2 dimerization is the key event required for its activation. Following dimerization, caspase-2 undergoes proximity-induced autocatalytic processing and cleaves itself at three well-conserved aspartic acid residues. The first cleavage separates the large (p19) and small (p14) subunits of the enzyme via cleavage of aspartic acid residue 333. These subunits remain stably associated and form the catalytic or active site of the mature enzyme. The prodomain is then removed by cleavage of aspartic acid residue 169 and finally, the linker portion of the small subunit

is removed by cleavage of aspartic acid residue 347. The fully mature caspase-2 enzyme is a heterodimer consisting of two large subunits (p19) and two small subunits (p12) (Figure 1.4).

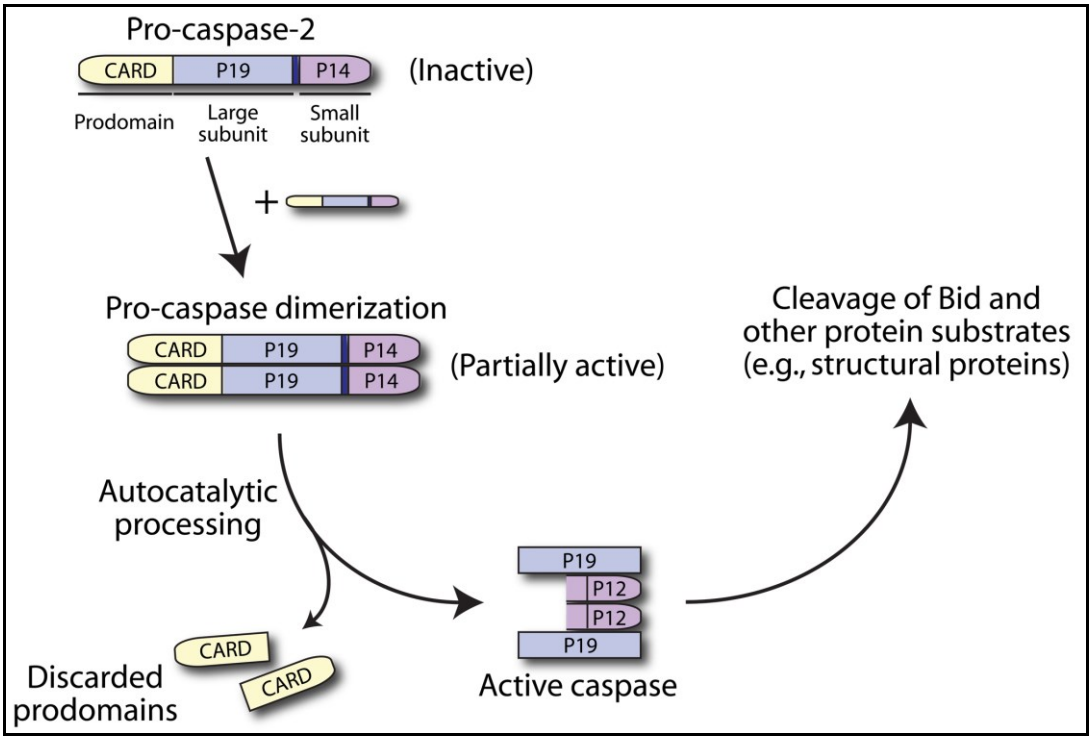

Figure 4.4: Mechanism of caspase-2 processing

Figure 1.4: Procaspase-2 monomers are recruited into close proximity via adaptor protein interactions (e.g. RAIDD, PIDD). Once in close proximity, caspase-2 proteins can dimerize, forming a partially active enzyme. The catalytic domains of caspase-2 dimers can promote auto-catalytic cleavage between the large and small subunits of each monomer (at D333). This cleavage results in stabilization of enzyme activity and promotes additional cleavages to remove the prodomain and linker region of the small subunit. The fully processed enzyme is a stable tetrameric complex with maximal enzymatic activity.

It is important to note that the proximity-induced processing of caspase-2 is not required for its activation, since a non-cleavable mutant is still able to maintain catalytic activity toward its substrates (Baliga et al., 2004). Cleavage of caspase-2 appears to be required for stabilization of its enzymatic activity, following initial activation. Thus, the current model is that caspase-2 activation in triggered solely by dimerization and that the proximity-induced processing of the proenzyme occurs secondary to its oligomerization (Baliga et al., 2004). The distinction between these two biochemical mechanisms is important, since many publications use caspase-2 processing as a readout of enzymatic activation. Perhaps a more appropriate method for measuring caspase-2 activation would be to evaluate enzyme dimerization or cleavage of a caspase-2-specific substrate.

1.2.4 Caspase-2 activating stimuli

Caspase-2 has been implicated in the induction of cell death by a number of cellular stressors, including DNA damage, neuronal stress, cytoskeletal disruption, and ER stress, among others (Table 1.1). While this list is not exhaustive, it does suggest that there are only a limited number of cellular conditions in which caspase-2 can function as an initiator of cell death. Our group, in addition to others, has found that caspase-2 dependency can be both cell-type and stimulus specific, making it difficult to identify cellular stressors that universally engage caspase-2. Because of these inconsistencies,

there has been much debate over caspase-2 activating stimuli and the contribution of caspase-2 to cell death in these scenarios.

Table 1.1: Examples of stimuli that have been reported to activate caspase-2

Stimulus	Examples	Cell Type	Caspase-2 Activity Assessment	References
DNA damage	Etoposide	Jurkat, IMR90E1A, Hela	Cleavage, siRNA, VDVAD-fmk, VDVADase, BiFC	(Bouchier-Hayes et al., 2009; Franklin and Robertson, 2007; Lassus et al., 2002; Robertson et al., 2002)
	Cisplatin	LLC-PK1, Caov4	VDVAD-fmk, VDVADase, cleavage, siRNA	(Seth et al., 2005; Vakifahmetoglu et al., 2008)
	5-FU	HCT116	VDVAD-fmk, VDVADase, siRNA	(Vakifahmetoglu et al., 2006)
	Doxorubicin	Mouse oocytes	Oocyte survival	(Bergeron et al., 1998)
	γ-irradiation	HEK293, thymocytes, zebrafish embryos	bVAD pulldown, cleavage, c2 morpholino	(Fushimi et al., 2008; O'Reilly et al., 2002; Shi et al., 2009)
	Daunorubicin	H1299	VDVAD-fmk, siRNA	(Baptiste-Okoh et al., 2008)
	UV	HCT116	Cleavage	(He et al., 2004)
Cytoskeletal disruptors	Zoledronic acid	MEF	Caspase2 KO MEF resistance	(Ho et al., 2008)
	Cytochalasin D	MEF, Hela	Caspase2 KO MEF resistance, BiFC	(Bouchier-Hayes et al., 2009; Ho et al., 2008)
	Vincristine	MEF, Hela	Caspase2 KO MEF resistance, BiFC	(Bouchier-Hayes et al., 2009; Ho et al., 2008)
	Paclitaxel	MEF, MCF-7, SK-BR-3	Caspase2 KO MEF resistance, Cleavage, VDVADase, siRNA	(Ho et al., 2008; Jelinek et al., 2013)
Neuronal stress	β-amyloid	Hippocampal neurons, sympathetic neurons, PC12	Cleavage, Caspase-2 KO cell resistance	(Troy et al., 2000)
	Transient global ischemia	hippocampal CA1 neurons	Cleavage	(Niizuma et al., 2008)
	Hypoxia	SK-N-MC,	Cleavage,	(Araya et al., 1998; Carlsson et

		Neonatal rat brain	Caspase-2 KO cell resistance, siRNA	al., 2011; Carlsson et al., 2012)
	NGF Withdrawal	Neuronal PC12 cells, sympathetic neurons	Cleavage, Antisense	(Stefanis et al., 1998; Troy et al., 1997)
	NGF	Mature oligodendrocytes	Cleavage	(Gu et al., 1999)
ER Stress	Brefeldin A	Bax/Bak deficient MEF, Hela	Cleavage and siRNA	(Cheung et al., 2006; Upton et al., 2008; Upton et al., 2012)
	Tunicamycin	U937, Hela	Cleavage, VDVADase, siRNA	(Cheung et al., 2006; Huang et al., 2009)
	Bortezomib	Human myeloma (H929, 8226/S)	siRNA, VDVAD-fmk	(Gu et al., 2008)
	Sorafenib	U937	siRNA	(Rahmani et al., 2007)
Miscellaneous	Oxidative Stress (ROS)	U937, CEM, Neural stem cells	Cleavage, siRNA VDVADase, VDVAD-fmk	(Peart et al., 2003; Rosato et al., 2008; Tamm et al., 2008)
	Death Receptor Activation	Jurkat, HCT116, SKW6.4, U937, Human fibroblasts, Hela	siRNA, Cleavage, VDVADase, BiFC	(Berube et al., 2005; Bouchier-Hayes et al., 2009; Wagner et al., 2004)
	Heat Shock	Mouse splenocytes, Jurkat, Hela	bVAD pulldown, BiFC	(Bouchier-Hayes et al., 2009; Tu et al., 2006b)
	Metabolic Stress	Xenopus oocytes and eggs	Cleavage, VDVADase	(Nutt et al., 2005)

Note: This table has been adapted from Bouchier-Hayes (2010).

Importantly, caspase-2 activation can be assessed by a number of different assays, many of which have been annotated for the caspase-2 activating stimuli listed in Table 1.1. The differences among these methodologies have contributed to the controversy surrounding caspase-2-activating stimuli and highlight the need for a more streamlined assessment of caspase-2 activation. For example, many of the published papers use fluorogenic substrates or inhibitors based on the preferred substrate cleavage site for caspase-2 (VDVAD). The problem with using such indicators is that they are not

specific for caspase-2, also being efficiently cleaved by executioner caspases, such as caspase-3 (McStay et al., 2008). Proteolytic processing is also used as a common read-out of caspase-2 activation. As discussed previously, cleavage is not required for caspase-2 activation and can sometimes occur as a secondary consequence of apoptotic signaling, serving as a positive feedback loop to amply caspase activity (Baliga et al., 2004; Li et al., 1997a; Swanton et al., 1999). Thus, it can be difficult to interpret conclusions that are based solely on measuring caspase-2 cleavage by western blot.

Another tool that is widely used to study caspase-2 activation is transient silencing via siRNA. Aside from the potential off-target effects of siRNA-target sequences, this approach is probably one of the best ways to determine whether a cell depends upon caspase-2 for cell death. Similar studies can also be performed using cells derived from caspase-2 KO mice. Such investigations could confirm the necessity of caspase-2, while at the same time ruling out the contribution of positive feedback loops. While inconsistencies between siRNA and KO cell experiments may arise, they do not immediately rule out caspase-2 as an initiator of cell death. There are a number of reasons why differences between these two approaches may arise. For example, the expression of caspase-2 and/or its regulatory factors may differ between transient and stable KO settings or there may be differences in caspase-2 requirements in humans versus mice. Moreover, there could be possible compensatory mechanisms in caspase-2 KO mice that could mask the true function of caspase-2. Because of these differences,

experiments that utilize transient silencing of caspase-2 can be useful in identifying functions of the enzyme that can be concealed in the KO setting.

Due to the difficulty in assessing caspase-2 dependency and activation, research on this enigmatic caspase has remained challenging. Going forward, biochemical and genetic assessments should be used combinatorially to determine the contribution of caspase-2 to stimulus-induced cell death. Studies should also be performed in multiple cell types to determine the true contribution of caspase-2 to cell death across a broad range of tissue types.

1.2.5 Caspase-2 regulation

In addition to adaptor protein binding, transcriptional, translational, and post-translational regulation of caspase-2 provides further control of apoptotic initiation. The amount and accessibility of caspase-2 protein can significantly influence its activation status following cellular insult. Importantly, caspase-2 protein levels have been shown to be transcriptionally regulated by p53, as well as post-transcriptionally by microRNAs (Baptiste-Okoh et al., 2008; Upton et al., 2012). Post-translational regulation of caspase-2 has also been shown to influence activation, serving to inhibit or, less commonly, activate the enzyme through changes in protein modifications (Andersen et al., 2009; Nutt et al., 2005; Shin et al., 2005; Yi et al., 2011). These additional modes of caspase regulation are often influenced by cellular stress and can therefore, provide an added level of control to avoid inappropriate caspase-2 activation.

1.2.5.1 Transcriptional and translational regulation

Caspase-2 levels have been shown to be regulated at the transcriptional level by a p53/p21-dependent pathway (Baptiste-Okoh et al., 2008). The induction of p53 in damaged cells results in a reduced level of caspase-2 mRNA and protein. This negative regulation of caspase-2 may be indirectly mediated by p53 through the induction of p21, since expression of the p21 transcription factor is sufficient to mediate the transcriptional repression of caspase-2 (Baptiste-Okoh et al., 2008). Interestingly, the p53-mediated downregulation of caspase-2 was reported to occur in both damaged and non-stimulated cells and may, therefore, serve as an apoptotic break in healthy cells to prevent an inappropriate activation of cell death signaling. Although this type of regulation may seem counterintuitive for apoptotic cells, it may well be that this apoptotic break can be overcome once DNA damage reaches a certain threshold.

Recent findings have also demonstrated that caspase-2 protein levels can be regulated at the post-transcriptional level by microRNAs. This pathway, which was uncovered in the setting of ER stress, identified four distinct microRNAs that normally repress caspase-2 mRNA translation, miR-17, -34a, -96, and -125b (Upton et al., 2012). These microRNAs bind to the 3′ end of caspase-2 mRNA sequences and inhibit gene expression by blocking mRNA translation. Interestingly, during periods of ER stress, the dual endoribonuclease and kinase, inositol requiring enzyme 1 alpha (IRE1α), reduces the levels of these mircoRNAs through RNA cleavage (Upton et al., 2012). This

lifts the block on caspase-2 translational repression, resulting in increased expression of the protease. Increased expression of caspase-2 then contributes to apoptotic cell death through proteolytic cleavage of Bid, which causes cytochrome *c* release from mitochondria.

1.2.5.2 Post-translational modification

In addition to protein level changes, caspase-2 activation can also be influence by post-translational modifications. To date, caspase-2 has been shown to be post-translationally modified by phosphorylation and n-terminal acetylation (Andersen et al., 2009; Nutt et al., 2005; Shin et al., 2005; Yi et al., 2011). Our group has specifically identified two independent phosphorylation sites on caspase-2, one in the prodomain and one in the linker region of the small subunit.

Caspase-2 prodomain phosphorylation occurs on serine 135 (*Xenopus* numbering) and is catalyzed by the calcium/calmodulin-dependent protein kinase type II (CaMKII) (Nutt et al., 2005). Interestingly, in cell-free *Xenopus* egg extracts, this phosphorylation has been shown to be regulated by metabolism, whereby abundant nutrient flux through the pentose phosphate pathway stimulates the activation of CaMKII via the production of coenzyme A (CoA) (McCoy et al., 2013; Nutt et al., 2005). This phosphorylation inhibits the binding between caspase-2 and its adaptor protein, RAIDD, and thus functions as an inhibitory phosphorylation on caspase-2 (Figure 1.5).

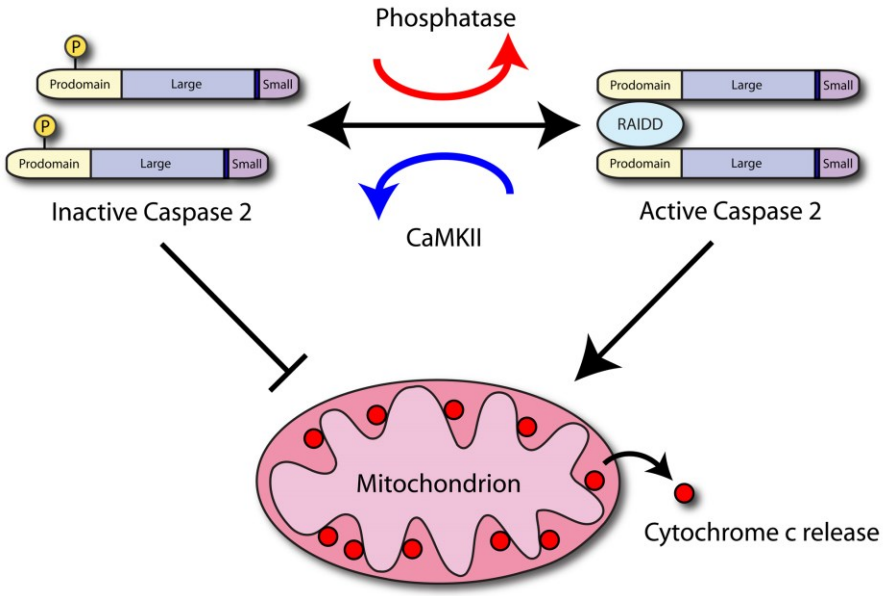

Figure 5.5: Metabolic regulation of caspase-2 by phosphorylation

Figure 1.5: Caspase-2 is suppressed in the *Xenopus* egg extract by CaMKII-catalyzed phosphorylation at serine 135. This prodomain phosphorylation, which is stimulated by coenzyme A-induced activation of CaMKII in the extract, is critical in preventing binding of caspase-2 to the CARD-containing adaptor protein, RAIDD.

Caspase-2 is also suppressed by phosphorylation of the linker region of the small subunit. This phosphorylation, which occurs on serine 308 (*Xenopus* numbering), is catalyzed by the M phase-promoting kinase, cyclin dependent kinase-1 (Cdk1) (Andersen et al., 2009). Upon entering mitosis, the Cdk1-cyclin B1 complex phosphorylates caspase-2 and inhibits its activation by an unknown mechanism. This phosphorylation may serve as a sort of cross-talk between apoptotic and cell cycle machineries, ensuring that apoptosis is not activated during normal cell cycle progression (Andersen et al., 2009).

In addition to the two phosphorylations characterized by our lab, caspase-2 has also been shown to be phosphorylated by protein kinase casein kinase 2 (PKCK2) at serine 157 (Shin et al., 2005). This phosphorylation was, again, shown to be inhibitory and could prevent caspase-2 from initiating cell death in response to receptor-induced caspase-8 activation (Shin et al., 2005).

Caspase-2 has also been shown to be post-translationally modified by N-terminal acetylation. This modification promotes activation of caspase-2 by enhancing its binding to the pro-apoptotic adaptor protein, RAIDD (Yi et al., 2011). Interestingly, it has recently been suggested that the abundance of acetylation can be regulated by the availability of its metabolite cofactor, acetyl-CoA. These observations, along with the metabolically-sensitive phosphorylation discussed above, suggest that caspase-2 could function as a critical gauge of cellular fate, coupling apoptotic sensitivity to metabolism through dynamic changes in post-translational modifications that influence its activation.

1.2.6 Caspase-2 substrates

Caspase-2 is unique among other initiator caspases in that it does not directly cleave executioner caspases (Guo et al., 2002). Instead, caspase-2 initiates the apoptotic cascade by cleaving the pro-apoptotic BH3-only protein, Bid, which is able to promote Bax activation, mitochondrial outer membrane permeabilization, and cytochrome *c* release (Luo et al., 1998). Mitochondrial release of cytochrome *c* facilitates the activation

of executioner caspases and cell death. In addition to promoting mitochondrial cytochrome *c* release, caspase-2 propagates the apoptotic pathway through cleavage of other substrates which aid in the dismantling of the cell.

In general, most caspases recognize a four-residue consensus sequence on their substrate counterparts. Interestingly, caspase-2 is the only family member that prefers a pentapeptide instead of a tetrapeptide, with VDVAD being its optimal substrate sequence (Talanian et al., 1997). While small peptide-inhibitors based on this consensus work well to inhibit caspase-2, they also appear to have some activity toward caspase-3 and -7 *in vivo*, suggesting that they lack specificity(McStay et al., 2008). Because the original biochemical studies performed to determine caspase specificity and activity relied on the use of synthetic peptide libraries, they are limited in their interpretation and cannot be used to unambiguously determine caspase substrates.

Fortunately, recent findings have utilized high throughput methods based on mass spectrometry in order to profile caspase-2 cleavage specificity. This study, whose results have been summarized in Table 1.2, identified close to 40 novel caspase-2 substrates (Wejda et al., 2012). Remarkably, many of these substrates shared overlapping specificity with executioner caspases, caspase-3 and -7, suggesting that caspase-2 could function as a pro-apoptotic caspase once released from it activating complex.

Table 2.2: Putative caspase-2 substrates and cleavage sites

Protein name	Cleavage site	Other caspases
Eukaryotic translation initiation factor 4B	ESDRKD¦GKKD	
Signal recognition particle 54-kDa protein	ELDSTD¦GAKV	Caspase-3
Thymosin ß-10	MADKPD¦MGEI	
Actin, cytoplasmic 2	SYELPD¦GQVI	
Prothymosin a	DGEEED¦GDED	
Clathrin light chain A	GPDAVD¦GVMN	Caspase-3
Myosin-14	LEDTLD¦STNA	
E3 ubiquitin-protein ligase HUWE1	ELLERD¦GGSG	
Filamin-A	VVDNAD¦GTQT	
Thimet oligopeptidase	AGDMAD¦AASP	Caspase-3
TAR DNA-binding protein 43	KmDETD¦ASSA	Caspase-3
G patch domain & KOW motif-containing protein	LPDRQD¦GPAA	
Keratin, type I cytoskeletal 18	LGDALD¦SSNS	Caspase-3, -7
Vimentin	LQDSVD¦FSLA	Caspase-3, -7
PRKC apoptosis WT1 regulator protein	DEEEPD¦GVPE	Caspase-3
Eukaryotic translation initiation factor 4?1	GEEDAD¦GSKT	
Aspartyl/asparaginyl ß-hydroxylase	EQENPD¦SSEP	
Microtubule-associated protein 1B	KTDATD¦GKDY	Caspase-3, -7
Prothymosin a	EEEEGD¦GEEE	
Zinc finger CCCH domain-containing protein 15	GGDEVD¦DSVS	
Heterogeneous nuclear ribonucleoprotein A0	SPHAVD¦GNTV	
Uncharacterized protein KIAA0174	ETDLID¦VGFT	
Lysyl-tRNA synthetase	AEVKVD¦GSEP	Caspase-3
Nucleosome assembly protein 1-like 1	LQERLD¦GLVE	
40 S ribosomal protein S18	QKDVKD¦GKYS	
Endoplasmin	EAIQLD¦GLNA	
Myosin-9	LEDTLD¦STAA	Caspase-3
Non-POU octamer-binding protein	ATMMPD¦GTLG	Caspase-3
Transcription intermediary factor 1-ß	SLDGAD¦STGV	Caspase-3
Acidic leucine-rich nuclear phosphoprotein 32	EEGYND¦GEVD	
Protein HEXIM1	DQEEPD¦LKTG	
Eukaryotic translation initiation factor 4H	EFDEVD¦SLKE	Caspase-3
Eukaryotic translation initiation factor 4B	DENKVD¦GMNA	Caspase-3
Filamin-A	PVDVVD¦NADG	
ATP synthase subunit a, mitochondrial	LGNAID¦GKGP	Caspase-3
Pyruvate kinase isozymes M1/M2	ANAVLD¦GADC	

In addition to the novel substrates listed in Table 1.2, caspase-2 has also been shown to cleave and inactivate a number of proteins which contribute to the structural disassembly of the cell. These include structural proteins, Golgin 160, αII-spectrin, and plakin, as well as proteins which contribute to the maintenance of genomic stability, such as ICAD, PARP, and histone deacetylase 4 (HDAC4) (Aho, 2004; Gu et al., 2008; Mancini et al., 2000; Paroni et al., 2004; Rotter et al., 2004; Sakahira et al., 1998). Cleavage of these substrates will help facilitate many of the morphological features of apoptosis often observed in dying cells, including loss of cellular attachment, cellular rounding and DNA fragmentation.

Interestingly, caspase-2 has recently been suggested to promote apoptotic cellular disassembly through the disruption of the cytoskeleton (Vakifahmetoglu-Norberg et al., 2013). Unexpectedly, caspase-2 mediated cytoskeletal breakdown was shown to be mediated by proteasomal degradation of four proteins including, tropomyosin, profilin, stathmin-1 and myotrophin in the setting of DNA damage, cytoskeleton disruption and ER stress. Degradation of these cytoskeleton proteins was blunted by siRNA targeting of caspase-2 and none of these proteins was directly cleaved by the protease (Vakifahmetoglu-Norberg et al., 2013). This study demonstrates a novel role for caspase-2, being the first to link this protease to proteasomal degradation. It will be interesting to see whether caspase-2 plays a role in promoting the degradation of other proteins, beyond just cytoskeletal targets, during apoptosis.

1.2.7 Studying apoptosis in *Xenopus laevis* cell-free egg extract

Eggs from the African clawed frog, *Xenopus laevis*, are poised to undergo multiple rounds of cellular division following fertilization. *Xenopus* eggs are densely packed with cellular components and can divide sequentially in the absence of any transcriptional input until they reach the 4,000-cell stage. *Xenopus* eggs are arrested at metaphase II of meiosis with high Cdc2/Cyclin B activity. By crushing these eggs via centrifugation, internal stores of calcium are released, mimicking fertilization and leading to the degradation of Cyclin B and exit from mitosis. The resulting cell-free extract can perform protein biosynthesis, allowing Cyclin B to be re-synthesized in the ensuing interphase to promote re-entry into mitosis (Murray, 1991). The degradation and re-synthesis of cyclin B will repeat itself, creating an extract that "cycles" between interphase and mitosis. These "cycling" extracts are ideal for examining biochemical modifications, changes in binding partners, and alterations in protein levels throughout the cell cycle.

The addition of cycloheximide to the eggs, prior to centrifugation, prevents the re-synthesis of cyclin B and results in an extract that is stably arrested in interphase (Smythe and Newport, 1991). Interphase egg extracts can be utilized as a cell-free model system to study signaling pathways, as they are capable of recapitulating DNA replication , entry into mitosis, and movement through the nuclear pore complex (Blow

and Laskey, 1986; Kluck et al., 1997; Murray and Kirschner, 1989; Newport and Forbes, 1987).

Initially characterized in 1994 by Newmeyer and colleagues, it was noted that the prolonged incubation of *Xenopus* egg extracts at room temperature resulted in the spontaneous activation of apoptosis (Newmeyer et al., 1994). Subsequent studies further demonstrated that this system executes many of the key biochemical events that define apoptosis, including mitochondrial cytochrome *c* release, nuclear fragmentation, and caspase activation (Kluck et al., 1997; von Ahsen and Newmeyer, 2000). Many years later, our lab has put forth effort to understand why *Xenopus* egg extracts undergo apoptosis. Although this thesis suggests more complexity, previous studies by our laboratory have suggested the initiating event to be metabolic stress; specifically depletion of the pentose phosphate pathway byproduct, nicotinamide adenine dinucleotide phosphate (NADPH). Caspase-2 functions as the initiator caspase in this system and it was demonstrated by our lab to be necessary for activation of the apoptotic cascade (Nutt et al., 2005).

In recent years, the *Xenopus* egg extract system has become a powerful research tool for studying the biochemical signaling events of apoptosis. This is primarily due to the ease of manipulation, as the extract lacks a plasma membrane and is therefore, not constrained by cell permeability. Recombinant proteins, pharmacological inhibitors, and metabolites can all be easily added to the extract, making it an ideal model for

biochemical manipulation. The influence of such manipulations on apoptotic signaling can be easily monitored by assessing caspase activation through the use of colorimetric assays or western blotting. Most importantly, apoptotic signaling pathways are well-conserved and our laboratory has repeatedly demonstrated the utility of the *Xenopus* egg extract as a model system by confirming many of our findings in mammalian cells.

1.3 Metabolism

The complex signaling pathways that control cellular fate can be intimately influenced by cellular metabolic status. Although the ability of nutrients to influence intracellular decisions has been appreciated for some time, the complex signaling mechanisms linking metabolic inputs to cell proliferation and death are not fully understood. Recently, our lab has demonstrated that caspase-2 is a metabolically-sensitive enzyme, undergoing dynamic changes in post-translational modification in response to alterations in metabolic activity. Metabolic changes in post-translational modifications appear to sensitize caspase-2 to activation and therefore, suggest that caspase-2 could function as a critical gauge of cellular fate, coupling apoptotic sensitivity to cellular nutrient status. Understanding the connection between caspase-2 and metabolism is the principal goal of this dissertation and thus, a short overview of metabolic pathways has been included in this section. Please note that the specific details of these pathways have been summarized and adapted from *Biochemistry* by Berg et al., (2002).

1.3.1 Cellular metabolism

Cellular metabolism refers to the set of intracellular reactions that (1) provide the cell with energy from the breakdown of environmental fuel sources and (2) synthesize the macromolecules necessary for growth, survival, and proliferation. Processes which breakdown extracellular fuel sources are known as catabolic metabolism and include glycolysis, the tricarboxylic acid (TCA) cycle, and fatty acid oxidation (beta-oxidation). These pathways, which supply the cell with reducing equivalents in the form of NADH and $FADH_2$, fuel the production of cellular ATP. Processes which synthesize molecules necessary for cell growth and survival are known as anabolic metabolism. The major anabolic pathway relevant to this thesis work is fatty acid synthesis, which utilizes acetyl-CoA and NADPH to manufacture long-chain fatty acids. For a summary of these major metabolic pathways, see Figure 1.6.

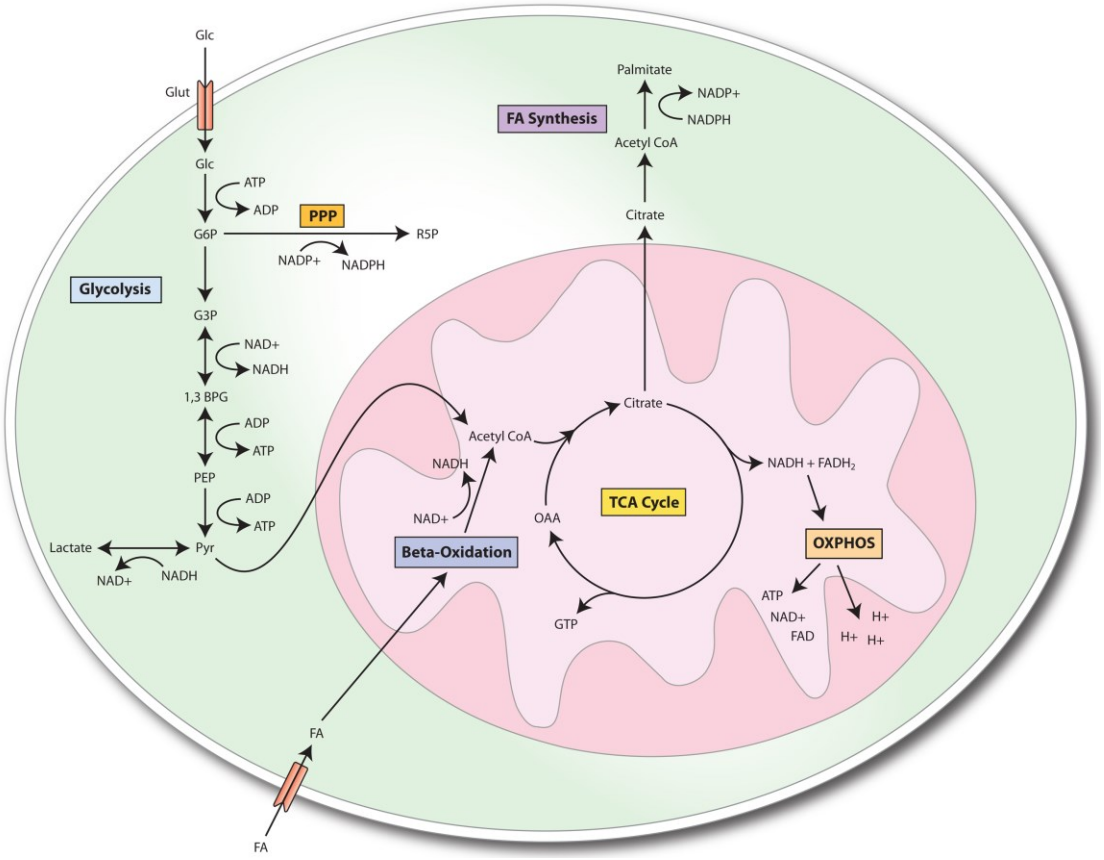

Figure 6.6: Cellular metabolic pathways

Figure 1.6: Glucose enters the cell through specialized membrane transporters, called Gluts, and is phosphorylated to glucose 6-phosphate (G6P) to prevent its re-exit. Once phosphorylated, G6P can either be used in the pentose phosphate pathway (PPP) to form ribose 5-phosphate and produce NADPH or is can enter glycolysis for the production of ATP and reducing equivalents. In the glycolytic pathway, G6P is converted into 2 molecules of pyruvate (pyr) through a series of reactions that form ATP and NADH. Pyr can then be shuttled into the mitochondrial matrix, where it is converted into acetyl-CoA for oxidation in the tricarboxylic cycle (TCA cycle), or under anaerobic conditions, pyr can be converted to lactate to regenerate NAD+ for glycolysis. In the TCA cycle, acetyl-CoA and oxaloacetate (OAA) condense to from citrate, which then undergoes a series of reactions that produce NADH, $FADH_2$ and GTP, eventually reforming OAA for subsequent cycles. The β−oxidation of fatty acids also occurs in the mitochondrial matrix, producing acetyl-CoA (for use in TCA cycle) and NADH. The NADH and $FADH_2$ produced by these reactions are used in oxidative phosphorylation to produce ATP, or energy, for the cell. Citrate, which is formed when acetyl-CoA condenses with OAA, can also be exported out of the mitochondria, converted to acetyl-CoA, and used in the production of palmitate through the NADPH-dependent reactions of fatty acid synthesis. Adapted from Lindblom and Kornbluth (2014).

1.3.2 Glucose metabolism

Glucose is the most important simple sugar in human metabolism, supplying the cell with both energy and reducing power. Glucose enters the cell through glucose transporters, which undergo a conformational change following glucose binding. Once cytosolic, glucose is prevented from exiting the cell via its phosphorylation by the enzyme hexokinase, forming glucose-6-phophate (G6P) (Note: this is the first step in glycolysis). G6P can either continue down the glycolytic pathway onto the tricarboxylic acid (TCA) cycle, which supports the mitochondrial production of ATP via oxidative phosphorylation, or it can be shunted into the pentose phosphate pathway (PPP) to produce NADPH through a series of oxidative reactions. While glycolysis is critical for maintaining cellular respiration and ATP production, NADPH is used in the reductive biosynthesis of lipids and helps to neutralize toxic reactive oxygen species (ROS) in the cell. Thus, glucose can be utilized in a number of catabolic pathways important for both cell growth and defense against damage. Metabolic flux of glucose may very well be dictated by the specific needs of the cell.

1.3.2.1 Glycolysis

Glycolysis is a series of ten cytosolic reactions that convert glucose into two molecules of pyruvate, with a net gain of two molecules of ATP. In order for glycolysis to occur, NAD+ must be present to act as an electron acceptor in the oxidation of glyceraldehyde 3-phosphate, which is the sixth step in the glycolytic breakdown

process. The NADH formed in this reaction can, under aerobic conditions, be re-oxidized into NAD+ by transferring its electrons to O_2 as part of the electron transport chain. Alternatively, under anaerobic conditions, NAD+ can be regenerated through the reduction of pyruvate to lactate in an enzymatic process that is catalyzed by lactate dehydrogenase.

1.3.2.2 The tricarboxylic acid cycle

In order to generate more energy from glucose, the pyruvate produced in glycolysis is further broken down in the mitochondria through a series of nine reactions, known as the tricarboxylic acid cycle or TCA cycle. Prior to entering the TCA cycle, pyruvate is converted to acetyl-CoA in the mitochondrial matrix by pyruvate dehydrogenase. Acetyl-CoA then undergoes a condensation reaction with oxaloacetate to form citrate, a reaction catalyzed by citrate synthase. Citrate then undergoes a series of isomerizations, oxidative decarboxylations, and hydration reactions to eventually regenerate oxaloacetate. Oxaloacetate can then re-combine with another acetyl-CoA molecule and repeat the process.

For every molecule of acetyl-CoA that enters the cycle, two molecules of CO_2 will be produced. Additionally, 3 molecules of NAD+ will be reduced to NADH, 1 molecule of FAD will be reduced to $FADH_2$, and one molecule of GDP will be phosphorylated to GTP. The reduced electron carriers generated by this process will be oxidized by the electron transport chain to produce an additional nine molecules of ATP. Oxidation of

these electron carriers is necessary to regenerate electron acceptors for use in subsequent TCA cycles and consequently, restricts function of this cycle to aerobic conditions when electrons can be transferred to O_2 as part of the electron transport chain.

1.3.2.3 Oxidative phosphorylation

The major source of ATP in aerobic organisms is formed through the reactions of the electron transport chain, which is also referred to as oxidative phosphorylation. These reactions, which utilize the NADH and $FADH_2$ formed in glycolysis, TCA cycle, and fatty acid oxidation (discussed in section 1.3.3.2), transfer electrons from these donors to molecular oxygen in a series of reactions that form a proton motive force and result in the pumping of protons from the mitochondrial matrix into the intermembrane space. ATP is generated when protons flow back into the matrix through the ATP synthase enzyme complex.

The respiratory chain transfers electrons through a series of three proton pumps and two mobile electron carriers. The three main proton pumps consist of large transmembrane protein complexes and are named NADH-Q reductase (Complex I), cytochrome reductase (Complex III), and cytochrome oxidase (Complex IV). These complexes pump protons across the inner mitochondrial membrane while transferring electrons from NADH to the final electron acceptor,O_2. Electrons from NADH are first transferred to Complex I and then moved to Complex III by the electron acceptor, ubiquinone. Cytochrome *c* then shuttles electrons from Complex III to Complex IV, and

Complex IV catalyzes their transfer to molecular oxygen to form water. The process of electron transport is similar for electrons donated from $FADH_2$, only this donor first transfers its electrons to succinate dehydrogenase (Complex II) before ubiquinone picks them up and transfers them to Complex III. Importantly, succinate dehydrogenase also catalyzes the conversion of succinate to fumarate as part of the TCA cycle. Succinate dehydrogenase is the only enzyme that participates in both the TCA and the electron transport chain and serves to link the glycolytic flux between these two metabolic processes.

The proton gradient created by the transport of electrons across the respiratory complexes is utilized by the ATP synthase enzyme to catalyze the phosphorylation of ADP to ATP. The oxidation of NADH and $FADH_2$ is tightly regulated by the level of ATP, such that when the ATP levels are high, electron transport is halted since additional energy production is not needed.

1.3.3 Lipid metabolism

Lipid metabolism is a complex process that involves several different pathways that interdependently regulate the breakdown and synthesis of fats. For the purposes of this dissertation, the discussion will focus on fatty acids, the most commonly stored and circulating forms of lipid energy. Fatty acids are carboxylic acids with long hydrocarbon chains that can be either saturated (without double bonds) or unsaturated (containing one or more carbon-carbon double bonds). Fatty acids can exist as uncombined fatty

acids, known more commonly as free fatty acids, which circulate in the blood while bound to serum albumin. Fatty acids can also exist as triglycerides or phospholipids. These more inert forms of fatty acids can facilitate the transport of lipids from adipose tissues to other areas of the body as well as serve as a major component of cellular membranes. Fatty acids, both free and glycerol-bound (triglycerides), can originate from four major sources: de novo fatty acid synthesis, cytoplasmic triglyceride stores, circulating lipoproteins, and circulating free fatty acids.

Due to their water insolubility, free fatty acids are transported in the blood in a complex with the protein serum albumin. Once taken up by a cell, fatty acids have several fates: (1) They can enter the mitochondria (in a reaction that requires carnitine) and be used for energy production (through the TCA cycle) via beta-oxidation or (2) they can recombine with glycerol to form triglycerides for storage purposes or in the case of the liver, get packaged into very-low-density-lipoprotein (VLDL) through condensation with cholesterol and apolipoprotein for export into the blood. The uptake of triglycerides usually results in the release of free fatty acids and a glycerol molecule. While free fatty acids are processes as above, glycerol is usually taken up by the cell and used for glucose production or recycled for triglyceride formation.

Healthy individuals contain very low concentrations of free fatty acids in the blood. An increase in circulating free fatty acids typically occurs when: (1) the body is breaking down fat, which occurs when the glucose supply is unable to meet energy

demands or (2) during periods of over-nutrition, when free fatty acids accumulate to levels that exceed the storage capacity of adipose tissue. Such an imbalance between energy demand and food supply can be detrimental, predisposing animals to liver steatosis (excessive fatty acid storage within the hepatocyte). The negative consequences of liver steatosis will be discussed in greater detail in section 1.4.

1.3.3.1 Fatty acid synthesis

Fatty acids are synthesized in the cytoplasm by a large enzyme complex known as fatty acid synthase (FASN). This complex performs a four-step energy-consuming reaction that results in the elongation of a carbon chain by 2 carbon units every cycle. It uses acetyl-CoA as a substrate and through the consumption of ATP and CO_2, first activates this molecule to malonyl-CoA, a 3-carbon compound. Malonyl-CoA is then added to the growing carbon chain through a series of reduction reactions which consume NADPH and elongate the growing chain by 2 carbon units. The final product of fatty acid synthesis is palmitate, a 16-carbon chain saturated fatty acid. Modification of palmitate leads to other shorter and longer chain fatty acids, while desaturation of the carbon chain is performed by specific enzymes, known as fatty acid CoA desaturases. Fatty acid synthesis is required for the production of fatty acids used in phospholipid biosynthesis and it functions to store excess cellular energy in the form of fat.

1.3.3.2 Beta-oxidation

When it is necessary to utilize fats as energy, beta-oxidation of fatty acids takes place in the mitochondrial matrix. In order to enter the matrix, cytosolic fatty acids must first be activated through a thioester linkage to CoA, which is catalyzed by acyl CoA synthetase and occurs on the outer mitochondrial membrane. Next, fatty acid CoAs are conjugated to carnitine to form acylcarnitines, which can be shuttled across the inner mitochondrial membrane into the matrix. Once in the matrix, carnitine is removed and the acyl CoA is degraded through a series of four reactions: oxidation by flavin adenine nucleotide (FAD), hydration, oxidation by NAD+, and thiolysis by CoA. Each round of reactions will reduce the acyl CoA chain by two carbon units, producing acetyl-CoA , NADH, and $FADH_2$. The reduced electron carriers generated by this process help fuel energy production via oxidative phosphorylation (section 1.3.2.3), while the acetyl-CoA molecule can be further utilized in the TCA cycle for energy generation (see section 1.3.2.2).

1.4 Obesity and apoptosis

During periods of overnutrition, long-chain fatty acids (LCFAs) accumulate and saturate the storage capacity of adipose tissue. As a result, LCFA levels become elevated in the plasma, resulting in increased import and storage of these molecules in non-adipose tissues (Frayn, 2002; Kusminski et al., 2009; Lewis et al., 2002). The over-accumulation of lipids in non-adipose tissues can result in chronic cellular dysfunction

and programmed cell-death. These processes, which are now commonly referred to as lipotoxicity and lipoapoptosis, have profound impact on tissue function and appear to be a critical part of the etiology of diseases associated with metabolic syndrome (Cazanave and Gores, 2010; Kusminski et al., 2009; Listenberger and Schaffer, 2002; Unger et al., 2010).

1.4.1 Lipotoxicity and lipoapoptosis

In normal cellular settings, the uptake and production of lipids is carefully balanced with their oxidation and transport. Overnutrition, inactivity, and environment are all factors that can increase the amount of free fatty acids circulating in the blood, resulting in an increased uptake of these molecules without a corresponding increase in their oxidation. This type of metabolic imbalance will lead to an over-accumulation of free fatty acids within the cell and without proper neutralization of these lipids, can result in chronic cellular dysfunction (Schaffer, 2003).

Upon entering a cell, fatty acids can be converted into different types of lipids for storage, most often being converted into triglycerides, which are considered the most neutral and harmless of intracellular lipids. Triglycerides are stored as cytoplasmic lipid droplets and while adipose cells have a unique capacity to store large amounts of lipids, non-adipose cells do not. Thus, an excess accumulation of lipid droplets in non-adipose cells will result in dysfunction, which in the case of the pancreas means diminished insulin secretion and in the case of the liver means impaired insulin-stimulated glucose

transport (Schaffer, 2003). The detrimental effects of lipid accumulation depend on the cell type and the degree of lipid overload. Prolonged exposure to high amounts of lipids can trigger apoptotic cell death, a process which is now commonly referred to as lipoapoptosis.

Lipoapoptosis has been shown to affect many cell types, including hepatocytes in the liver, cardiomyocytes in the heart, and islet beta cells in the pancreas. These cells, which specifically undergo apoptosis in response to treatment with saturated fatty acids, display several characteristic features of the intrinsic apoptotic pathway, including mitochondrial permeabilization, cytochrome *c* release, and effector caspase activation. While the role of the mitochondria and cytochrome *c* release has been well-established in LCFA-induced lipoapoptosis, the core apoptotic machinery engaged by toxic concentrations of LCFA upstream of the mitochondria has not yet been reported and will be discussed in this dissertation.

Understanding how lipids induce cell death is important for managing diseases that are exacerbated by lipid-induced cytotoxicity. Thus, multiple studies have focused on identifying the specific lipid species that triggers apoptosis. Data demonstrating that a non-metabolizable fatty acid (2-bromoplamitate) induces apoptosis in islet beta cells suggests that free fatty acids may be the toxic offenders (Cnop et al., 2001) . Moreover, there have been several studies showing the toxic effects of saturated but not unsaturated fatty acids, suggesting that saturated fatty acids may be central to apoptotic

induction (de Vries et al., 1997; Furstova et al., 2008; Hardy et al., 2003; Kim et al., 2008; Mei et al., 2011; Staiger et al., 2006). For example, saturated fatty acids serve as a precursor molecule for the de novo synthesis of ceramide, a lipid signaling molecule that is known to induce apoptosis. While ceramide synthesis can be increased following the treatment of cells with LCFAs, ceramide only induces apoptosis in some cell types and thus, may not be the critical effector triggering lipoapoptosis (de Vries et al., 1997; Listenberger et al., 2001). In addition to ceramide production, free fatty acids may induce lipoapoptosis through the production of ROS either by increased production of nitric oxide or reactive oxygen radicals coming from oxidative phosphorylation (Kong and Rabkin, 2002; Piro et al., 2002; Shimabukuro et al., 1997).

1.4.2 Lipoapoptosis as a critical mediator of nonalcoholic fatty liver disease

Lipoapoptosis has recently gained recognition as a critical mediator of nonalcohlic fatty liver disease (NAFLD). NALFD is a progressive liver disease in which excessive fatty acid uptake by the liver results in hepatocyte cell death (Neuschwander-Tetri, 2010). Hepatocellular lipoapoptosis has been demonstrated to be a critical mechanism driving the progression of NAFLD to the more advanced stage of the disease, nonalcoholic steatphepatitis (NASH). NASH is characterized by an increase in liver cell injury as well as cell death (Feldstein et al., 2003) . NASH can result in an irreversible scarring of the liver, which is known as cirrhosis, and upon prolonged

stress, can cause liver failure. Currently, NASH-related cirrhosis is the third leading cause of liver transplantation in the United States (Charlton et al., 2011).

NAFLD affects 25% of the population here in the United States, although many believe this to be an underestimation, as patients usually have little to no symptoms often only complaining of fatigue or mild abdominal discomfort. NAFLD is typically diagnosed by abnormal liver enzyme levels during routine blood tests, which may indicate that there is a decrease in liver function. Mild to moderate elevations of the serum aminotransferases (aspartate aminotransferase (AST) and alanine aminotransferase (ALT)) are most commonly found but serum alkaline phosphatase and g-glutamyl transpeptidase levels can also be abnormal. A liver biopsy is then usually performed to differentiate NAFLD from NASH. If the tissue shows lipid deposits without inflammation or cellular damage, NAFLD is diagnosed. However, if the tissue shows infiltration of inflammatory cells, damage to hepatocytes and liver scarring, NASH is noted. Once patients have progressed to this state, there is little that can be done to reverse liver damage. Therefore, it is important to find a therapeutic entry point for halting the progression of NAFLD.

Lipoapoptosis has been shown to be a critical mediator of liver scarring, fueling the production of type I collagen in a process known as fibrogenesis (Figure 1.7). More specifically, hepatocyte apoptosis promotes the activation of a group of cells in the liver known as hepatic stellate cells (HSCs). These cells, which activate upon the engulfment

of apoptotic bodies, begin secreting type I collagen (collagen 1α1) (Canbay et al., 2003). Collagen secretion results in fibrosis or cirrhosis and correlates with negative patient outcomes (Malhi et al., 2010). Since lipoapoptosis is a critical mediator of fibrosis in NASH, it is important to understand the apoptotic signaling events regulating cell death in order to find a potential therapeutic target. In Chapters 5 of this dissertation, we evaluate the hypothesis that lipoapoptosis of hepatocytes is mediated by the activation of caspase-2, thereby driving the progression and pathogenesis of NASH-related cirrhosis.

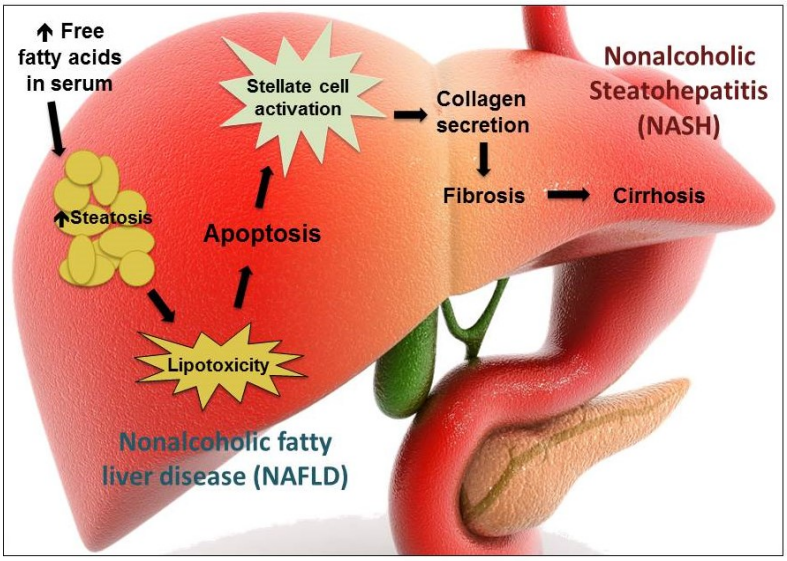

Figure 7.7: Progression of NAFLD

Figure 1.7: An increased level of free fatty acids in the serum promotes the uptake and deposit of excess fatty acids in the liver, resulting in steatosis. Steatosis triggers cellular dysfuction, or lipotoxicity, resulting in the nonalchoholic fatty liver disease (NAFLD). Prolonged exposure to excess fatty acids will trigger apoptotsis of hepatocytes, resulting in the activation of hepatic stellate cells (HSCs). Following activation, HSCs secrete collagen to promote liver fibrosis and cirrhosis. Fibrosis is indicative of the more advanced stage of liver disease, known as nonalchoholic steatohepatitis, or NASH.

2. Materials and Methods

2.1 Xenopus techniques

2.1.1 *Xenopus* egg extract

Mature *Xenopus laevis* female frogs were induced to lay eggs by injection of exogenous β-human chorionic gonadotropin (β-HCG) hormone as described previously (Smythe and Newport, 1991). 24h post-injection, eggs were collected and jelly coats were removed from the eggs with 2% cysteine (pH 8.0). Eggs were washed three times with modified Ringer's solution (MMR: 1 M NaCl, 20 mM KCl, 10 mM $MgSO_4$, 25 mM $CaCl_2$, 5 mM Hepes, pH 7.8, 0.8 mM EDTA) and then three times with egg lysis buffer (ELB: 250 mM sucrose, 2.5 mM MgCl2, 1.0 mM dithiothreitol, 50 mM KCl, 10 mM Hepes, pH 7.7). Eggs were centrifuged at 400 g, excess buffer was removed, and cytochalasin B (5 μg/mL; Calbiochem), aprotinin/leupeptin (5 μg/mL), and cyclohexamide (50 μg/mL) were added. Egg lysis was performed by centrifugation at 10,000 g for 12 minutes. Crude cytosolic egg extracts were collected using a syringe and stored on ice until time of use. Prior to use, egg extract was supplemented with an energy regenerating mix (2 mM ATP, 50 μg/mL creatine kinase, and 20 mM phosphocreatine).

2.1.2 Caspase Assay

Xenopus egg extract caspase assays were performed using crude cytosolic extract, as described previously by our lab (Deming et al., 2004). Caspase-3 activity was measured spectrophotometrically by assessing the cleavage of the colorimetric substrate

Ac-DEVD-pNA. Briefly, 5 μL of crude cytosolic egg extract was removed and incubated in 85 μL of DEVDase buffer (50 mM Hepes (pH 7.5), 100 mM NaCl, 0.1% CHAPS, 10 mM DTT, 1 mM EDTA, 10% glycerol) and kept on ice. Following collection of all samples, 10 μl of the colorimetric peptide substrate, Ac-DEVD-pNA (200 mM final concentration; BIOMOL Research Labs, INC.), was added to each sample and incubated at 37°C for 30–60 minutes. Absorbance of the colorimetric product was measured at 405 nm using a Bio-Rad microplate reader (Bio-Rad Microplate Reader, Model 680). Absorbance data was analyzed using data-plotting software.

Caspase-2 activity assays were performed according to the BioVision caspase-2 colorimetric assay kit specifications (BioVision). Briefly, 10 μL of crude cytosolic egg extract was removed and incubated in 40 μL cell lysis buffer. All samples were diluted with 50 μL of 2X reaction buffer and then incubated with 10 μL of VDVAD-pNA (4mM final concentration) at 37°C for 60–120 minutes. Absorbance of the colorimetric product was measured at 405 nm using a Bio-Rad microplate reader and the absorbance data was analyzed using data-plotting software.

2.1.3 *In vitro* translated caspase-2 protein synthesis

^{35}S-labeled, *in vitro* translated, full-length caspase-2 proteins were synthesized using the TNT SP6 quick-coupled transcription/translation system (Promega). Briefly, 20 ng/μl of pSP64T *Xenopus* caspase-2 cDNA was added to rabbit reticulocyte lysate containing 0.4 mCi/mL ^{35}S-Translabel, 1x (minus-cysteine, minus-methionine) amino

acid mixture, and additional components in accordance with the manufacturer's protocol. The reactions were incubated at 30°C for one hour and then stored at -80°C until needed.

2.1.4 Analysis of *in vitro* translated caspase-2 protein processing

^{35}S-labeled, *in vitro* translated, full-length caspase-2 proteins were added to the extract at a 1:10 ratio. Samples of extract containing radiolabelled caspase-2 were removed over time, denatured by SDS sample buffer, resolved on SDS-PAGE. Proenzyme processing was assayed by autoradiography using a phosphorimager (Molecular Dynamics).

2.1.5 Fatty acid preparation and supplementation

20 mM fatty acid stock solutions were made by complexing sodium palmitate to 10% fatty-acid free bovine serum albumin (BSA). For palmitate, 74.24 mg of sodium palmitate (Sigma #P9767) was dissolved in 4 mL of water in a small glass beaker. The solution was heated on a hot plate, stirring constantly until the solution went clear. A cold mixture of 13.3 mL of 30% fatty acid free BSA (Sigma A-9205) and 20 mL of water was added to the fatty acid solution and brought to a final volume of 40 mL. The 20 mM stock solution was then filtered sterilized through a 0.45 μm filter, followed by filtration through a 0.20 μm filter. A control BSA stock solution was made by adding BSA to water only, followed by filtration as described above. Stock solutions were aliquoted and frozen at -20°C for later use. To test the effects of exogenous fatty acid

supplementation on extract apoptosis, BSA or BSA-conjugated palmitate was added to a final concentration of 4 mM after extract preparation. Extracts were then warmed to room temperature and caspase assays were performed.

2.1.6 NAD+/NADH nucleotide analysis

NAD+ and NADH levels were measured using the NAD+/NADH quantitation kit (BioVision). Briefly, extract samples were removed at the indicated time points a diluted 1:40 in NAD+/NADH extraction buffer. Samples were vortexed, spun through a 10kDa molecular weight cutoff filter, and then divided evenly. Half the sample was used for the measurement of total NAD+ and NADH (NADt) and the other half was used to measure NADH following decomposition of NAD+ by incubating at 60°C for 30 minutes. All samples were added to a 96-well plate and the cycling reaction was performed at room temperature for 2 hours. Absorbance of the colorimetric product was measured at 450 nm using a Bio-Rad microplate reader and the absorbance data was analyzed using data-plotting software.

2.1.7 Oxygen consumption analysis

Oxygen (O_2) consumption rates were measured using the Seahorse extracellular flux XF24 analyzer (Seahorse Biosciences). Briefly, freshly prepared egg extracts were added in triplicate to a 24-well plate and analyzed for 4 h. O_2 consumption rates were measured every 10 minutes and analyzed using the "(Level) Direct (Ksv)" method and data-plotting software.

2.2 Metabolomic profiling (performed in collaboration with Dr. Chris Newgard)

2.2.1 Sample preparation

Metabolic profiling was performed on both freshly prepared *Xenopus* egg extracts (fresh) and extracts incubated at room temperature for 3-4 h, but harvested prior to caspase activation (aged). 300 μL of extract was removed from fresh and aged samples followed by protein precipitation with either methanol (1200 μL) or acidified acetonitrile (750 μL ACN + 450 μL 1% formic acid). Samples were mixed well by vortex, spun down, and supernatants were removed immediately and stored at -80°C until sample analysis.

2.2.2 Amino acid and acylcarnitine analysis

Measurements of amino acid (AA) and acylcarnitine (AC) were made by flow-injection electrospray tandem mass spectrometry of their butyl and methyl esters, as described previously (An et al., 2004; Wu et al., 2004). Briefly, supernatants were supplemented with a mixture of internal standards and then evaporated under nitrogen using a SPE Dry-96 Jones chromatography apparatus. Residues were incubated with 3M MeOH-HCl (Supelco Inc.) or 3M BuOH-HCl (Regis Chemical Company), depending on whether methyl ester or butyl ester derivatives of the samples were to be prepared, followed by evaporation of the reagent under nitrogen. 200 μL methanol:water (85:15, v/v) was added to each sample and AA and AC analytes were measured by direct injection electrospray tandem mass spectrometry, using a Waters Acquity™ UPLC

system equipped with a TQ (triple quadrupole) detector and a data system controlled by MassLynx 4.1 operating system (Waters). AA were detected by positive neutral loss scans of 102, 119, and 161 Da, and AC profiles were generated using a precursor scan function (m/z 99 for methylesters or m/z 85 for butyl esters). The ratios of molecular signals to their respective internal standards were used to quantify the analytes. For several analytes, the lack of available analytical standards required reporting a dimensionless value based on the analyte to internal standard ratio.

2.2.3 Organic acid analysis

Organic acid (OA) analytes were extracted into ethyl acetate, dried and then converted to trimethyl silyl esters by *N,O*-bis (trimethylsilyl) trifluoroacetamide, with protection of α-keto groups by oximation with ethoxyamine hydrochloride. OA were analyzed by capillary gas chromatography/mass spectrometry (GC/MS) using a TRACE DSQ instrument (Thermo Electron Corporation). All MS analyses employed stable-isotope dilution with internal standards from Isotec (St. Louis, MO), Cambridge Isotope Laboratories (Andover, MA), and CDN Isotopes (Pointe-Claire, Quebec, Canada).

2.3 Mammalian cell techniques

2.3.1 Cell culture

Hek 293T, HeLa, HepG2, and AML12 cell lines were obtained from the American Type Culture Collection (ATCC). Hek 293T, HeLa, and HepG2cells were grown in high-glucose Dulbecco's Modified Eagle Medium (DMEM) supplemented with 10% fetal

bovine serum (FBS). AML12 cells were maintained according to the specifications of the ATCC in a 1:1 mixture of DMEM and Ham's F12 medium with 0.005 mg/ml insulin, 0.005 mg/ml transferrin, 5 ng/ml selenium, and 40 ng/ml dexamethasone and supplemented with 10% FBS. Hek 293T and HeLa cells were passaged via incubation in 0.05% Trypsin-EDTA, while HepG2 and AML12 cells were passaged via incubation in 0.25% Trypsin-EDTA. All cultures were maintained at 37°C with 5% CO_2.

2.3.2 siRNA transfection

For siRNA-mediated knockdown of caspase-2 in human cell lines (Hek 293T and HepG2), custom caspase-2 oligos targeting to the 3′ untranslated region of caspase-2 were ordered from Sigma-Aldrich. The sequence for the caspase-2 siRNA used was UGGAAGUAUUUGAGAGAGA[dT] [dT]. For siRNA-mediated knockdown of caspase-2 in murine cells (AML12), Smartpool siRNA targeting mouse caspase-2 (catalog number M-044184-00) and ON-TARGETplus control siRNA #1 (catalog number D-001810-01-05) were obtained from Dharmacon. RNAi reagents were transfected using RNAi Max (Invitrogen) following the manufacturer's protocol and media was changed 24 h post-transfection. siRNAs were transfected for 48 to 72 hours and cells were collected either by gentle scraping or using trypsinization. Collected cells were washed once in ice-cold PBS, pelleted by centrifugation, and then further processed or snap-frozen in liquid nitrogen for storage at -80°C.

2.3.3 Fatty acid preparation and treatments

In order to avoid the addition of organic solvents to the cell culture medium, solutions containing fatty acid sodium salts bound to albumin were prepared from stock solutions of the fatty acid sodium salt and media containing fatty acid-free BSA (2%). Fatty acid stock solutions were prepared by dissolving the fatty acid sodium salt in water at 70°C to a final concentration of 100 mmol/L. For example, palmitate solutions were made by dissolving 28 mg of sodium palmitate in 1 mL sterile H_2O and heating at 70°C until the solution was clear. This solution was then added to the cell culture media containing 2% fatty acid-free BSA and these solutions were used after filtration through 0.22-μm filters.

2.3.4 Caspase assay

Caspase-2 activity assays were performed according to the BioVision caspase-2 colorimetric assay kit specifications (BioVision).

2.3.5 Western blot analysis

For western blot analysis, mammalian cells were lysed in RIPA buffer (50 mM Tris Base, 1 mM EDTA, 1% NP-40, 0.25% NaDoC, 0.1% SDS, pH 7.4) with 100 mM PMSF and 5 μg/mL aprotinin and leupeptin. Lysates were centrifuged at 4°C for 15 minutes at 14,000 g and protein concentration of the supernatant was determined using the BioRad protein assay reagent. 50 μg of protein was separated on a 12% SDS PAGE gel and then transferred to PVDF membrane at 80 volts for 90 minutes. Membranes were blocked

with 5% non-fat dry milk in TBST (0.25 M Tris Base, 4.5% NaCl, pH 7.4, 0.1% Tween-20) for 30 minutes at room temperature and then incubated with primary antibodies (1:1,000 dilution in TBST) overnight at 4°C. The next day, membranes were washed 3 x 5 minutes with TBST and then incubated with infrared fluorescent secondary antibodies (1:10,000 dilution in TBST) for 1 hour at room temperature. Membranes were washed 3 x 5 minutes with TBST and then analyzed using the Li-Cor Odyssey Infrared Imaging System (Lincoln, NE). Antibodies used were anti-caspase-2 (polyclonal, Abcam (ab7979)); anti-caspase-2 (monoclonal, BD Transduction Laboratories (Clone G310-1248)); and anti-actin (polyclonal, Santa Cruz (I-19)). Secondary antibodies were IRDye® 800CW Goat (polyclonal) anti-mouse from Odyssey and Alexa Fluor ® 680 Goat anti-rabbit from Invitrogen.

2.3.6 Gel filtration chromatography

293T cells were treated with 2% BSA or 2% BSA + 1 mM palmitate for 18 hours before lysis by dounce homogenization in hypotonic lysis buffer (20 mM HEPES pH 7.5, 10 mM KCl, 1.5 mM $MgCl_2$, 1 mM EDTA, 1 mM EGTA, 1 mM DTT, and 5 μg/ml each aprotonin and leupeptin). Lysates were centrifuged at 4°C for 15 minutes at 16, 000 g and protein concentration of the supernatant was determined using the BioRad protein assay reagent. 500 μL of 8 mg/mL lysates were loaded onto a Superdex 200 column at a flow rate of 0.3 mL/minute. Fractions were collected and analyzed by western blotting.

2.3.7 Bimolecular fluorescence complementation

Caspase-2 bimolecular fluorescence complementation (BiFC) expression vectors were constructed by standard PCR cloning in a manner similar to the design by the Douglas R. Green Lab (Bouchier-Hayes et al., 2009). Briefly, caspase-2 prodomain (amino acids 1-169) was inserted into pBiFC-VN173 (Addgene, 22010) and pBiFC-VC155 (22011) at the N-termini of the split-venus fragments. Simultaneously, an N-terminal c-Myc tag was substituted for the pBiFC-VC155 HA tag. Flag-caspase-2-VN173 and c-Myc-caspase-2-VC155 fusions were then inserted into the MCSI and MCSII, respectively, of pTRE-Tight-BI (Clontech, 631068) for tetracycline-controlled expression.

To generate stable cell lines, the pTRE-Tight-BI caspase-2 BiFC construct was linearized and then co-transfected into HeLa Tet-Off cells (Clontech, 631156) with Clontech's Linear Hygromycin Marker (631625) at a 5:1 ratio. After 24 h, transfected cells were split to low confluency and then treated with 200ug/mL hygromycin for 2 weeks to select for clonal populations. Clones were harvested and then tested for protein expression and BiFC response.

Stable BiFC cells were maintained in DMEM supplemented with 10% FBS, 100ug/ml geneticin, 100ug/ml hygromycin, and 1ug/ml doxycycline (Dox). Prior to treatment, cells were washed twice with PBS to remove Dox and then switched to DMEM supplemented with 10% Tet-System Approved FBS (Clontech) for 24 h to allow expression of the caspase-2-BiFC fragments. Cells were then treated with 1mM

palmitate or 2% BSA for 24 h in the presence of 10μM of the pan caspase inhibitor Q-VD-OPh to prevent executioner caspase activation and cell death. To detect BiFC, cells were analyzed by flow cytometry.

2.3.8 Propidium ioidide staining

To assess cellular apoptosis, Hek293T, HepG2, and AML12 cells were analyzed for propidium iodide (PI) uptake. Cells were treated with 2% BSA or 2% BSA + fatty acids and then collected via trypsinization. Samples were washed once with 1X PBS and then resuspended in 1 μg/mL PI (dissolved in PBS), and kept on ice until analysis. Samples were protected from light and analyzed immediately at the Duke University flow cytometry core facility.

2.4 Mouse model techniques (performed in collaboration with Dr. Anna Mae Diehl)

2.4.1 Murine models

For caspase-2 expression studies, 5 male wild-type mice, strain C57BL/6, were obtained from Jackson Laboratories (Bar Harbor, ME). Animals were fed a methionine choline-deficient (MCD) diet (MP Biomedicals) for 8 weeks. Equal numbers of mice were fed standard rodent food (4.7 kcal/g: 13% calories as fat, 62% as carbohydrates and 24% as proteins) as a control.

For diet-induced disease studies, 10 caspase-2 knockout mice, strain B6.129S4-*Casp2*^{tm1Yuan}/J (stock no. 007899), and 10 wild-type mice, strain C57BL/6J (stock no. 000664), were purchased from Jackson Laboratories. Five animals per group were fed a

high fat (HF)/MCD diet or the same HF diet supplemented with methionine and choline (MP Biomedicals) for 8 weeks (4.5 kcal/g: 20% calories as fat, 58% as carbohydrates and 22% as proteins).

At the end of all treatments, mice were fasted for 6 hours and sacrificed. Livers were harvested and either formalin-fixed or snap frozen. All mice were maintained in a temperature- and light-controlled facility. Animals were age-matched and experiments were begun at approximately 8 weeks of age.

Animal care and procedures were approved by the Duke University Institutional Animal Care and fulfilled National Institutes for Health and Duke University IACUC requirements for humane animal care.

2.4.2 Hepatocyte isolation

Mouse hepatocytes were isolated from 3 caspase-$2^{-/-}$ mice and 3 control mice using *in situ* liver perfusion, collagenase digestion, and differential sedimentation (Berry and Phillips, 2000). Viability/purity was assessed by trypan blue exclusion. Hepatocytes were seeded onto plastic culture dishes in DMEM/F12 (Invitrogen) supplemented with 10% FBS, ITS (1:200; Invitrogen), dexamethasone (1 mM; Sigma) and antibiotics (Life Technologies). After 24 hours, cells were treated with similar media but supplemented with 2% BSA with or without 1 mM palmitate (Sigma #P9767) for 48 h.

2.4.3 Histopathological Analysis

Formalin-fixed, paraffin-embedded liver biopsies were cut into 5 μm serial sections and for immunohistochemistry, sections were deparafinized with xylene and rehydrated. Slides were incubated in 3% hydrogen peroxide/methanol and antigen retrieval was performed by heating in 10 mM sodium citrate (pH 6.0). Sections were blocked (X9090; Dako Envision) and incubated overnight at 4ºC with caspase-2 antibody, 1:3000 (Santa Cruz Biotechnology, sc-626R). Horseradish peroxidase (HRP)-conjugated IgG secondary antibody was used and antigens were demonstrated by diaminobenzidine (DAB) (Dako Envision, K3466). Tissue sections were counterstained with Aqua Hematoxylin-INNOVEX (Innovex Biosciences). Morphometric analysis with Metamorph Software (Molecular Devices Corporation) was performed for quantification.

2.4.4 TUNEL staining

Terminal deoxynucleotidyl transferase-mediated dUTP nick-end labeling (TUNEL) assay (Boehringer Mannheim, Mannheim, Germany) was performed according to the manufacturer's protocol.

2.4.5 Fibrosis staining

To assess liver fibrosis, sections were stained with Picrosirius red (Sigma) and counterstained with Weigert's haematoxylin (Polysciences, Inc). Quantification was done by morphometric analysis with Metamorph Software (Molecular Devices

Corporation) in sections that were randomly chosen (under x10 magnification, 20 fields each from sample)(Choi et al., 2006).

2.5 Reagents

2.5.1 Antibodies

Anti-caspase-2 (polyclonal, 1:1000) was purchased from Abcam (ab7979); anti-caspase-2 (monoclonal, 1:1000) from BD Transduction Laboratories (Clone G310-1248); and anti-actin (polyclonal, 1:1000) from Santa Cruz (I-19).

2.5.2 Additional Reagents

Aminooxyacetate (Sigma-Aldrich) was used at 10 mM. D-Glucose 6-phosphate sodium salt (Sigma-Aldrich) was used at 20 mM. Triacsin C, etomoxir, and fatty acid sodium salts were purchased from Sigma-Aldrich, with the exception of sodium palmitoleate, which was purchased from Nu-Chek Prep, Inc. Bovine Serum Albumin (Fraction V, heat shock, fatty acid ultra-free) was purchased from Roche, unless otherwise specified.

2.6 Statistics

The results represent the means ± S.E. of the mean. For mammalian cell studies, statistical significance was determined using a two-tailed Student's *t* test for three independent experiments, with significance at $p < 0.05$. For murine model experiments, significance was established using Student's test and Spearman correlation, with significance at $p < 0.05$.

3. Metabolic stress-induced activation of caspase-2 in *Xenopus laevis* egg extracts

This chapter appears in modified form in the Journal of Biological Chemistry. 2013 May 17; 288(20): 14463-75.

3.1 Introduction

As discussed in Chapter 1, apoptosis is a form of programmed cell death that is activated in response to pro-death stimuli. Characterized by rapid cellular fragmentation and phagocytosis, apoptosis eliminates damaged or unneeded cells, while preserving the integrity of the surrounding tissue. Disruption of the apoptotic program can result in inappropriate cell survival, enabling cancer cells to continue propagating despite the presence of pro-death signals from hypoxia, chemotherapeutics, and DNA damage. In contrast, too much apoptosis can result in tissue dysfunction and is often a hallmark of chronic degenerative disorders.

Apoptosis is characterized by the activation of a group of cysteine proteases known as caspases. Caspases, which are divided into two classes, initiator or executioner, based on their position in the apoptotic hierarchy, dismantle the cell in an orderly, energy-dependent manner. Caspase-2, which is the most evolutionarily conserved caspase, functions as an initiator and activates the intrinsic apoptotic cascade. The prevailing model is that caspase-2, once activated, cleaves the BH3-only protein Bid to generate truncated Bid (tBid), which activates Bax to promote mitochondrial

cytochrome *c* release. Despite being one of the most conserved caspases, the regulation and precise functions of caspase-2 have remained somewhat unclear.

Physiologically, the role of caspase-2 is not entirely clear. The only overt developmental phenotype in the caspase-2 KO mouse was an overabundance of oocytes, suggesting a central role for caspase-2 in controlling oocyte cell death (Bergeron et al., 1998). Extending our understanding of the role of caspase-2 in oocytes, our laboratory has used *Xenopus laevis* oocytes and eggs to study the metabolic regulation and activation of caspase-2. Previously, our lab demonstrated that incubation of *Xenopus* egg extract at room temperature leads to activation of the apoptotic cascade via caspase-2 and that caspase-2 is required to execute apoptosis in this system (Nutt et al., 2005). Moreover, it was discovered that caspase-2 activation occurred only after specific metabolic changes (e.g., depletion of NADPH) and was regulated through suppressive binding of the small, acidic protein 14-3-3ζ (Nutt et al., 2009). Release of 14-3-3ζ, and thus activation of caspase-2, could be blocked by supplementing the extract with metabolites leading to NADPH production, either through malic enzyme or the pentose phosphate pathway (Nutt et al., 2009; Nutt et al., 2005). Based in part on these observations, it was hypothesized that the activation of caspase-2 in this system was regulated by cellular metabolic status, whereby extract incubation results in nutrient starvation, loss of 14-3-3ζ binding, and activation of caspase-2.

Recently, our lab demonstrated that the removal of 14-3-3ζ from caspase-2 is regulated via changes in 14-3-3ζ protein acetylation. Interestingly, we found that the metabolically-sensitive deacetylase, sirtuin 1 (Sirt1), is a direct regulator of 14-3-3ζ acetylation and demonstrated that a loss of Sirt1 activity in aging *Xenopus* egg extracts contributes to 14-3-3ζ release and activation of caspase-2 (Andersen et al., 2011). As an NAD+ dependent deacetylase, Sirt1 activity can be regulated by the availability of this metabolite co-factor. As such, Sirt1 is typically activated by starvation conditions (i.e., increased NAD+/NADH ratios), rather than nutrient excess. Given this, we were surprised to observe a decrease in Sirt1 activity upon extract incubation, when nutrient levels were thought to be decreasing. Given the inconsistencies between Sirt1 activity and the extract starvation hypothesis, we became interested in investigating the metabolic stress triggering caspase-2 activation in our cell-free extract system.

In an attempt to more thoroughly understand the metabolic changes underlying caspase-2 activation in this setting, we performed metabolomic profiling on egg extract at time points leading up to caspase-2 activation. Consistent with previous studies on egg metabolism, we observed a robust decrease in aspartate upon extract incubation, indicating the usage of amino acids as a fuel source in this cell type (Dworkin and Dworkin-Rastl, 1990, 1991). The most notable change preceding caspase-2 activation, however, was a marked increase in LCFA metabolites. Metabolic treatments that suppress caspase-2 activation specifically block the observed increase in LCFA

metabolites, suggesting that a buildup of lipids may engage the apoptotic pathway/caspase-2 in *Xenopus* egg extract. Moreover, the caspase-suppressive effect of such metabolic treatments could be overridden by supplementing the extract with the saturated LCFA, palmitate. Together, these data provide evidence that lipid accumulation plays a critical role in triggering caspase-2 activation and apoptosis in *Xenopus* egg extract.

3.2 Results

Active caspase-2 has been shown to trigger mitochondrial cytochrome c release in a number of settings and our lab has shown that it is required upstream of mitochondria to induce cell-free apoptosis in the *Xenopus* egg extract system (Nutt et al., 2005). We initially observed that activation of caspase-2 in this setting could be blocked by supplementing egg extract with metabolic intermediates, suggesting that metabolic changes preceded caspase-2 activation. However, the precise nature of these metabolic changes was unclear. Thus, in an effort to understand the mechanisms underlying caspase-2 activation, we performed metabolomics on *Xenopus* egg extract, comparing fresh, unaged extract to extract incubated at room temperature for several hours and harvested just prior to caspase-2 activation (aged). All samples were analyzed for amino acid, organic acid, and acylcarnitine changes.

3.2.1 Amino acid metabolism and the accumulation of succinate precede caspase activation in *Xenopus* egg extract

In agreement with previous studies on egg metabolism, the two most abundant amino acids in *Xenopus* egg extract were aspartate and glutamate (Shiokawa et al., 1986; Vastag et al., 2011). Interestingly, upon room temperature incubation of the extract, we observed a notable decrease in aspartate, along with a corresponding increase in alanine, with very little change in the other amino acids profiled (Figure 3.1A). These changes are likely occurring via transamination reactions, whereby aspartate is converted to oxaloacetate and pyruvate is converted to alanine via transamination of α-ketoglutarate and glutamate, respectively (Figure 3.1B). The decrease in aspartate suggests that this amino acid is likely serving as a carbon source to support extract metabolism, as has previously been shown in intact *Xenopus* eggs (Dworkin and Dworkin-Rastl, 1990). We also observed changes in the organic acid profile of fresh and aged extracts, including an increase in both pyruvate and lactate following extract incubation (Figure 3.1C). In contrast, intermediates of the TCA cycle decreased moderately, with the exception of succinate, which showed significant accumulation (Figure 3.1C).

Increased levels of succinate are often observed under conditions in which the electron transport chain (ETC) is inhibited (Folbergrova´ et al., 1974; Kotarsky et al., 2012; Wiesner et al., 1989). Hypoxia, or the lack of oxygen, has been shown to inhibit ETC function, as well as result in increased levels of succinate. Interestingly, under hypoxic conditions, the formation of succinate has been shown to be coupled to amino

acid utilization, specifically that of aspartate and glutamate (Hochachka et al., 1975; Taegtmeyer, 1978). Given the similarities between these observations and our data, we wanted to determine whether there were any other metabolic changes that might indicate a loss of mitochondrial respiration.

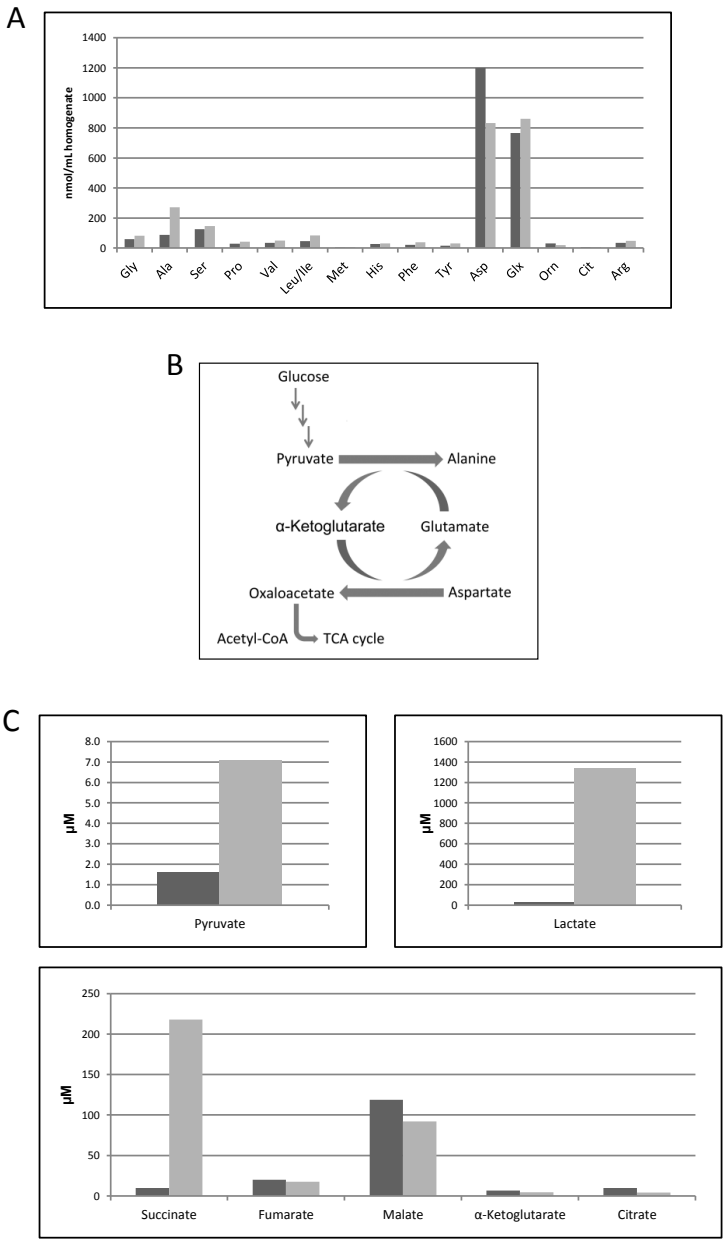

Figure 3.1: Amino acid metabolism and the accumulation of succinate precede caspase activation in *Xenopus* egg extract.

Figure 3.1: A. Freshly prepared *Xenopus* egg extract (dark gray bars) or extract incubated at room temperature for 4 h (light gray bars) was analyzed for amino acid profile following protein precipitation. B. Figure of carbon flux via transamination reactions in the egg extract. C. Egg extracts, treated as in panel A, were analyzed for organic acids.

3.2.2 The absence of mitochondrial respiration in incubated extract results in the accumulation of long-chain acylcarnitines and a decrease in the NAD+/NADH ratio

Since ETC inhibition results in a block in beta-oxidation and a decrease in the NAD+/NADH ratio, we examined both the lipid profile and redox status of incubated extract. Consistent with a lack of ETC function, we observed an accumulation of multiple long-chain acylcarnitines, reflective of the long-chain acyl-CoA pools, as well as a progressive decrease in the NAD+/NADH ratio following extract incubation (Figure 3.2A and 3.2B). Furthermore, since changes in the cytosolic levels of NADH and NAD+ are reflected in the balance between lactate and pyruvate, we assessed the lactate/pyruvate ratio and found that the ratio was significantly increased from 17.3 to 188.7 in aged extracts, supporting the observed accumulation of NADH.

Given these data, we wanted to more directly assess whether the extract might be experiencing hypoxia. Rather than assessing the dissolved oxygen content in the extract as a readout of hypoxia, as it would be hard to define what dissolved oxygen percentage in egg extracts would result in hypoxic phenotypes, we chose to more directly assess mitochondrial respiration. Using the Seahorse Bioscience XF24 extracellular flux analyzer, we monitored the O_2 consumption rate of aging egg extracts for 4 h. Indeed, extracts showed little O_2 consumption, with respiration going to virtually zero over time (Figure 3.2C).

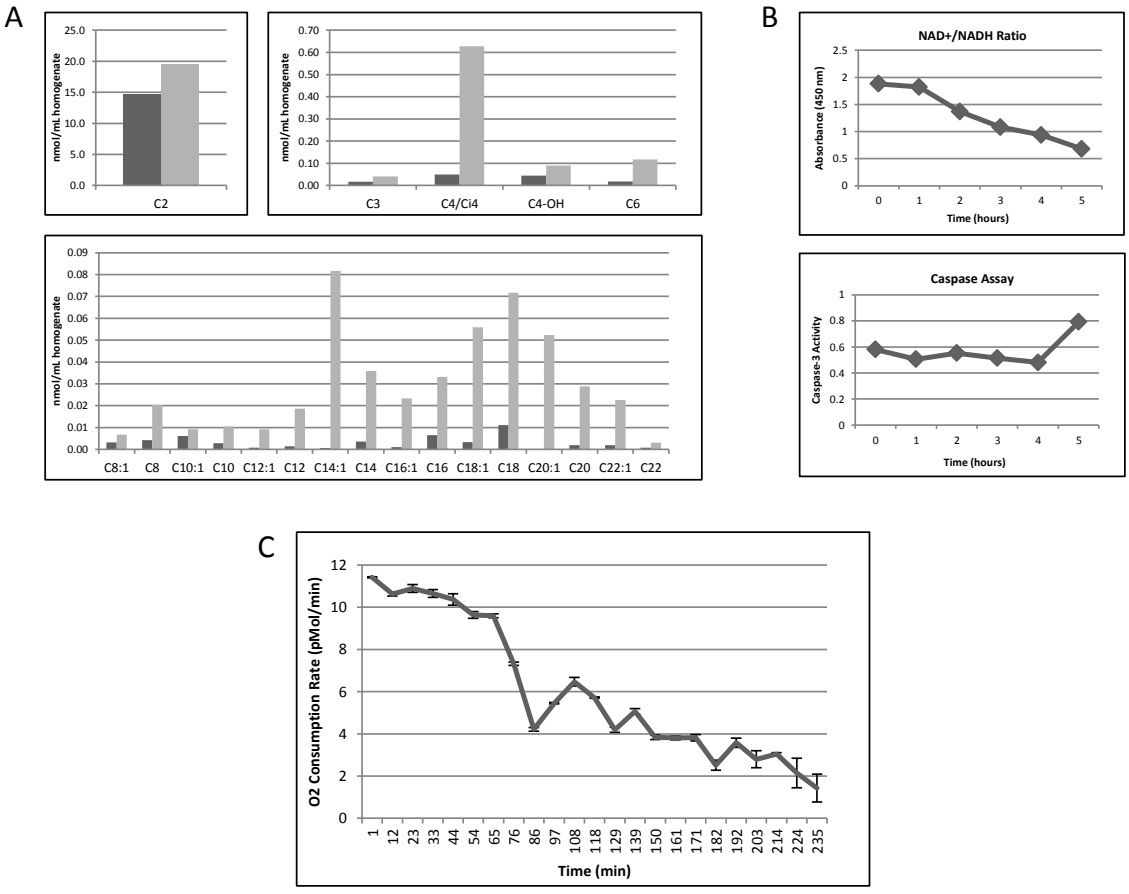

Figure 3.2: The absence of mitochondrial respiration results in the accumulation of long-chain acylcarnitines and a decrease in the NAD+/NADH ratio

Figure 3.2: A. Freshly prepared *Xenopus* egg extract (dark gray bars) or extract incubated at room temperature for 4 h (light gray bars) was analyzed for acylcarnitines. B. Samples of egg extract were collected at the indicated times and analyzed for NAD+/NADH ratio changes by spectrophotometric color change (kit supplied by BioVision). The same samples were used to measure caspase-3 activity using the caspase substrate Ac-DEVD-*p*NA. Substrate cleavage was measured spectrophotometrically at 405 nm. F. The O_2 consumption rate of aging egg extracts was monitored for 4 h using the Seahorse Bioscience XF24 extracellular flux analyzer. The results represent the means ± S.D. of three technical replicates.

Together, these data suggest that the observed metabolic changes are linked to inhibited mitochondrial respiration, including the formation of succinate from the amino acid aspartate, the build-up of NADH, and the accumulation of LCFA metabolites (acylcarnitines/acyl-CoAs). Since we knew from previous studies that the activation of caspase-2 and downstream apoptotic events could be blocked in this system by supplementing the extract with metabolites (Nutt et al., 2005), we postulated that one of these underlying metabolic changes might be triggering caspase-2 activation.

3.2.3 Inhibition of amino acid transamination by aminooxyacetate blocks caspase activation

Given the potential dependence of the egg extract on amino acid utilization and previous observations that hypoxia-induced succinate formation could be abrogated by inhibiting transamination reactions (Taegtmeyer, 1978), we wanted to determine whether the inhibition of transaminase activity would affect caspase activation in the extract. To test this, we treated the extract with the general transaminase inhibitor, aminooxyacetate (AOA), and monitored caspase-2 activity via cleavage of the model substrate, VDVAD-pNA, over time. Surprisingly, the inhibition of transaminase activity suppressed VDVAD cleavage activity in the extract (Figure 3.3A; note that the absolute time course of caspase activation varies from extract to extract, but the relative rates of caspase activation following different treatments is constant). We also found that caspase-2 processing, which occurs following caspase-2 activation as a means to stabilize the active dimeric protease, was suppressed by AOA treatment (Figure 3.3B).

Furthermore, downstream activation of the executioner caspase, caspase-3, was also suppressed by AOA treatment (Figure 3.3C), suggesting that the loss of amino acid transamination can suppress caspase activation in the extract.

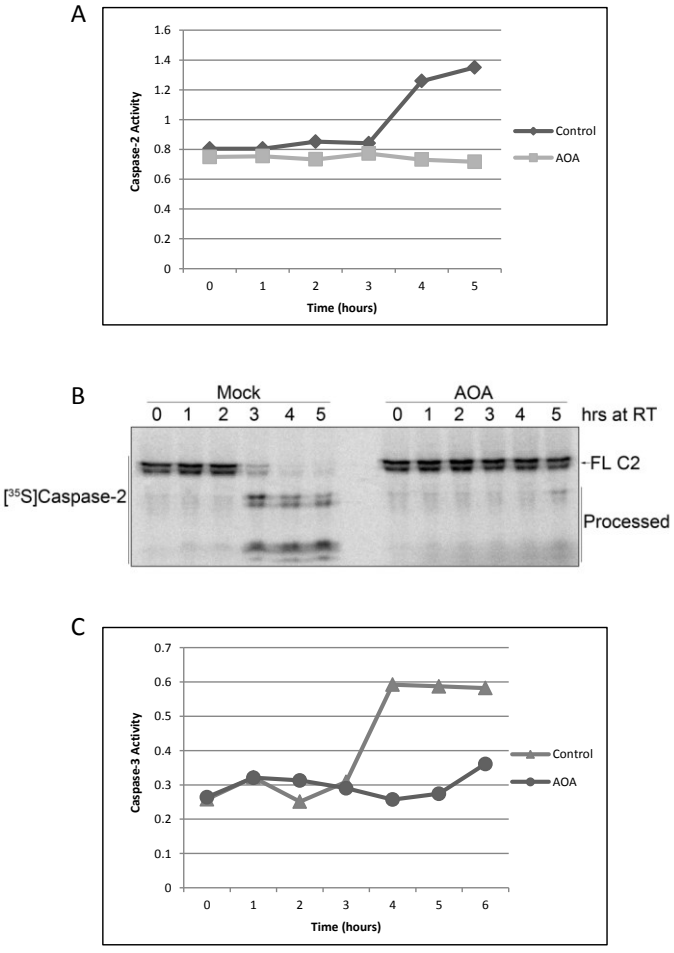

Figure 3.3: The inhibition of amino acid transamination by aminooxyacetate blocks caspase activation

Figure 3.3: A. Egg extracts supplemented with AOA (10 mM) or buffer were analyzed for caspase-2 activity at the indicated time points using the BioVision caspase-2 colorimetric assay kit B. ^{35}S-labeled caspase-2 was incubated in AOA- or mock-treated extracts and samples were resolved by SDS-PAGE/phosphorimager. C. Egg extracts, treated as in panel A, were analyzed for caspase-3 activity at the indicated time points using the caspase substrate Ac-DEVD-*p*NA.

3.2.4 Metabolic treatments that block caspase activation also prevent the accumulation of long-chain fatty acid metabolites

In an effort to understand how inhibition of amino acid transamination can suppress caspase activation, we compared the metabolic profiles of extracts treated with and without AOA. AOA caused aspartate and alanine levels to return to basal levels in aged extracts, consistent with our suggestion that the changes in these amino acids are driven by aspartate transamination and further catabolism (Figure 3.4A). Treatment of extracts with AOA caused a substantial decrease in TCA cycle intermediates and blocked the accumulation of succinate, suggesting that aspartate plays an important role in energy metabolism, particularly in supplying the extract with anaplerotic substrates (Figure 3.4B). Glycolytic activity appeared to be unaffected by transaminase inhibition, as demonstrated by the accumulation of pyruvate and lactate in the presence of AOA (Figure 3.4B). Strikingly, we observed a decrease in long-chain acylcarnitine accumulation in the presence of AOA, suggesting that inhibition of amino acid transamination was able to suppress the increase in LCFA metabolites (Figure 3.4C).

Since LCFA accumulation may be linked to redox changes in the extract (i.e. high levels of NADH inhibits the oxidation of LCFAs), we assessed whether AOA could modify the observed decrease in the NAD+/NADH ratio preceding caspase activation. As shown in Figure 3.4D, AOA was able to delay the decrease in NAD+/NADH, supporting the notion that acylcarnitine accumulation may be resulting from increasing levels of NADH, which can then feedback to inhibit beta-oxidation. Although we

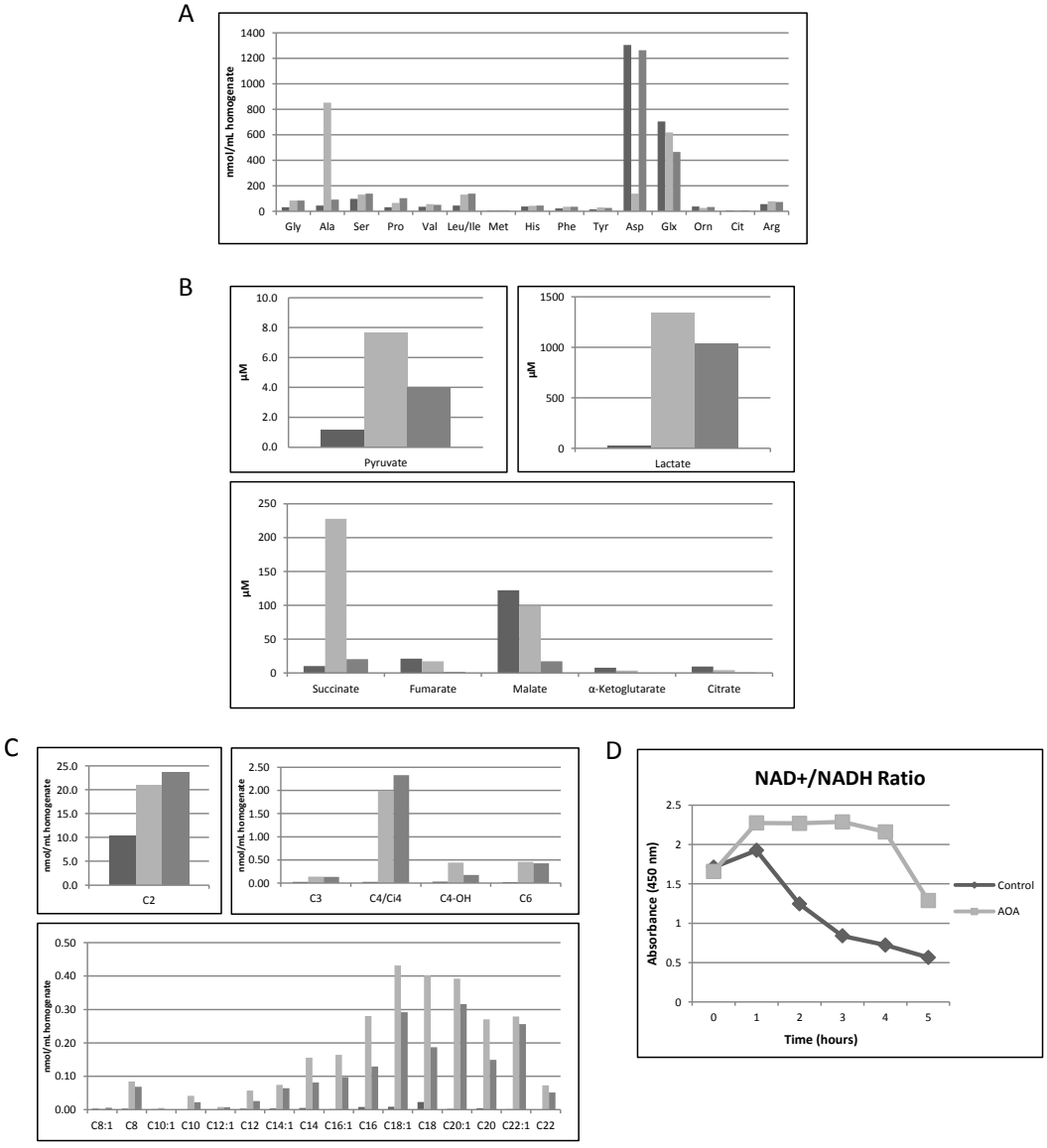

Figure 3.4: Metabolic treatments that block caspase activation also prevent the accumulation of long-chain fatty acid metabolites

Figure 3.4: A. Amino acid profiling was performed on egg extracts immediately following preparation (black bars) or after room temperature incubation in the absence (light gray bars) or presence of 10 mM AOA (dark gray bars). B. Egg extracts, treated as in panel A, were analyzed for organic acids. C. Egg extracts, treated as in panel A, were analyzed for acylcarnitines. D. Samples of egg extract treated with and without 10 mM AOA were collected at the indicated times and analyzed for NAD+/NADH ratio changes by spectrophotometric color change (kit supplied by BioVision).

observed a delay of NADH accumulation in AOA-treated extracts, the lactate/pyruvate ratio was still increased in comparison to fresh extracts. Although there may be some effect of AOA on cytosolic NAD+/NADH pools, as there is delayed accumulation of lactate (Figure 3.4B), it is more likely that AOA is blocking the mitochondrial shift of NAD+ to NADH by inhibiting TCA cycle flux. This, in turn, may delay the decrease in total NAD+/NADH.

3.2.5 Supplementation of the extract with glucose-6-phosphate blocks long-chain fatty acid metabolite accumulation

The ability of AOA to both suppress caspase activation and block significant metabolic changes in the extract, including the catabolism of aspartate and the accumulation of long-chain acylcarnitines, suggests that one or both of these metabolic alterations is necessary for caspase-2 activation (and thus downstream caspase-3 activation) in this system. To further investigate this, we examined the metabolic profile of egg extract treated with a pentose phosphate pathway intermediate, G6P, which we have previously shown can suppress caspase-2 activation in this setting (Nutt et al., 2005). While G6P was able to block the accumulation of long-chain acylcarnitines, it was unable to suppress aspartate transamination and succinate formation (Figure 3.5 A and B). Collectively, these data suggest that the accumulation of LCFA metabolites is the pivotal metabolic change underlying caspase-2 activation. Moreover, the previously observed protection from apoptosis in egg extracts conferred by G6P may be mediated, at least in part, by preventing the accumulation of LCFAs. These findings raise the

interesting possibility that caspase-2 is, more broadly, an initiator caspase for lipoapoptosis.

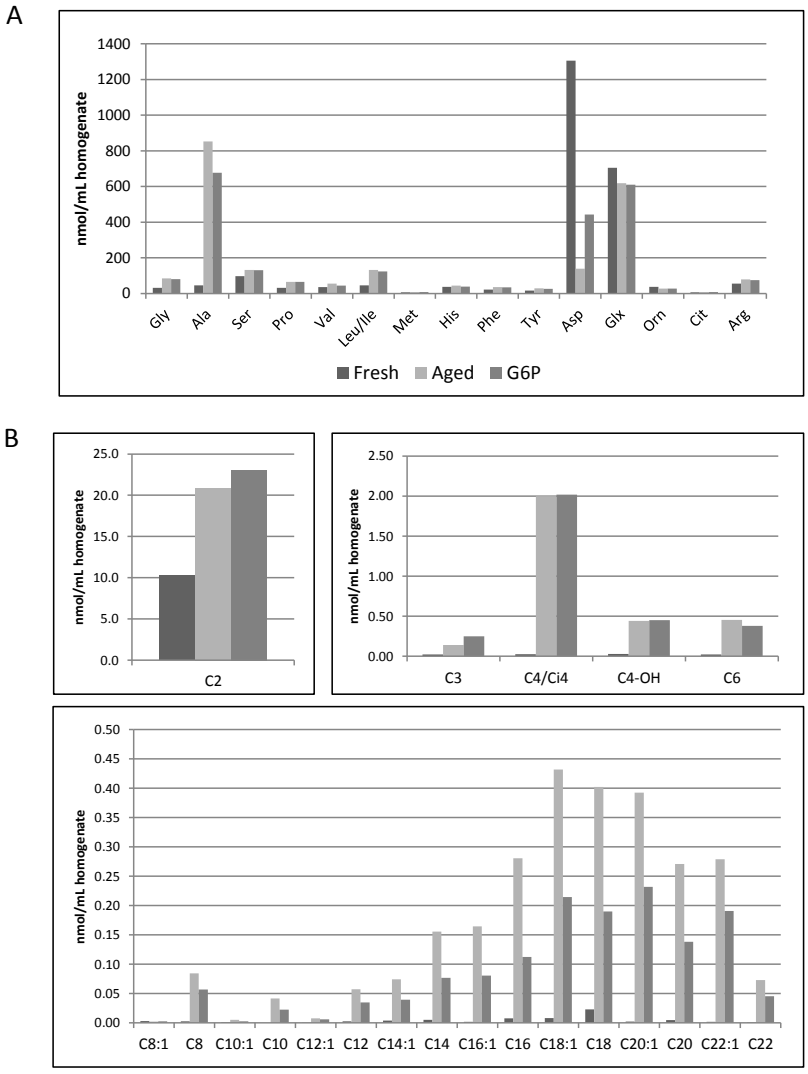

Figure 3.5: Supplementation of the extract with glucose-6-phosphate blocks long-chain fatty acid metabolite accumulation

Figure 3.5: A. Amino acid profiling was performed on egg extracts immediately following preparation (black bars) or after room temperature incubation in the absence (light gray bars) or presence of 20 mM G6P (dark gray bars). B. Egg extracts, treated as in panel A, were analyzed for acylcarnitines.

3.2.6 Palmitate accelerates caspase activation and overrides the protective effect of AOA

Given the data above and previous publications implicating LCFAs in cell death, we were interested in determining whether treatment of the extract with an LCFA that increased in abundance with extract incubation (palmitate, C16) might accelerate caspase activation (Arici et al., 2003; de Vries et al., 1997; El-Assaad et al., 2003; Lupi et al., 2002; Malhi et al., 2006) (Figure 3.2A and 3.4C). To test this, we treated extracts with BSA-conjugated palmitate or BSA as a control and performed a caspase activity assay. As shown in Figure 3.6A, palmitate accelerated caspase-3 activation, and this acceleration could be blocked by the addition of the anti-apoptotic protein, B cell lymphoma XL (Bcl-xL), suggesting that palmitate is specifically engaging the apoptotic pathway upstream of mitochondria. Furthermore, we verified that the pro-apoptotic effect of palmitate was being exerted at the level of caspase-2 by monitoring enzyme processing and found that it was, indeed, accelerated after palmitate treatment (Figure 3.6B). Together, these data suggest that palmitate can promote caspase-2 activation. Therefore, we reasoned that if AOA was simply blocking the buildup of LCFAs as a means to inhibit apoptosis, then palmitate treatment should be able to override the protective effect of AOA. Indeed, palmitate addition was able to overcome the anti-apoptotic effect of AOA, accelerating caspase activation (Figure 3.6C). Taken together, these data suggest that an over-abundance of LCFA metabolites can engage the

apoptotic pathway in *Xenopus* egg extract, where caspase-2 is the critical initiator caspase.

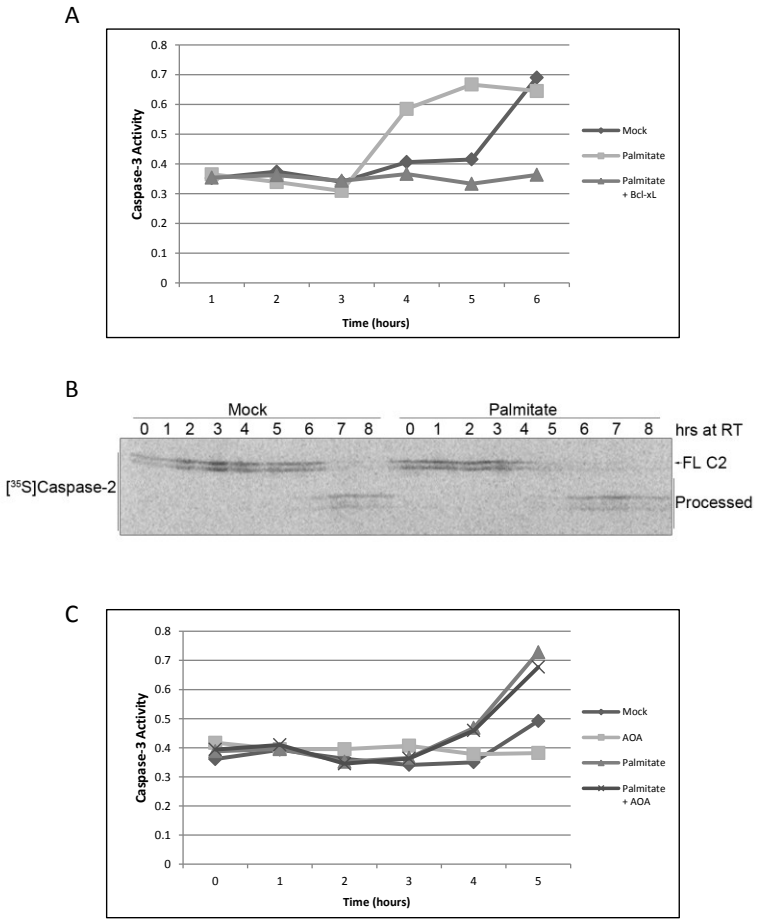

Figure 3.6: Palmitate accelerates caspase activation and overrides the protective effect of AOA

Figure 3.6: A. Mock-treated (BSA) or palmitate-treated (BSA-conjugated palmitate, 4 mM) egg extracts were incubated in the presence or absence of Bcl-xL and analyzed for caspase-3 activity at the indicated time points. Caspase-3 activity was assessed using the caspase substrate Ac-DEVD-*p*NA and cleavage was measured spectrophotometrically at 405 nm. B. ^{35}S-labeled caspase-2 was incubated in mock- or palmitate-treated extracts and samples were resolved by SDS-PAGE/phosphorimager. C. Egg extracts were incubated with combinations of palmitate (4 mM) and AOA (10 mM) and caspase-3 activity was assessed using the caspase substrate Ac-DEVD-*p*NA.

3.3 Discussion

Metabolomic profiling of *Xenopus* egg extract revealed that a clear metabolic signature emerges upon extract incubation. Prior to caspase activation, several robust metabolic changes occur, including: a decrease in aspartate with a corresponding increase in alanine, an accumulation of succinate, and a buildup of multiple long-chain acylcarnitines (which reflect the cognate acyl CoA pools). While the utilization of amino acids as a carbon source was not surprising, as this had been previously observed in *Xenopus* eggs (Dworkin and Dworkin-Rastl, 1990), the buildup of succinate and LCFA metabolites was not anticipated- especially given our previous hypothesis that extract incubation results in nutrient depletion/starvation that leads to caspase-2 activation. Conventionally, cells starved of nutrients (i.e., glucose) activate fatty acid oxidation as a means to supply the mitochondria with reducing power, or NADH, for making ATP. Therefore, if the extract was, indeed, suffering from nutrient depletion, we would expect to see a decrease in fatty acid levels following extract incubation, which is not what was observed. Rather, the metabolic profile of incubated extract showed striking similarity to previous studies of hypoxic systems. Thus, we measured mitochondrial oxygen consumption and discovered that extracts fail to consume oxygen during the assessed room-temperature incubation period. Based on previous findings and the lack of oxygen consumption in this system, we speculate that the observed metabolic changes are the result of inhibited electron transport chain activity, as described below.

3.3.1 Potential mechanism of extract metabolism

A decrease in electron transport chain function or activity would ultimately result in a significant decline of oxidized electron carriers (i.e., NAD+). Furthermore, succinate dehydrogenase, which is the only enzyme which participates in both the electron transport chain and the TCA cycle, would be unable to efficiently oxidize succinate, leading to its accumulation and a decrease in TCA cycle flux. A block in succinate metabolism would cause a decrease in anaplerotic substrates, mainly oxaloacetate, resulting in the accumulation of acetyl-CoA (C2) and pyruvate, as we have observed in our metabolomics analysis.

Furthermore, the inefficient flux of substrates through the TCA cycle without the ability to efficiently regenerate NAD+ via the ETC would likely lead to a redox imbalance, resulting in increased levels of NADH. A significant shift in the redox status of the extract from an oxidized state (NAD+ > NADH) to a reduced state (NADH > NAD+) will inhibit glycolytic flux. Thus, to compensate for such redox changes, pyruvate will be converted to lactate, in a process which will regenerate NAD+ from NADH. The large increase in lactate that occurs upon extract incubation is likely driven by NADH accumulation. Furthermore, we speculate that the buildup of LCFA metabolites are also linked to increasing levels of NADH which, in combination with high levels of acetyl-CoA, can feedback and inhibit beta-oxidation, as well as stimulate the process of fatty acid elongation.

3.3.2 Inhibition of extract metabolism and long-chain fatty acid stress

Our metabolomics data were not consistent with a cellular starvation profile, making it unlikely that the stress triggering caspase-2 activation was nutrient depletion. As such, we aimed to further understand extract metabolic flux in order to determine which of the observed metabolic changes were triggering caspase-2 activation. Using an inhibitor of aminotransferases, we demonstrated that blocking the use of aspartate as a carbon source could delay caspase-2 activation in aging extracts. This effect did not appear to be due to amino acid stabilization, but rather appeared to be the result of a decrease in LCFA accumulation.

The ability of AOA to suppress buildup of LCFA metabolites is likely mediated by its ability to block carbon flux through the TCA cycle, which helps to stabilize early changes in NAD+/NADH (i.e. slowing the decrease we observed in untreated extracts, Figure 3D), allowing continued beta-oxidation. AOA treatment was unable to restore mitochondrial respiration (data not shown), making it more likely that AOA is delaying NADH accumulation, rather than accelerating NAD+ regeneration. Palmitate treatment can likely override the suppressive effect of AOA by accelerating lipid overload. The ability of palmitate to both accelerate caspase activation and override the suppressive effect of AOA suggests that an excess of saturated LCFAs can trigger the activation of caspase-2.

3.3.3 The extract as a model of metabolic stress

While the *Xenopus* egg extract metabolomics may not reflect the metabolic state of unstressed mammalian cells, the observed metabolic signature was very reminiscent of several pathophysiological disease states. For example, succinate and LCFA accumulations have been observed in hypoxia, diabetes, and cancer and have been attributed to an imbalance between energy demand and food/oxygen supply (Goldberg et al., 1966; Sadagopan et al., 2007; Selak et al., 2005). Although the underlying cause of such an imbalance remains uncertain in the extract, we hypothesized that the critical metabolic stress triggering caspase-2 activation and apoptosis was the accumulation of LCFAs.

The accumulation of LCFA metabolites in hypoxia has been appreciated for some time. Interestingly, caspase-2 has recently gained recognition as a regulator of hypoxia-induced toxicity in several models, including porcine proximal tubule cells (LLC-PK1), human neuroblastoma cells (SK-N-MC), and neonatal mouse brains (Carlsson et al., 2011; Carlsson et al., 2012; Nakagawa et al., 2008; Park et al., 2007b). Given our data, it seems likely that the buildup of LCFA metabolites in these hypoxic settings may be triggering the activation of caspase-2. Interestingly, these studies highlight a potential correlation between lipid accumulations and caspase-2 activation which warrants further investigation. Looking specifically at whether caspase-2 can function as a more general initiator of cell death in response to lipotoxicity, specifically in mammalian cell

systems, is an important step toward furthering this research. Chapter 4 of this thesis discusses our work to address this question.

4. Caspase-2 as an initiator of lipid-induced cell death in mammalian cells

This chapter appears in modified form in the Journal of Biological Chemistry. 2013 May 17; 288(20): 14463-75.

4.1 Introduction

During periods of overnutrition, LCFAs accumulate to levels that exceed the storage capacity of adipose tissue. As a result, LCFAs become elevated in the plasma, resulting in increased import and storage of these molecules in non-adipose tissues (Frayn, 2002; Kusminski et al., 2009; Lewis et al., 2002). The over-accumulation of lipids in non-adipose tissues can be toxic, resulting in chronic cellular dysfunction and ultimately apoptotic cell death, a process more generally referred to as lipoapoptosis. Lipoapoptosis can profoundly compromise tissue function and appears to be an underlying cause of diseases associated with metabolic syndrome (Cazanave and Gores, 2010; Kusminski et al., 2009; Listenberger and Schaffer, 2002; Unger et al., 2010).

LCFA-induced lipoapoptosis has been shown to occur in many cell types, including hepatocytes, cardiomyocytes, proximal tubule cells in the kidney, and islet beta cells in the pancreas (Arici et al., 2003; de Vries et al., 1997; El-Assaad et al., 2003; Malhi et al., 2006). These cells, which specifically undergo apoptosis in response to treatment with saturated fatty acids, display several characteristic features of the intrinsic apoptotic pathway, including mitochondrial permeabilization, cytochrome c

release, and effector caspase activation (Unger and Orci, 2002). While the role of the intrinsic apoptotic pathway has been well-established in LCFA-induced apoptosis, the core apoptotic machinery engaged by toxic concentrations of saturated LCFAs upstream of the mitochondria has not yet been revealed.

Accumulating evidence suggests that caspase-2 is not universally engaged by apoptotic signaling pathways but instead responds to specific cellular stressors. Given our findings on caspase-2 activation and LCFA accumulation in *Xenopus* egg extract, we aimed to determine whether caspase-2 might be mediating lipoapoptosis in mammalian somatic cells. Our data suggest that caspase-2 is, indeed, activated upon LCFA treatment in mammalian cells. We demonstrate that caspase-2 shifts into a high molecular weight complex following the treatment of HEK 293T cells with the saturated LCFA, palmitate. Down-regulation of caspase-2 also significantly impairs cell death induced by saturated LCFA treatment, suggesting that caspase-2 activates LCFA-induced lipoapoptosis in mammalian cells. These findings, which reveal a conserved, critical role for caspase-2 as an initiator of lipoapoptosis, may have clinical implications for the treatment of diseases associated with lipid accumulations.

4.2 Results

4.2.1 Caspase-2 plays a central role in mediating lipotoxicity in 293T cells

With ample evidence showing that palmitate can induce cell death in a number of mammalian cell lines at physiologically relevant concentrations (0.03-1.0 mM)

(Furstova et al., 2008), we first wished to extend our observations from the *Xenopus* egg extract system and determine whether caspase-2 is activated in lipid-induced apoptosis in mammalian cells. To test this, we transfected HEK 293T cells with siRNA directed against caspase-2 or a scrambled siRNA control and then treated cells with 1 mM palmitate for 18 h. We then assessed caspase-2 activation via cleavage of the model substrate, VDVAD-pNA, and found that the enzymatic activity of caspase-2 was increased following palmitate treatment (Figure 4.1A). The observed increase in activity appears to be specific to caspase-2, as knockdown of the protease was able to block the palmitate-induced increase in substrate cleavage (Figure 4.1A). Additionally, since caspase-2 has been shown to undergo proteolytic processing following its activation in mammalian cells, we also monitored caspase-2 cleavage via western blot and found that caspase-2 was processed following palmitate treatment (Figure 4.1B).

As an initiator caspase, caspase-2 is activated following the binding of adaptor proteins, which facilitate its oligomerization into a high molecular weight (HMW) complex. Therefore, to determine whether caspase-2 is engaged and activated in this fashion during LCFA-induced apoptosis, we performed gel filtration analysis on HEK 293T cell extracts derived from control and palmitate-treated cells. While we consistently observed trace amounts of caspase-2 in the HMW fractions of mock treated cells, in palmitate treated cells, recruitment of caspase-2 into HMW fractions was robust

(Figure 4.1C). We further confirmed that the caspase-2 present in these HMW fractions was, indeed, enzymatically active by performing a caspase-2 activity assay (Figure 4.1C).

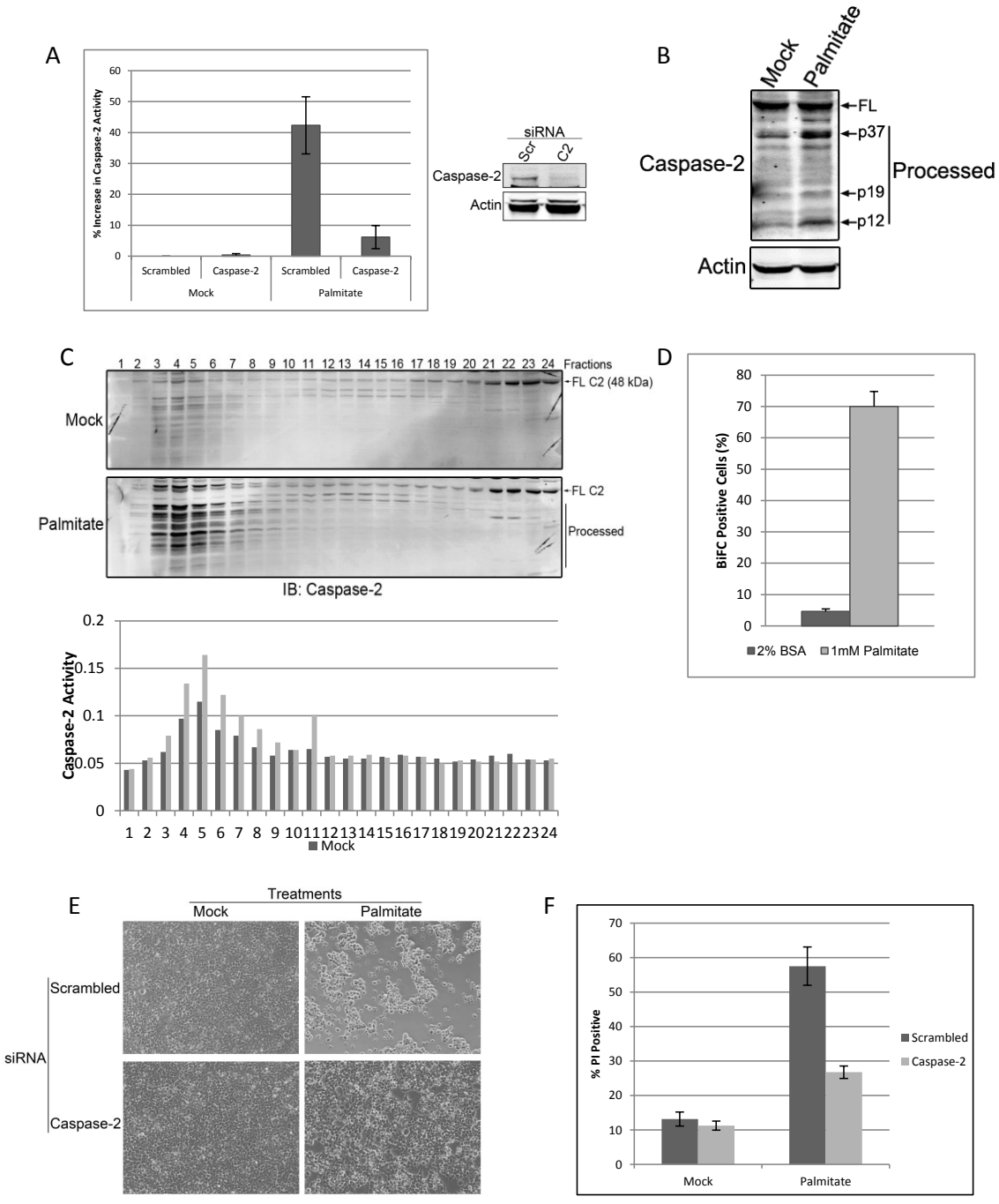

Figure 4.1: Caspase-2 plays a central role in mediating lipotoxicity in 293T cells

Figure 4.1: A. 293T cells were transfected with 50 nM scrambled or C2-targeted siRNA. At 48 h post-transfection, cells were mock-treated with BSA or treated with 1 mM palmitate for 18 h and caspase-2 activity was assessed using the BioVision caspase-2 colorimetric assay kit. Knockdown efficiency was determined by immunoblot. The results represent the means ± S.E. for percent increase in activity compared to siCTRL, mock-treated samples for three independent experiments. Statistical significance was determined using a two-tailed Student's *t* test. *, $p < 0.05$ *versus* control. B. 293T cells were treated with BSA or palmitate for 24 h and immunoblotted for caspase-2 and actin. The top caspase-2 panel is a short exposure (to show changes in full length caspase-2 levels) and the bottom caspase-2 panel is a long exposure (to reveal the p12 fragment). C. 293T cells were treated with BSA or palmitate for 18 hours before lysis by dounce homogenization in hypotonic lysis buffer. Cell lysates were separated on a Superdex 200 column and relevant fractions were immunoblotted for caspase-2. Full length caspase-2 and processed caspase-2 are indicated. Fractions were also tested for caspase-2 activity by assessing cleavage of the caspase-2 model substrate, VDVAD-*p*NA, as part of the BioVision caspase-2 colorimetric assay kit. D. 293T cells were treated as in panel A and at 24 h post-treatment, phase-contrast images were captured on an EVOS FL digital inverted microscope. E. 293T cells were treated as in panel A and cell death was measured 24 h after palmitate treatment by propidium iodide staining and flow cytometric analysis. The results represent the means ± S.E. for four independent experiments.

Finally, we confirmed the activation of caspase-2 *in situ* following palmitate treatment using BiFC (Bouchier-Hayes et al., 2009). To do this, we stably transfected HeLa Tet-Off cells with a construct encoding a caspase-2 prodomain fused to each of the split Venus proteins and under the control of a central, bidirectional tetracycline-response element (TRE). These cells were allowed to express the constructs in DMEM supplemented with tetracycline-free FBS for 24 h and then treated with 1 mM palmitate and 10 μM Q-VD-OPh, to block downstream executioner caspase activation, for 24 h. As expected, we obtained a strong BiFC signal with caspase-2/prodomain constructs following palmitate treatment (Figure 4.1D), suggesting that caspase-2 is dimerized and activated in mammalian cells in response to palmitate-induced lipotoxicity.

We next wanted to determine whether caspase-2 was required for lipoapoptosis in mammalian cells. To do this, we treated scrambled or caspase-2 knockdown cells with palmitate for 24 h before measuring cell viability. Palmitate induced significant cell death in the scrambled control cells, whereas caspase-2 deficient cells were protected from apoptosis, as shown by maintenance of cell density over 24 h of treatment (Figure 4.1E). We further quantified cell death by PI staining and found that down-regulation of caspase-2 could significantly block palmitate-induced cell death in 293T cells (Figure 4.1F), suggesting that caspase-2 is required for lipoapoptosis in these cells.

4.2.2 Caspase-2 mediates saturated fatty acid-induced lipoapoptosis via acyl-CoA cytotoxicity

Previous studies have shown in multiple cell types that only saturated LCFAs exert cytotoxic effects(de Vries et al., 1997; Furstova et al., 2008; Hardy et al., 2003; Kim et al., 2008; Mei et al., 2011; Staiger et al., 2006). Therefore, we wanted to determine whether caspase-2 was required for cell death induced by other saturated LCFAs, as well as validate that only saturated LCFAs could induce apoptosis. To do this, we treated scrambled or caspase-2 knockdown cells with either the monounsaturated fatty acids, palmitoleate (16:1) and oleate (18:1), or the saturated fatty acids, palmitate (16:0) and stearate (18:0). Cell death was assessed by PI staining. As expected, only saturated fatty acids induced prominent cell death (Figure 4.2A). Interestingly, the loss of caspase-2 was able to significantly protect against cell death induced by both saturated LCFAs, suggesting that caspase-2 can function as a general initiator of cell death in saturated

fatty acid-induced lipotoxicity (Figure 4.2A). Moreover, since the combination of saturated and unsaturated fatty acids has been shown to reduce the cytotoxic effects of saturated fatty acids (Coll et al., 2008; Gao et al., 2009; Listenberger et al., 2003; Miller et al., 2005; Yuzefovych et al., 2010), we also assessed whether oleate addition could protect against caspase-2 mediated cell death induced by palmitate or stearate. Consistent with previous findings, oleate was able to block cell death induced by these saturated fatty acids, suggesting that it could prevent palmitate and stearate-induced caspase-2 activation (Figure 4.2A).

In some settings, the ability of oleate to suppress the cytotoxic effects of saturated LCFAs has been attributed to its ability to decrease palmitate-induced ROS and ceramide generation (Hu et al., 2011; Yuzefovych et al., 2010). To test whether the cell death induced by palmitate in 293T cells was being mediated by either of these two stresses, we treated cells with the ROS scavenger, N-acetyl cysteine (NAC), or the serine palmitoyltransferase inhibitor, myriocin, to inhibit ceramide synthesis. Neither treatment was able to suppress cell death induced by palmitate, suggesting that palmitate-induced apoptosis is not dependent on ROS or ceramide formation in these cells (data not shown). Thus, in order to more thoroughly understand how palmitate exerts its pro-apoptotic effects on caspase-2, we tested whether metabolism of palmitate to its corresponding long-chain acyl-CoA and/or long-chain acylcarnitine form was required to induce caspase-2 activity and cell death.

Activation of other caspases, specifically caspase-3, -7, and -8, has been shown to be directly induced by palmitoylcarnitine in vitro (Mutomba et al., 2000), and therefore, it seemed possible that caspase-2 was being activated by palmitate via its conversion to palmitoylcarnitine. To explore this possibility, we treated cells with the long-chain acyl-CoA synthetase inhibitor, triacsin C, and the carnitine palmitoyltransferase I inhibitor, etomoxir, and assessed caspase-2 activity following palmitate treatment. Triacsin C, which inhibits the formation of palmitoyl-CoA, significantly prevented palmitate-induced caspase-2 activation, while etomoxir, which inhibits the formation of palmitoylcarnitine, had no significant effect (Figure 4.2B). Consistent with caspase-2 being the initiator of apoptosis in this setting, triacsin C was also able to inhibit cell death, while etomoxir failed to show any effect (Figure 4.2C). Together, these data suggest that while palmitate activation via acyl-CoA formation was essential to induce caspase-2 activation, palmitoylcarnitine formation was not required. It is important to note that in our experimental setting, triacsin C revealed cytotoxic effects in the absence of palmitate, which may be due to a reduction of basal intracellular acyl-CoA concentrations below a level necessary for cell viability (data not shown).

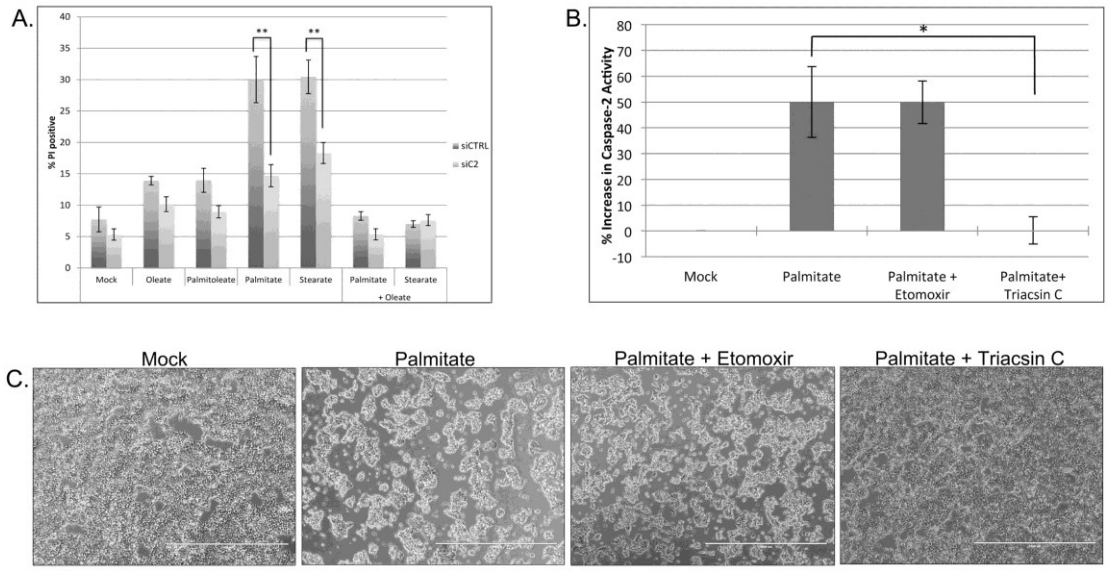

Figure 4.2 Caspase-2 mediates saturated fatty acid-induced lipoapoptosis via acyl-CoA cytotoxicity

Figure 4.2: A. 293T cells were transfected with 50 nM scrambled or C2-targeted siRNA. At 48 h post-transfection, cells were mock-treated with BSA or 1 mM fatty acids and cell death was measured 24 h post-treatment by propidium iodide staining and flow cytometric analysis. The results represent the means ± S.E. for four independent experiments. Statistical significance was determined using a two-tailed Student's *t* test. **, $p < 0.01$ *versus* control. B. 293T cells were mock-treated with BSA or treated with 1 mM palmitate with or without 200 μM etomoxir or 5 μM triacsin C. At 24 h post-treatment, phase-contrast images were captured on an EVOS FL digital inverted microscope. C. 293T cells were treated as in B. At 18 h post-treatment, caspase-2 activity was assessed using the BioVision caspase-2 colorimetric assay kit. The results represent the means ± S.E. for percent increase in activity compared to mock-treated samples for four independent experiments. Statistical significance was determined using a two-tailed Student's *t* test. *, $p < 0.05$ *versus* control.

4.2.3 Caspase-2 is required for LCFA-induced apoptosis in hepatocytes

To more thoroughly evaluate the importance of caspase-2 in lipoapoptosis, we examined the role of caspase-2 in saturated LCFA-induced hepatocyte cell death. Accumulating evidence suggests that lipoapoptosis plays an important role in the

pathogenesis of NAFLD, specifically in the progression from NAFLD to the more advanced state of liver disease, NASH (Cazanave and Gores, 2010; Ibrahim et al., 2011).

To determine whether caspase-2 is required for lipoapoptosis in hepatocytes, we tested whether knockdown of caspase-2 in HepG2 cells would protect against palmitate-induced cell death. As shown in Figure 4.3A, down-regulation of caspase-2 was able to dampen cell death, as determined by PI staining. While the decrease in cell death is clear upon caspase-2 knockdown, it is not complete. The lack of a larger effect may be due to residual caspase-2, as we were only able to achieve partial knockdown in this cell type (Figure 4.3A). Therefore, we also investigated whether caspase-2 was activated in normal mouse hepatocytes (AML12 cells) following palmitate treatment by measuring VDVAD-pNA cleavage. We observed a 45% increase in enzymatic activity, consistent with a role for caspase-2 in palmitate-induced cell death in hepatocytes (data not shown). To determine whether caspase-2 was required for cell death, we pre-treated AML12 cells with scrambled or caspase-2 siRNA and assessed cell death after palmitate treatment. Down-regulation of caspase-2 significantly inhibited cell death in these normal mouse hepatocytes (Figure 4.3B), revealing a conserved, critical role for caspase-2 in saturated LCFA-induced cell death.

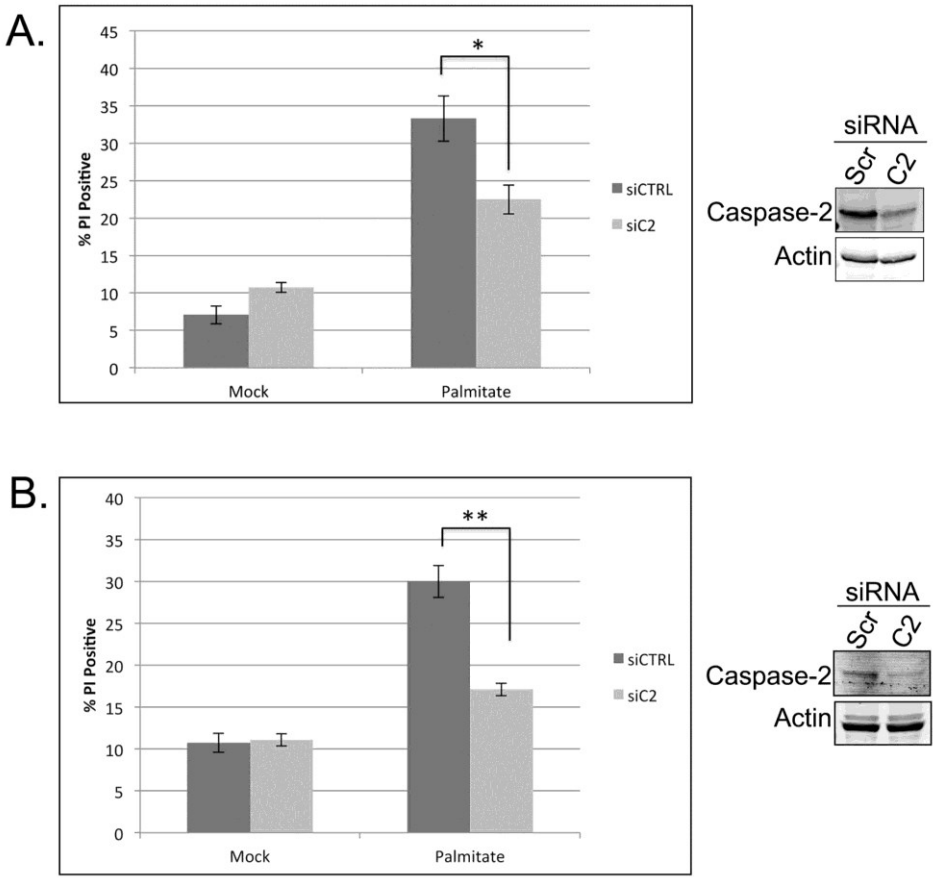

Figure 4.3: Caspase-2 is required for LCFA-induced apoptosis in hepatocytes

Figure 4.3: A. HepG2 cells were transfected with 50 nM scrambled or C2-targeted siRNA. At 48 h post-transfection, cells were mock-treated with BSA or treated with 0.7 mM palmitate for 24 h and cell death was measured by propidium iodide staining and flow cytometric analysis. Knockdown efficiency was determined by immunoblot. B. AML12 cells were treated with 50 nM scrambled or mouse caspase-2-targeted smartpool siRNA. At 48 h post-transfection, cells were mock- or palmitate-treated and analyzed for cell death as in panel A. Knockdown efficiency was determined by immunoblot. The results represent the means ± S.E. for three or more independent experiments. Statistical significance was determined using a two-tailed Student's *t* test. *, $p < 0.05$ *versus* control. **, $p < 0.01$ *versus* control.

4.3 Discussion

With the prevalence of obesity and metabolic syndrome rising sharply world-wide, it has become increasingly important to define the molecular mechanisms underlying the pathogenesis and progression of diseases associated with lipid-induced cytotoxicity. Cardiovascular disease, type-2 diabetes mellitus (T2DM), and NAFLD have all recently gained recognition as diseases that are exacerbated by lipoapoptosis (Cazanave and Gores, 2010; Kusminski et al., 2009; Listenberger and Schaffer, 2002). In this chapter, we demonstrated that caspase-2 is not only engaged, but makes a significant contribution to saturated LCFA-induced cell death both in 293T cells and several hepatocyte cell lines. Together, these findings reveal a previously unknown role for caspase-2 as an initiator caspase and provide a missing link in the signaling pathways functioning upstream of the mitochondria in lipoapoptosis. The relevance and potential impact of this novel finding are discussed below.

4.3.1 Caspase-2 initiates saturated LCFA-induced lipoapoptosis in 293T cells

Our data suggest that caspase-2 is activated in 293T cells following palmitate treatment as shown by both cleavage of the preferred caspase-2 substrate, VDVAD, as well as proteolytic processing of the caspase-2 proenzyme. We also verified that caspase-2 is activated following palmitate treatment by recruitment to a HMW complex and that only the HMW fractions containing caspase-2 exhibited enzymatic VDVAD cleavage activity. Caspase-2 was also required for full activation of palmitate-induced

cell death, specifically in HEK 293T cells. Delving further into caspase-2-induced lipotoxicity, we confirmed that only saturated fatty acids induced cell death and that this cell death was dependent on caspase-2. Interestingly, as has previously been observed in other cells types, palmitate-induced cytotoxicity was not dependent on ROS, ceramides, or oxidative LCFA catabolism in our 293T cell model (Hardy et al., 2003; Kim et al., 2008; Staiger et al., 2006). Rather, the activation of palmitate via acyl-CoA formation was required to induce cell death. Understanding how saturated LCFAs and their respective acyl-CoA derivatives induce caspase-2 is the focus of ongoing studies.

Currently, we are testing the hypothesis that conversion of palmitoyl-CoA into lysophosphatidylcholine (LPC), which functions as a minor phospholipid in cellular membranes, could be mediating caspase-2 activation by acting as the toxic effector. Recent findings in the literature have suggested that palmitate toxicity is exerted indirectly via generation of the lipid metabolite, LPC (Han et al., 2008; Kakisaka et al., 2012). Upregulation of LPC can change plasma membrane lipid dynamics and activate apoptosis by influencing signaling pathways via the activation of JNK, GSK-3, and/or PKC (Kakisaka et al., 2012; Masamune et al., 2001). Although the data have not been included in this thesis, we have preliminary data which suggests that caspase-2 is necessary for cell death in response to LPC. Caspase-2 knockdown cells treated with LPC are significantly protected from cell death, suggesting that LPC may be the downstream effector of palmitate that activates caspase-2 and results in apoptosis. The

conversion of phosphatidylcholine to lysophosphatidylcholine downstream of palmitate treatment can be inhibited by blocking the activity of phospholipase A2. Future studies will evaluate whether inhibition of this lipase can protect against palmitate-induced cell death, which would suggest that the formation of saturated LPC from palmitate is responsible for caspase-2 activation in our cell model of lipoapoptosis.

4.3.2 Implications for hepatocyte lipoapoptosis and NAFLD/NASH

In addition to HEK 293T cells, we also showed that caspase-2 could function as an initiator of cell death in hepatocytes treated with saturated LCFAs. This hepatocyte finding is of particular interest, as lipoapoptosis plays a critical role in the development and progression of NAFLD, the most common form of chronic liver disease in both children and adults in the United States (Browning et al., 2004; Wieckowska and Feldstein, 2005). Furthermore, lipoapoptosis is the key molecular event driving the progression of NAFLD to the more advanced state of liver disease, NASH (Feldstein et al., 2003; Witek et al., 2009). Hepatocyte apoptosis is significantly increased in patients with NASH and there are currently no effective therapies to halt NAFLD progression. Thus, insight into the molecular mediators of lipoapoptosis may be useful in developing effective therapies for this syndrome.

NAFLD is characterized by an increased level of lipids in the liver, which in overweight or obese patients, often results from the elevated levels of LCFAs in the blood. The retention of lipids in the liver causes the over-accumulation of cellular lipids

in hepatocyte (steatosis) and triggers lipoapoptosis. Hepatocyte apoptosis results in the activation of HSCs and the phagocytosis of apoptotic bodies by HSCs induces their production of type I collagen (Canbay et al., 2003). Collagen secretion by HSCs enhances liver fibrogenesis and the development of cirrhosis, both of which correlate with negative patient outcomes (Malhi et al., 2010).

Since apoptosis plays such an important role in NAFLD progression, inhibition of apoptosis has been proposed as a useful therapeutic strategy. In support of this idea, recent studies performed in both humans and mice have shown moderate success of pan-caspase inhibitors on NAFLD/NASH symptoms (Ratziu et al., 2012; Witek et al., 2009). Excitingly, our data suggest that an inhibitor which more specifically targets caspase-2 may enhance the effectiveness of caspase-targeted therapies. The loss of this apical initiator caspase doesn't appear to compromise viability in a knock-out setting and thus, caspase-2 is an attractive therapeutic target for both blocking apoptosis and maintaining mitochondrial integrity in NAFLD/NASH.

Finally, while our studies have focused on the importance of caspase-2 in hepatocyte lipoapoptosis, there are several additional settings where caspase-2 may be relevant in lipoapoptotic therapies, including cardiomyocytes in the heart, proximal tubule cells in the kidney, and islet beta cells in the pancreas. Future studies will evaluate the physiological relevance of caspase-2 in these lipotoxicity settings.

5. Caspase-2 as a regulator of hepatocyte lipoapoptosis in a mouse model of nonalcoholic fatty liver disease

Please note that these experiments were performed in collaboration with Dr. Anna Mae Diehl's laboratory at Duke University.

5.1 Introduction

Lipoapoptosis, which is the cell death induced by lipids, plays an important role in the pathogenesis of liver disease. Overnutrition, inactivity, and environment are all factors which can increase body fat content, putting you at a higher risk for lipid-induced toxicity. For example, in the case of the liver, increasing body fat content results in fatty deposits in the liver, and the development of NAFLD. NAFLD affects 25% of the population here in the United States, although many believe this to be an underestimation, as patients usually have little to no symptoms often only complaining of fatigue or mild abdominal discomfort. NAFLD is typically diagnosed by abnormal liver enzyme levels during routine blood tests, which may indicate that there is a decrease in liver function.

Failure of patients to reduce elevated lipid levels can result in lipid-induced apoptosis of hepatocytes and progression of NAFLD to the more advance state of liver disease, known as NASH. A major difference between NAFLD and NASH is the extent of hepatocyte apoptosis, which is significantly increased in the case of NASH (Feldstein et al., 2003). NASH is also characterized by fibrosis of the liver and can often lead to an

irreversible state of liver cirrhosis. Once patients have progressed to this state, there is little that can be done to reverse liver damage. Therefore, it is important to find a therapeutic entry point for halting the progression of NAFLD prior to liver fibrogenesis.

Hepatocellular apoptosis has been demonstrated to be a critical mechanism driving the progression of NAFLD, as well as many other liver diseases, including viral hepatitis, Wilson's disease, cholestatic liver disease, and alcohol-induced injury (Galle and Krammer, 1998). Importantly, the apoptosis observed in these settings has been shown to contribute significantly to liver fibrosis through the activation of HSCs, which upon transformation to a myofibroblastic state begin secreting type I collagen (collagen 1α1)(Canbay et al., 2003). Type I collagen makes up the majority of fibrosis observed in liver cirrhosis. Since lipid-induced apoptosis is a critical mediator of fibrosis in NASH, it is important to understand the apoptotic signaling events controlling cell death in order to find a potential therapeutic target.

The most frequently employed animal model of NASH is a nutritional restriction of methionine and choline in the diets of mice. This model, which is known as the methionine-choline deficient diet, or MCD, induces severe liver steatosis by inhibiting the secretion of VLDL from the liver. The retention of fatty acids in the liver results in physiological changes similar to those observed in human NASH, including aminotransferase elevations, steatosis, hepatocyte apoptosis, and fibrosis (Hebbard and George, 2011; Larter and Yeh, 2008; Takahashi et al., 2012). Although the MCD diet is

easy to use, there are some concerns about its efficacy, as the metabolic profile induced by the diet goes against what has been observed in individuals with fatty liver. For example, mice fed an MCD diet show significant weight loss, peripheral insulin sensitivity, and low insulin and leptin levels (Larter et al., 2008; Leclercq et al., 2007; Nagasawa et al., 2006; Rinella and Green, 2004). Patients with NASH most often have symptoms of the metabolic syndrome, including excessive weight gain, insulin insensitivity, and high blood pressure. As such, this diet should only be used to assess changes in liver injury and repair pathways and should not be used to evaluate the impact of experimental treatments on metabolic status.

Since lipid-induced apoptosis is critical for NASH and our data suggest that caspase-2 can function an initiator of lipoapoptosis, we hypothesized that caspase-2 might play a role in the development of NASH *in vivo*. To test this hypothesis, we assayed caspase-2 protein levels following MCD diet feeding as well as determined whether caspase-2 KO mice were protected from hepatocyte lipoapoptosis and fibrosis. Interestingly, we found that caspase-2 protein levels were significantly increased after an 8-week MCD diet regimen. This was consistent with what we observed in NASH patients, where caspase-2 was also upregulated. Moreover, we show that caspase-2 KO mice fed the MCD diet are protected from apoptosis, HSC activation, and fibrosis. These data provide substantial evidence that caspase-2 is a potential therapeutic target for both blocking apoptosis and preventing fibrogenesis in NAFLD/NASH.

5.2 Results

5.2.1 Caspase-2 KO hepatocytes are protected from palmitate-induced apoptosis *in vitro*

In Chapter 4, we discussed our data demonstrating that caspase-2 is a critical regulator of lipoapoptosis in mammalian cells. We aimed to further validate these findings using a genetic model of caspase-2 depletion and thus, we tested whether caspase-2 KO hepatocytes were protected against a palmitate-induced death *in vitro*. To do this, we isolated hepatocytes from WT or caspase-2 KO C57BL/6J mice and treated them with 2% BSA or 2% BSA + 1 mM palmitate for 48 h. We then assayed hepatocyte viability using the cell counting kit-8 and found that while only 35% of WT hepatocytes were alive at 48 h, 58% of KO hepatocytes survived (Figure 5.1). The observed increase in KO viability further supports a role for caspase-2 in hepatocyte lipoapoptosis.

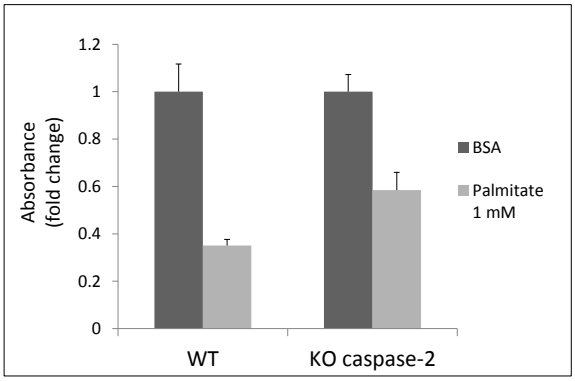

Figure 5.1: Caspase-2 KO hepatocytes are protected from palmitate-induced apoptosis *in vitro*

Figure 5.1: Hepatocytes isolated from WT or caspase-2 KO mice were treated with BSA or 1 mM palmitate for 48 h and viability was measured using the cell counting kit-8.

5.2.2 Caspase-2 is significantly upregulated in patients with NASH and in mice fed an MCD diet

Given the importance of hepatocyte lipoapoptosis in the pathogenesis of NAFLD, we aimed to extend our novel findings from mammalian cells and determine whether caspase-2 plays an important role in mediating lipoapoptosis in a mouse model of NAFLD. To test this, we placed WT mice on either a control or MCD diet for 8-weeks. We then harvested the livers and assessed caspase-2 protein levels using both immunohistochemistry and western blotting. Unexpectedly, we observed a significant increase in hepatic caspase-2 staining in mice fed the MCD diet as compared to the control (Figure 5.2 A). These results were further confirmed by immunoblot, which showed that administration of the MCD diet caused significant upregulation of caspase-2 protein (Figure 5.2 B). Given this, we were curious whether caspase-2 protein levels would be significantly upregulated in patients with NASH. To examine this, we took tissue sections from NASH patients and stained for caspase-2. Encouragingly, caspase-2 was upregulated in the livers of patients with NASH just as it was in mice fed an MCD diet (Figure 5.2 C). Taken together, these data demonstrate that caspase-2 is significantly upreglated in NASH and suggests that it may make a significant contribution to the hepatocyte lipoapoptosis observed in this disease.

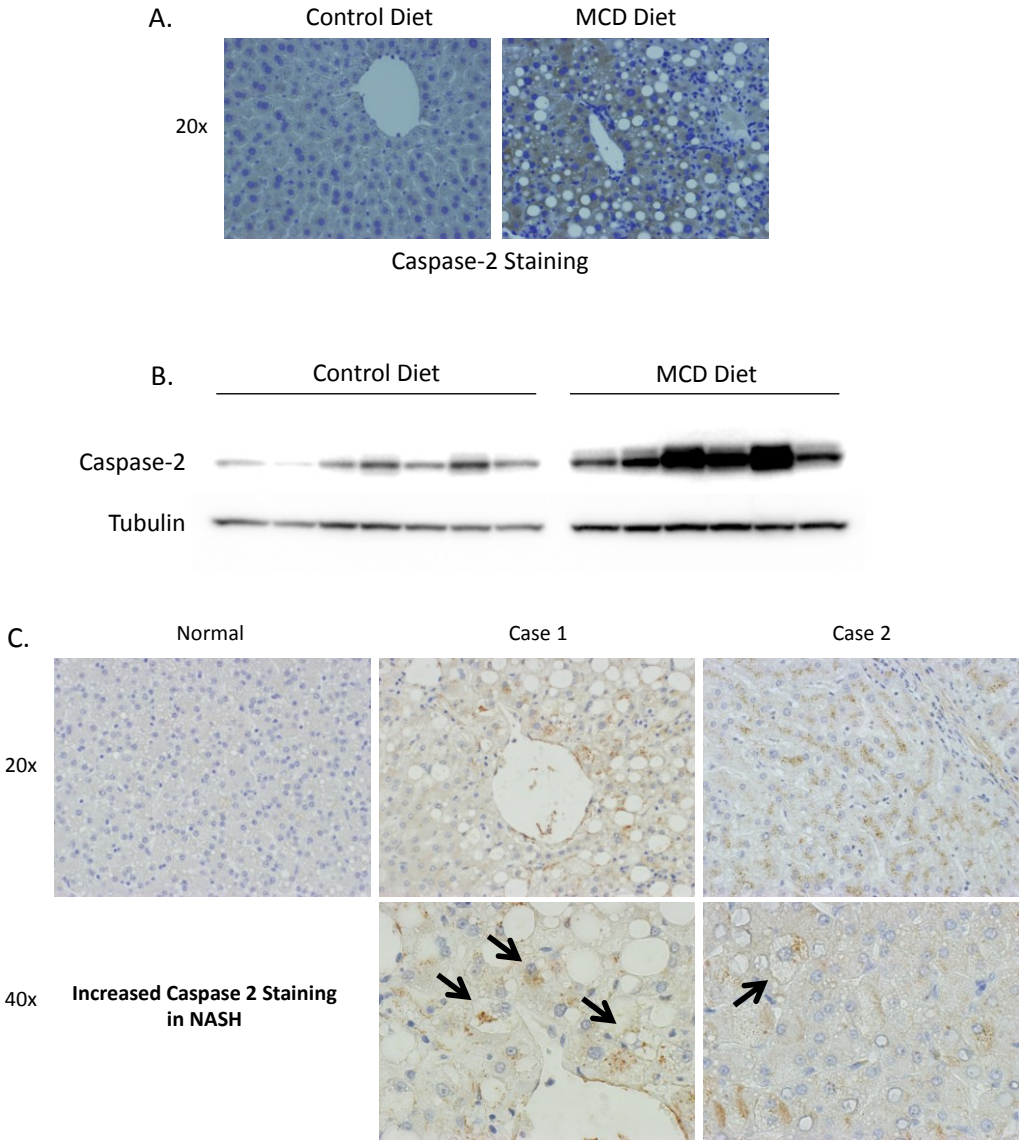

Figure 5.2: Caspase-2 is significantly upregulated in patients with NASH and in mice fed an MCD diet

Figure 5.2: A. Representative caspase-2 immunohistochemistry (brown) in livers from WT mice fed regular chow (control diet) or methionine choline deficient (MCD) diet. B. Western blot analysis of livers of WT mice fed as above. Each lane represents an individual mouse sample and tubulin serves as a loading control. C. Representative caspase-2 immunohistochemistry (brown) in a healthy human liver and in NASH patients (n= 2).

5.2.3 Caspase-2 KO mice are protected from MCD diet-induced apoptosis and fibrosis

After observing significant upregulation of caspase-2 in multiple NASH settings, we aimed to determine whether the loss of caspase-2 would offer protection against hepatocyte apoptosis and the consequential liver fibrosis induced by this disease. To test this, we subjected WT and caspase-2 KO mice to either a control or MCD diet for 8-weeks and assayed hepatocyte apoptosis using TUNEL staining. Caspase-2 KO mice showed significantly fewer TUNEL positive cells following the administration of the NASH-inducing diet (Figure 5.3 A and B). These data demonstrate that caspase-2 KO mice are protected from hepatocyte apoptosis and suggest that caspase-2 is necessary to elicit the full lipoapoptotic response induced by the MCD diet.

Since hepatocyte lipoapoptosis contributes to an increased risk of liver fibrosis, specifically by triggering the myofibroblastic transformation of HSCs through the phagocytosis of apoptotic bodies, evaluating markers of liver fibrosis can be helpful in assessing the contribution of caspase-2 to NASH progression. Therefore, we assessed HSC activation using α-SMA as a marker of myofibroblastic transformation. We performed immunohistochemistry on the livers of both WT and caspase-2 KO mice and found that caspase-2 KO mice showed reduced α-SMA staining, suggesting a reduced activation of HSCs (Figure 5.4 A).

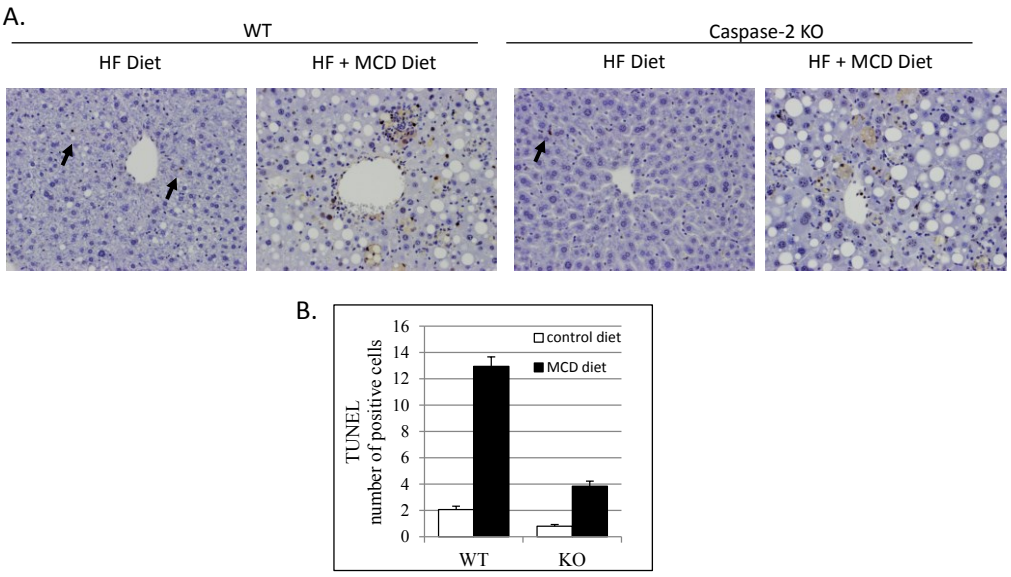

Figure 5.3: Caspase-2 KO mice are protected from MCD diet-induced apoptosis

Figure 5.3: A. Representative TUNEL assays of liver sections from WT or caspase-2 KO mice fed a high fat diet (control) or a methionine choline deficient (MCD) diet. Arrows indicate TUNEL-positive cells in control livers. B. TUNEL-positive cells were counted and graphed as mean ± SEM (n=3 mice/group).

To determine if the reduced accumulation of α-SMA was accompanied by changes in liver fibrosis, liver sections were stained with Sirius Red and collagen 1α1 to evaluate the abundance of collagen fibrils. Consistent with there being a reduced activation of HSCs, caspase-2 KO mice showed a reduced accumulation of Sirius Red-stained fibrils and a reduced expression of collagen 1α1 (Figure 5.4 B and C). These data are furthered supported by a reduction in collagen 1α1 mRNA, as determined by QRT-PCR analysis (Figure 5.4 C). Taken together, these data suggest that loss of caspase-2 leads to a reduction in NASH-associated fibrogenesis. This reduction, combined with the decreased HSC activation, suggests that caspase-2 KO mice are protected from

hepatic lipoapoptosis induced by the MCD diet and identify caspase-2 as a potential therapeutic target for preventing the progressive fibrogenesis observed in NASH.

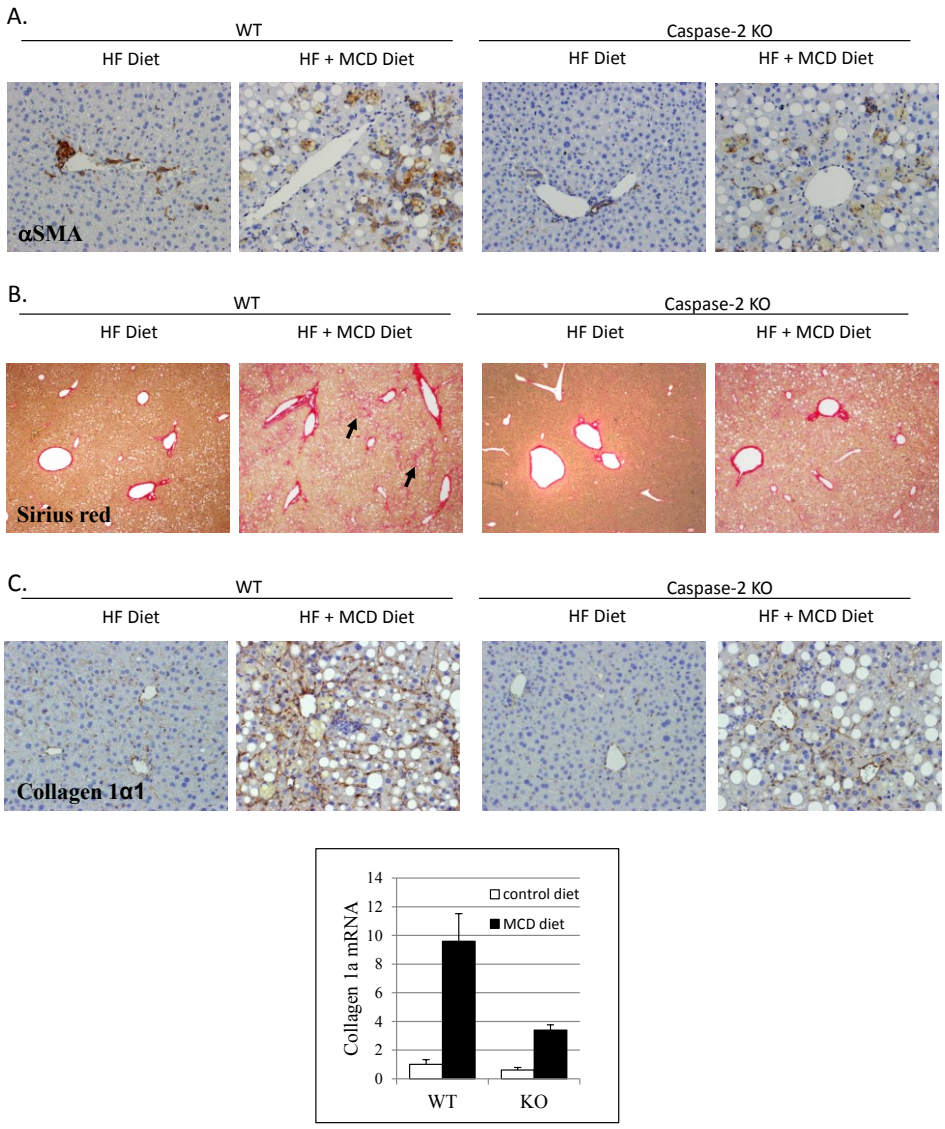

Figure 5.4: Caspase-2 KO hepatocytes are protected from MCD diet-induced fibrosis

Figure 5.4: A. Representative αSMA immunohistochemistry (brown) of liver sections from WT or caspase-2 KO mice fed a high fat diet (control) or a methionine choline deficient (MCD) diet. B. Sirius red staining of collagen fibrils. C. Collagen 1α1 immunohistochemistry (brown) and qRT-PCR analysis of liver RNA normalized to expression in HF diet-fed WT mice and expressed as mean ± SEM.

5.3 Discussion

Previously, we demonstrated that caspase-2 is activated in response to an over-abundance of long-chain fatty acids and that the loss of caspase-2 could protect mammalian cell lines from lipotoxicity *in vitro*. In order to determine the therapeutic significance of these findings, experiments evaluating the importance of caspase-2 in an *in vivo* model of lipotoxicity needed to be performed. In this chapter, we treated caspase-2 KO mice with a diet deficient in methionine and choline, which induces severe liver steatosis, and evaluated the degree of disease protection as compared with control mice. We first demonstrated that caspase-2 KO hepatocytes are protected from lipid-induced cell death *in vitro*, just as we observed in mammalian cell lines depleted of caspase-2 with siRNA. Interestingly, we observed increased expression of caspase-2 in the livers of mice fed the MCD diet. These findings were of particular interest when we noted an increase in caspase-2 expression in NASH patients. Lastly, we found that caspase-2 KO mice administered the NASH-inducing diet were protected from apoptosis and fibrosis, suggesting that caspase-2 is critical regulator of lipid-induced hepatocyte cell death in NASH.

5.3.1 Caspase-2 expression is significantly increased in hepatocytes in NASH

In this study, we showed that caspase-2 expression is significantly increased in both patient samples and our mouse model of NASH. Increased expression of caspase-2 was largely detected in fatty hepatocytes and appeared to be enriched near fibrotic

septa. Such a distribution suggests that caspase-2 might be triggering apoptosis and consequently, activation of fibrogenesis in the surrounding areas. While we have had little success detecting elevations of caspase-2 protein in mammalian cell lines treated with LCFAs, several recent publications have noted increased expression of the protease following high fat feeding *in vivo* (Jobgen et al., 2009; Miller et al., 2014). It is possible that the observed increase in caspase-2 protein is an event which requires whole tissue signaling triggered by physiological lipid accumulation. Thus, it is possible that our cell culture model of exogenous LCFA supplementation doesn't fully recapitulate the lipotoxic stress triggered *in vivo* and thus, we are unable to observe similar changes in caspase-2 protein levels.

Although historically, changes in the level of caspase-2 have not been shown to promote enzyme activation, recent findings have suggested that increased levels of caspase-2 stemming from translational upregulation are, indeed, required for activation of the caspase, at least in the setting of ER stress (Upton et al., 2012). The prevailing model is that ER stress triggers activation of IRE1α, an RNase, which causes rapid decay of select microRNAs that translationally repress caspase-2. Degradation of these microRNAs lifts this repression, resulting in increased translation and thus, expression of caspase-2. Interestingly, IRE1α has been shown to be activated in NASH and its activation has been shown to correlate with histologic disease severity (Puri et al., 2008). Having previously been implicated in the development of cellular injury in NASH, it is

tempting to hypothesize that activation of IRE1α might be initiating cell death via caspase-2 stabilization. We are actively trying to investigate this possibility by performing studies that will measure the level of target microRNAs following MCD diet treatment. If these studies prove to be fruitful, microRNA regulation of caspase-2 could be exploited for therapeutic purposes.

5.3.2 Potential mechanism for caspase-2 activation in NASH

While we have provided extensive evidence that the over-accumulation of lipids can trigger activation of caspase-2, we have failed to uncover the mechanism by which this activation occurs. Previously, our laboratory demonstrated that caspase-2 could be suppressed through CaMKII mediated phosphorylation at serine-135 in Xenopus egg extracts (see figure 1.5) (Nutt et al., 2005). Recent data has suggested that the activity of CaMKII can be modulated by the availability of CoA (McCoy et al., 2013). The accumulation of fatty acids can reduce the free CoA/acyl-CoA ratio, resulting in a decreased availability of free CoA. Reductions in free CoA could result in a reduced activation of CaMKII, which could make caspase-2 more susceptible to activation through reduced phosphorylation at serine-135. Studies to investigate the relevance of this mechanism should evaluate the level of caspase-2 phosphorylation and CaMKII activation following the induction of lipotoxicity in both cell and animal models.

5.3.3 Caspase-2 is a favorable therapeutic target in preventing apoptosis and fibrosis in NASH progression

The data presented in this chapter bolster the role of caspase-2 in lipid-induced cell death by validating its importance in an animal model of NASH. We confirmed that caspase-2 is an important initiator of lipoapoptosis in NASH by demonstrating that KO mice had significantly fewer TUNEL-positive cells in mice fed a NASH-inducing diet. Moreover, caspase-2 KO mice had less activation of HSC and less fibrosis, suggesting that caspase-2 is an attractive therapeutic target for blocking apoptosis, preventing fibrosis, and slowing the progression of NAFLD.

Since there are currently no therapies to halt NAFLD progression, our findings warrant further investigation. One potential drawback to targeting caspase-2 directly in patients with NAFLD would be that such a treatment could potentially increase their risk of tumor development. For example, although caspase-2 KO mice fail to show an increased susceptibility of tumorigenesis, loss of caspase-2 in combination with another tumor suppressor, such as the ataxia telangiectasia mutated (ATM) kinase which controls the DNA damage pathway, can result in an increased incidence of tumor development (Bergeron et al., 1998; Puccini et al., 2013). Since preventing apoptosis and fibrosis would likely require prolonged treatment so patients have time to reduce their lipid levels through diet and exercise, there is a chance that patients could be put at an increased risk of tumor development or progression. While we found no evidence that

inhibiting caspase-2 was unsafe in our mouse model of NASH, future studies should evaluate the significance of the aforementioned risks.

6. Conclusion and perspectives

With the prevalence of obesity and metabolic syndrome rising sharply world-wide, it has become increasingly important to define the molecular mechanisms underlying the pathogenesis and progression of diseases associated with lipid-induced cytotoxicity. Multiple studies have focused on identifying the specific lipid species that triggers lipoapoptosis and there is an overwhelming consensus the free fatty acids are the toxic offenders. The lipotoxic effects of free fatty acids are complex, since they can promote ER stress as well as trigger mitochondrial permeabilization, cytochrome *c* release, and executioner caspase activation. Although the role of the mitochondria in lipoapoptosis was well established, little attention had been given to the pro-death signaling pathways functioning upstream of the mitochondria. Work from this dissertation contributes to a better understanding of the early steps of lipoapoptosis, specifically identifying caspase-2 as the initiator, and should help to identify novel therapeutic approaches for this disease process.

6.1 Lipid accumulations promote the activation of caspase-2 in Xenopus egg extract

In Chapter 3 of this dissertation, we describe metabolomic profiling of *Xenopus* egg extract. The link between metabolism and caspase-2 was initially discovered by our lab and we have described a detailed molecular mechanism for how metabolism can influence caspase-2 modification and activation (Andersen et al., 2011; Nutt et al., 2009;

Nutt et al., 2005). While these studies lead to the hypothesis that *Xenopus* egg extract apoptosis occurs in response to metabolic starvation, there were conflicting data between this hypothesis and the nutrient-sensitive metabolic enzymes regulating caspase-2 modification. Thus, we aimed to determine the true metabolic stress triggering caspase-2 activation in these extracts.

Our metabolomics analysis revealed that Xenopus egg extracts experience a dramatic increase in LCFA metabolites prior to caspase activation. Interestingly, supplementation of the extract with metabolic intermediates or inhibitors that are able to block caspase-2 activation also blocked the accumulation of LCFAs. This data, although correlative, suggested that the buildup of lipids might be the metabolic stress triggering caspase-2 activation. To test this hypothesis, we attempted to overcome the metabolic suppression provided by extract supplementation and found that exogenous addition of the saturated LCFA, palmitate, could not only overcome caspase-2 inhibition but could accelerate it. These data heavily implicated LCFA accumulation in the activation of caspase-2.

Although strictly speculative, we have provided a hypothesis for the dramatic metabolic changes that were observed upon extract incubation. These speculations are based on the lack of mitochondrial respiration that was evident following measurement of mitochondrial oxygen consumption. The failure of mitochondria to utilize oxidative phosphorylation would results in several of the phenotypes we have observed,

including: (1) insufficient supply of oxidized electron carriers (i.e., decrease in the NAD+/NADH ratio) (2) increases in succinate, since succinate dehydrogenase participates in both the electron transport chain and the TCA cycle and (3) a decrease in anaplerotic substrates, mainly oxaloacetate, resulting in the accumulation of acetyl-CoA and pyruvate. The inefficient flux of substrates through glycolysis and the TCA cycle without the ability to regenerate NAD+ will lead to a redox imbalance, resulting in increased levels of NADH. We suspect that the accumulation of NADH results in the accumulation of LCFAs by both increasing fatty acid elongation (driven by increasing acetyl-CoA and NADH levels) and decreasing beta-oxidation (which would be inhibited by increasing NADH levels).

Interestingly, we have previously demonstrated that the exogenous addition of NAD+ can protect against caspase-2 activation in this system (Andersen et al., 2011). The mechanism for this suppression was suggested to be through Sirt1-mediated deacetylation of 14-3-3ζ, which enables this protein to bind to an inhibitory phosphorylation site on caspase-2 (Ser135) and protect it against dephosphorylation (See section 1.2.5.2 for a review). It would be interesting to know whether addition of this oxidized electron carrier also protects against caspase-2 activation by stabilizing the redox state of the extract and consequently, blocking the accumulation of long-chain lipids. It is tempting to speculate that changes in cellular redox status, which can trigger caspase-2 dephosphorylation through the loss of 14-3-3 binding because of a

decrease in sirt1 activity, actually sensitize caspase-2 to activation by LCFA accumulations through the removal of an inhibitory phosphorylation.

Moreover, it is still unclear how the buildup of LCFAs triggers the activation of caspase-2 in egg extract. Can LCFAs directly promote the activation of caspase-2 or do they mediate their toxicity through secondary pathways, via ceramide synthesis or the generation of ER stress? Although we initially focused on the translational aspects of this research, determining the relevance of LCFA-induced caspase-2 activation in cell and animal models, it would be helpful to know the mechanism of activation in this setting, especially for the purposes of therapeutic intervention. Fortunately, the Xenopus egg extract system is ideal for determining whether LCFAs can directly promote caspase-2 activation in the absence of any membrane components. As mentioned in the introduction, we have the ability to make pure cytosolic extracts, devoid of any membranes (i.e., ER, Golgi, mitochondria), which we can treat with palmitate to determine whether they are sufficient to activate caspase-2 in this setting. Additionally, we can add back individual membrane fractions, including purified mitochondria or ER membranes to determine which, if any of these membrane fractions, are necessary for exerting the toxic signaling events that promote caspase-2 activation. Future research efforts will be put toward understanding how the accumulation of LCFAs can promote caspase-2 activation in egg extract.

Finally, our studies from the Xenopus egg extract model system suggested that the buildup of LCFA metabolites could trigger the activation of caspase-2. Our metabolomic studies revealed a positive correlation between lipid accumulation and caspase-2 activation, which we felt warranted further investigation. Therefore, we looked specifically at whether caspase-2 could function as a more general initiator of cell death in response to lipotoxicity in mammalian cell system and this data is discussed below.

6.2 Caspase-2 regulates lipoapoptosis in mammalian cells

In Chapter 4 of this dissertation, we extend our findings from the Xenopus model system to mammalian somatic cells. We aimed to determine whether caspase-2 was activated in response to an over-accumulation of LCFAs through multiple approaches. As detailed in section 1.2.3, caspase-2 activity can be assessed by a number of different assays and differences among these methodologies have contributed to controversy surrounding caspase-2-activating stimuli. Because the caspase-2 research field lacks an efficient assay for evaluating caspase-2 activation, we performed several assays, including the depletion of caspase-2, to determine its importance.

Using an in vitro caspase-2 activity assay that measures VDVAD cleavage, we found that caspase-2 activity increased significantly following treatment with the saturated LCFA, palmitate. We also observed processing of the proenzyme by western blot following palmitate treatment. Importantly, we verified caspase-2 is activated by

recruitment to a HMW complex and that only the HMW fractions containing caspase-2 exhibited enzymatic activity. Finally, we confirmed the activation of caspase-2 following palmitate treatment *in situ* using BiFC.

Once we knew that palmitate could activate caspase-2, we aimed to determine whether caspase-2 was required for the cell death induced by this saturated LCFA. We observed that the depletion of caspase-2 by siRNA significantly protected 293T cells against lipoapoptosis, suggesting that caspase-2 is necessary for full activation of the apoptotic cascade in response to palmitate toxicity. Delving further into caspase-2-induced lipotoxicity, we confirmed that only saturated fatty acids induced cell death and that this cell death was dependent on caspase-2. Interestingly, the activation of palmitate via acyl-CoA formation was required for its toxicity and we have ongoing studies evaluating how saturated LCFAs and their respective acyl-CoA derivatives induce caspase-2 activation.

To evaluate the relevance of our findings in a more physiologic setting, we tested whether caspase-2 was necessary for hepatocyte lipoapoptosis. Interestingly, lipoapoptosis plays an important role in the pathophysiology of liver disease, contributing to the development and progression of NAFLD. Our data show that depletion of caspase-2 by siRNA significantly protects normal and transformed hepatocyte cell lines from saturated fatty acid induced cell death. These findings demonstrate that caspase-2 is necessary for hepatocytes lipoapoptosis and suggest that

caspase-2 may be a useful therapeutic target. At present, there are no effective therapies for halting the progression of NAFLD and thus, therapeutic targeting of caspase-2 may prove useful.

Although we know that caspase-2 is activated following its recruitment into a HMW complex in LCFA-induced cell death, attempts to identify its activation platform have, thus far, been unsuccessful. Moreover, we have had mixed results on the importance of the adaptor protein, RAIDD, in these studies. Despite these difficulties, we continue to try to define the activation platform necessary for caspase-2 activation in lipotoxicity. Encouragingly, our laboratory has recently developed a new methodology for identifying caspase-2 binding partners using a green fluorescent protein (GFP)-trap assay along with our stable BiFC expressing cells. Following its activation in situ, caspase-2 is immunoprecipitated by pulling down on the dimerized fragments of venus using GFP-trap. Initial experiments have been successful in isolating specific caspase-2 binding partners and thus, we aim to use this novel assay to identify the caspase-2 activation platform in lipoapoptosis. Insight into the molecular mediators of caspase-2 activation could reveal a favorable target for therapeutic intervention.

While our initial intent in performing these studies was to determine whether our findings from the Xenopus egg extract were applicable to mammalian cells, we have struggled to evaluate the relevance of our metabolically-regulated post-translational modification mechanism (Figure 1.5) in the mammalian cell setting. Caspase-2 phosphorylation at the conserved serine residue in mammalian cells (serine 164) appears to be low in abundance. As such, we have had difficult detecting the binding between caspase-2 and 14-3-3ζ, the small acidic protein which binds this phospho-site to inhibit dephosphorylation. Since this mechanism of caspase-2 regulation was originally identified in egg extracts treated with glucose-6-phosphate, it may well be that this mechanism is not conserved or that it is only applicable in mammalian cells under certain physiological conditions, which we have not yet determined. Future studies will need to evaluate the importance of this phosphorylation in mammalian cells before we can determine its relevance in the lipoapoptotic activation of caspase-2. Nevertheless, we would hypothesize that high levels of cellular lipids would result in inhibition of Sirt1, a regulator of 14-3-3ζ acetylation and binding to caspase-2, by decreasing cellular NAD+/NADH ratios via enhanced beta-oxidation. Thus, even if caspase-2 phosphorylation at serine 164 were found to be important in mammalian cells, we suspect that increases in intracellular lipids loads would remove this post-translational inhibition via changes in Sirt1 activity.

6.3 The loss of caspase-2 protects against lipoapoptosis and fibrosis in a mouse model of NASH

In Chapter 5 of this dissertation, we translated our findings from mammalian cell line to an *in vivo* mouse model of lipotoxicity. Since lipoapoptosis has been implicated as a key driver of NASH pathogenesis and progression, we aimed to determine whether caspase-2 plays a role in this process (Feldstein et al., 2003). Importantly, hepatocyte apoptosis strongly influences the severity of liver fibrosis in NASH, resulting in the transformation of HSCs to a myofibroblstic state, where they begin secreting collagen and can promote liver cirrhosis. The inhibition of lipoapoptosis is one potential therapeutic option for slowing the progression of NAFLD to NASH and thus, we were interested in determining whether caspase-2 could regulate lipotoxicity *in vivo*.

To investigate this possibility, we first tested whether hepatocytes derived from caspase-2 KO mice were protected from saturated fatty acid induced cell death *in vitro*. We found that caspase-2 KO hepatocytes underwent less cell death when treated with palmitate in culture. Unexpectedly, we found that caspase-2 protein expression was significantly increased in the livers of mice fed a NASH-inducing diet (MCD diet) and it appeared that this increased expression occurred mainly in fatty hepatocytes. Given this finding, we evaluated caspase-2 expression in the livers of patients who had been diagnosed with NASH and encouragingly, we observed that its expression was dramatically increased as well. These findings further substantiate the relevance of our NASH-inducing animal model for the study of NAFLD pathogenesis.

Finally to determine whether the loss of caspase-2 would offer protection against NASH progression, we treated caspase-2 KO cells with the MCD diet and found that they were protected against hepatocyte lipoapaoptosis, as shown by a decrease in TUNEL positive cells. Moreover, in comparing caspase-2 KO with control mice, we observed a decrease in HSC transformation and fibrotic staining. These data suggest that caspase-2 KO mice are also protected against the fibrogenesis prompted by apoptotic cells. Taken together, these data demonstrate a role for caspase-2 in inducing the cell death of hepatocytes in NASH-induced lipoapoptosis.

At present, there are no proven effective therapies for halting NASH progression. Our work suggests that targeting caspase-2 and/or its regulators may be used as a potential therapeutic strategy. Indeed, recent studies have shown moderate success of pan-caspase inhibitors on NAFLD/NASH symptoms in both patient and animal models (Ratziu et al., 2012; Witek et al., 2009). Excitingly, our data suggest that an inhibitor which more specifically targets caspase-2 may enhance the effectiveness of caspase-targeted therapies. The loss of this apical initiator caspase doesn't appear to compromise viability in a knock-out setting and thus, caspase-2 is an attractive therapeutic target for both blocking apoptosis and maintaining mitochondrial integrity in NASH. We hope that our work will contribute to the development of novel therapies for the treatment of this disease.

6.4 Concluding Remarks

The data presented in this dissertation have advanced our understanding of caspase-2, demonstrating a novel role of the pro-apoptotic initiator caspase in lipid-induced apoptosis. Using an unbiased metabolomics approach, we discovered that the activation of caspase-2, the initiator of apoptosis in *Xenopus* egg extract, was associated with an accumulation of LCFA metabolites. Metabolic treatments that blocked the build-up of LCFA metabolites also potently inhibited caspase-2. The caspase-suppressive effect of such metabolic treatments could be overridden by supplementing the extract with the saturated LCFA, palmitate, suggesting that the buildup of LCFAs could trigger caspase-2 activation in this system.

Importantly, we have extended these findings to the mammalian somatic cell system, where we have demonstrated that caspase-2 is activated following palmitate treatment. We demonstrated that caspase-2 was activated by both cleavage of the preferred caspase-2 substrate, VDVAD, as well as proteolytic processing of the caspase-2 proenzyme. Furthermore, we also discovered that caspase-2 was activated by recruitment to a HMW complex following palmitate treatment and that caspase-2 was required for full activation of palmitate-induced cell death. Delving further into caspase-2-induced lipotoxicity, we confirmed that only saturated fatty acids induced cell death and that this cell death was dependent on caspase-2. Interestingly, as has previously been observed in other cells types, palmitate-induced cytotoxicity was not

dependent on ROS, ceramides, or oxidative LCFA catabolism in 293T cells (Hardy et al., 2003; Kim et al., 2008; Staiger et al., 2006). Rather, the activation of palmitate via acyl-CoA formation was required to induce cell death. Taken together, these findings reveal a conserved, critical role for caspase-2 in mediating LCFA-induced lipoapoptosis.

Finally, to demonstrate the therapeutic significance of our findings, we evaluated the importance of caspase-2 in an *in vivo* model of lipotoxicity. We first demonstrated that caspase-2 KO hepatocytes are protected from lipid-induced cell death *in vitro*, just as we observed in mammalian cell lines depleted of caspase-2. Interestingly, we observed an increase in caspase-2 expression in the livers of wild-type mice following the administration of a NASH-inducing diet. These findings are of particular importance, as caspase-2 expression is also increased in patients diagnosed with NASH. Most importantly, we demonstrated that caspase-2 KO mice are protected from apoptosis and fibrosis when fed a NASH-inducing diet, suggesting that caspase-2 is major regulator of hepatocyte lipoapoptosis. These data suggest that caspase-2 is an attractive therapeutic target for blocking apoptosis, preventing fibrogenesis, and slowing the progression of NAFLD and we look forward to following up on these studies.

References

Ahmad, M., Srinivasula, S.M., Wang, L., Talanian, R.V., Litwack, G., Fernandes-Alnemri, T., and Alnemri, E.S. (1997). CRADD, a novel human apoptotic adaptor molecule for caspase-2, and FasL/tumor necrosis factor receptor-interacting protein RIP. Cancer research *57*, 615-619.

Aho, S. (2004). Plakin proteins are coordinately cleaved during apoptosis but preferentially through the action of different caspases. Exp Dermatol *13*, 700-707.

An, J., Muoio, D.M., Shiota, M., Fujimoto, Y., Cline, G.W., Shulman, G.I., Koves, T.R., Stevens, R., Millington, D., and Newgard, C.B. (2004). Hepatic expression of malonyl-CoA decarboxylase reverses muscle, liver and whole-animal insulin resistance. Nature medicine *10*, 268-274.

Andersen, J.L., Johnson, C.E., Freel, C.D., Parrish, A.B., Day, J.L., Buchakjian, M.R., Nutt, L.K., Thompson, J.W., Moseley, M.A., and Kornbluth, S. (2009). Restraint of apoptosis during mitosis through interdomain phosphorylation of caspase-2. Embo J *28*, 3216-3227.

Andersen, J.L., Thompson, J.W., Lindblom, K.R., Johnson, E.S., Yang, C.S., Lilley, L.R., Freel, C.D., Moseley, M.A., and Kornbluth, S. (2011). A biotin switch-based proteomics approach identifies 14-3-3zeta as a target of Sirt1 in the metabolic regulation of caspase-2. Molecular cell *43*, 834-842.

Araya, R., Uehara, T., and Nomura, Y. (1998). Hypoxia induces apoptosis in human neuroblastoma SK-N-MC cells by caspase activation accompanying cytochrome c release from mitochondria. FEBS letters *439*, 168-172.

Arici, M., Chana, R., Lewington, A., Brown, J., and Brunskill, N.J. (2003). Stimulation of Proximal Tubular Cell Apoptosis by Albumin-Bound Fatty Acids Mediated by Peroxisome Proliferator Activated Receptor-γ. Journal of the American Society of Nephrology *14*, 17-27.

Baliga, B.C., Colussi, P.A., Read, S.H., Dias, M.M., Jans, D.A., and Kumar, S. (2003). Role of prodomain in importin-mediated nuclear localization and activation of caspase-2. J Biol Chem *278*, 4899-4905.

Baliga, B.C., Read, S.H., and Kumar, S. (2004). The biochemical mechanism of caspase-2 activation. Cell Death Differ *11*, 1234-1241.

Baptiste-Okoh, N., Barsotti, A.M., and Prives, C. (2008). A role for caspase 2 and PIDD in the process of p53-mediated apoptosis. Proceedings of the National Academy of Sciences of the United States of America *105*, 1937-1942.

Berg, J.M., Tymoczko, J.L., and Stryer, L. (2002). Biochemistry, 5 edn (New York: W H Freeman).

Bergeron, L., Perez, G.I., Macdonald, G., Shi, L., Sun, Y., Jurisicova, A., Varmuza, S., Latham, K.E., Flaws, J.A., Salter, J.C., *et al.* (1998). Defects in regulation of apoptosis in caspase-2-deficient mice. Genes & development *12*, 1304-1314.

Berry, M.N., and Phillips, J.W. (2000). The isolated hepatocyte preparation: 30 years on. Biochemical Society transactions *28*, 131-135.

Berube, C., Boucher, L.M., Ma, W., Wakeham, A., Salmena, L., Hakem, R., Yeh, W.C., Mak, T.W., and Benchimol, S. (2005). Apoptosis caused by p53-induced protein with death domain (PIDD) depends on the death adapter protein RAIDD. Proceedings of the National Academy of Sciences of the United States of America *102*, 14314-14320.

Blow, J.J., and Laskey, R.A. (1986). Initiation of DNA replication in nuclei and purified DNA by a cell-free extract of Xenopus eggs. Cell *47*, 577-587.

Bonzon, C., Bouchier-Hayes, L., Pagliari, L.J., Green, D.R., and Newmeyer, D.D. (2006). Caspase-2-induced apoptosis requires bid cleavage: a physiological role for bid in heat shock-induced death. Molecular biology of the cell *17*, 2150-2157.

Bouchier-Hayes, L. (2010). The role of caspase-2 in stress-induced apoptosis. Journal of Cellular and Molecular Medicine *14*, 1212-1224.

Bouchier-Hayes, L., Oberst, A., McStay, G.P., Connell, S., Tait, S.W., Dillon, C.P., Flanagan, J.M., Beere, H.M., and Green, D.R. (2009). Characterization of cytoplasmic caspase-2 activation by induced proximity. Molecular cell *35*, 830-840.

Browning, J.D., Szczepaniak, L.S., Dobbins, R., Nuremberg, P., Horton, J.D., Cohen, J.C., Grundy, S.M., and Hobbs, H.H. (2004). Prevalence of hepatic steatosis in an urban population in the United States: Impact of ethnicity. Hepatology *40*, 1387-1395.

Butt, A.J., Harvey, N.L., Parasivam, G., and Kumar, S. (1998). Dimerization and autoprocessing of the Nedd2 (caspase-2) precursor requires both the prodomain and the carboxyl-terminal regions. The Journal of biological chemistry *273*, 6763-6768.

Canbay, A., Taimr, P., Torok, N., Higuchi, H., Friedman, S., and Gores, G.J. (2003). Apoptotic body engulfment by a human stellate cell line is profibrogenic. Laboratory investigation; a journal of technical methods and pathology *83*, 655-663.

Carlsson, Y., Schwendimann, L., Vontell, R., Rousset, C.I., Wang, X., Lebon, S., Charriaut-Marlangue, C., Supramaniam, V., Hagberg, H., Gressens, P., *et al.* (2011). Genetic inhibition of caspase-2 reduces hypoxic-ischemic and excitotoxic neonatal brain injury. Annals of neurology *70*, 781-789.

Carlsson, Y., Wang, X., Schwendimann, L., Rousset, C.I., Jacotot, E., Gressens, P., Thoresen, M., Mallard, C., and Hagberg, H. (2012). Combined effect of hypothermia and caspase-2 gene deficiency on neonatal hypoxic-ischemic brain injury. Pediatric research *71*, 566-572.

Cazanave, S.C., and Gores, G.J. (2010). Mechanisms and clinical implications of hepatocyte lipoapoptosis. Clinical Lipidology *5*, 71-85.

Charlton, M.R., Burns, J.M., Pedersen, R.A., Watt, K.D., Heimbach, J.K., and Dierkhising, R.A. (2011). Frequency and outcomes of liver transplantation for nonalcoholic steatohepatitis in the United States. Gastroenterology *141*, 1249-1253.

Cheung, H.H., Lynn Kelly, N., Liston, P., and Korneluk, R.G. (2006). Involvement of caspase-2 and caspase-9 in endoplasmic reticulum stress-induced apoptosis: a role for the IAPs. Experimental cell research *312*, 2347-2357.

Choi, S.S., Sicklick, J.K., Ma, Q., Yang, L., Huang, J., Qi, Y., Chen, W., Li, Y.X., Goldschmidt-Clermont, P.J., and Diehl, A.M. (2006). Sustained activation of Rac1 in hepatic stellate cells promotes liver injury and fibrosis in mice. Hepatology (Baltimore, Md *44*, 1267-1277.

Cnop, M., Hannaert, J.C., Hoorens, A., Eizirik, D.L., and Pipeleers, D.G. (2001). Inverse relationship between cytotoxicity of free fatty acids in pancreatic islet cells and cellular triglyceride accumulation. Diabetes *50*, 1771-1777.

Coll, T., Eyre, E., Rodriguez-Calvo, R., Palomer, X., Sanchez, R.M., Merlos, M., Laguna, J.C., and Vazquez-Carrera, M. (2008). Oleate reverses palmitate-induced insulin resistance and inflammation in skeletal muscle cells. The Journal of biological chemistry *283*, 11107-11116.

Colussi, P.A., Harvey, N.L., and Kumar, S. (1998). Prodomain-dependent nuclear localization of the caspase-2 (Nedd2) precursor. A novel function for a caspase prodomain. J Biol Chem *273*, 24535-24542.

Danial, N.N., and Korsmeyer, S.J. (2004). Cell death: critical control points. Cell *116*, 205-219.

de Vries, J.E., Vork, M.M., Roemen, T.H., de Jong, Y.F., Cleutjens, J.P., van der Vusse, G.J., and van Bilsen, M. (1997). Saturated but not mono-unsaturated fatty acids induce apoptotic cell death in neonatal rat ventricular myocytes. Journal of lipid research *38*, 1384-1394.

Deming, P.B., Schafer, Z.T., Tashker, J.S., Potts, M.B., Deshmukh, M., and Kornbluth, S. (2004). Bcr-Abl-mediated protection from apoptosis downstream of mitochondrial cytochrome c release. Molecular and cellular biology *24*, 10289-10299.

Dworkin, M.B., and Dworkin-Rastl, E. (1990). Regulation of carbon flux from amino acids into sugar phosphates in Xenopus embryos. Developmental biology *138*, 177-187.

Dworkin, M.B., and Dworkin-Rastl, E. (1991). Carbon metabolism in early amphibian embryos. Trends in biochemical sciences *16*, 229-234.

El-Assaad, W., Buteau, J., Peyot, M.L., Nolan, C., Roduit, R., Hardy, S., Joly, E., Dbaibo, G., Rosenberg, L., and Prentki, M. (2003). Saturated fatty acids synergize with elevated glucose to cause pancreatic beta-cell death. Endocrinology *144*, 4154-4163.

Feldstein, A.E., Canbay, A., Angulo, P., Taniai, M., Burgart, L.J., Lindor, K.D., and Gores, G.J. (2003). Hepatocyte apoptosis and Fas expression are prominent features of human nonalcoholic steatohepatitis. Gastroenterology *125*, 437-443.

Folbergrova´, J., Ljunggren, B., Norberg, K., and Siesjo¨, B.K. (1974). Influence of complete ischemia on glycolytic metabolites, citric acid cycle intermediates, and associated amino acids in the rat cerebral cortex. Brain Research *80*, 265-279.

Franklin, E.E., and Robertson, J.D. (2007). Requirement of Apaf-1 for mitochondrial events and the cleavage or activation of all procaspases during genotoxic stress-induced apoptosis. Biochem J *405*, 115-122.

Frayn, K.N. (2002). Adipose tissue as a buffer for daily lipid flux. Diabetologia *45*, 1201-1210.

Fridman, A., Pak, I., Butts, B., Hoek, M., Nicholson, D., and Mehmet, H. (2013). MerCASBA: an updated and refined database of caspase substrates. Apoptosis : an international journal on programmed cell death *18*, 369-371.

Furstova, V., Kopska, T., James, R.F., and Kovar, J. (2008). Comparison of the effect of individual saturated and unsaturated fatty acids on cell growth and death induction in the human pancreatic beta-cell line NES2Y. Life sciences *82*, 684-691.

Fushimi, K., Ray, P., Kar, A., Wang, L., Sutherland, L.C., and Wu, J.Y. (2008). Up-regulation of the proapoptotic caspase 2 splicing isoform by a candidate tumor suppressor, RBM5. Proceedings of the National Academy of Sciences of the United States of America *105*, 15708-15713.

Galle, P.R., and Krammer, P.H. (1998). CD95-induced apoptosis in human liver disease. Seminars in liver disease *18*, 141-151.

Gao, D., Griffiths, H.R., and Bailey, C.J. (2009). Oleate protects against palmitate-induced insulin resistance in L6 myotubes. The British journal of nutrition *102*, 1557-1563.

Goldberg, N.D., Passonneau, J.V., and Lowry, O.H. (1966). Effects of changes in brain metabolism on the levels of citric acid cycle intermediates. The Journal of biological chemistry *241*, 3997-4003.

Gu, C., Casaccia-Bonnefil, P., Srinivasan, A., and Chao, M.V. (1999). Oligodendrocyte apoptosis mediated by caspase activation. The Journal of neuroscience : the official journal of the Society for Neuroscience *19*, 3043-3049.

Gu, H., Chen, X., Gao, G., and Dong, H. (2008). Caspase-2 functions upstream of mitochondria in endoplasmic reticulum stress-induced apoptosis by bortezomib in human myeloma cells. Mol Cancer Ther *7*, 2298-2307.

Guo, Y., Srinivasula, S.M., Druilhe, A., Fernandes-Alnemri, T., and Alnemri, E.S. (2002). Caspase-2 induces apoptosis by releasing proapoptotic proteins from mitochondria. The Journal of biological chemistry *277*, 13430-13437.

Han, M.S., Park, S.Y., Shinzawa, K., Kim, S., Chung, K.W., Lee, J.-H., Kwon, C.H., Lee, K.-W., Lee, J.-H., Park, C.K., *et al.* (2008). Lysophosphatidylcholine as a death effector in the lipoapoptosis of hepatocytes. Journal of lipid research *49*, 84-97.

Hardy, S., El-Assaad, W., Przybytkowski, E., Joly, E., Prentki, M., and Langelier, Y. (2003). Saturated Fatty Acid-induced Apoptosis in MDA-MB-231 Breast Cancer Cells: A ROLE FOR CARDIOLIPIN. Journal of Biological Chemistry *278*, 31861-31870.

He, Q., Huang, Y., and Sheikh, M.S. (2004). Bax deficiency affects caspase-2 activation during ultraviolet radiation-induced apoptosis. Oncogene *23*, 1321-1325.

Hebbard, L., and George, J. (2011). Animal models of nonalcoholic fatty liver disease. Nature reviews. Gastroenterology & hepatology *8*, 35-44.

Ho, L.H., Read, S.H., Dorstyn, L., Lambrusco, L., and Kumar, S. (2008). Caspase-2 is required for cell death induced by cytoskeletal disruption. Oncogene *27*, 3393-3404.

Hochachka, P.W., Owen, T.G., Allen, J.F., and Whittow, G.C. (1975). Multiple end products of anaerobiosis in diving vertebrates. Comparative Biochemistry and Physiology Part B: Comparative Biochemistry *50*, 17-22.

Hu, W., Ross, J., Geng, T., Brice, S.E., and Cowart, L.A. (2011). Differential Regulation of Dihydroceramide Desaturase by Palmitate versus Monounsaturated Fatty Acids: IMPLICATIONS FOR INSULIN RESISTANCE. Journal of Biological Chemistry *286*, 16596-16605.

Huang, W.C., Lin, Y.S., Chen, C.L., Wang, C.Y., Chiu, W.H., and Lin, C.F. (2009). Glycogen synthase kinase-3beta mediates endoplasmic reticulum stress-induced lysosomal apoptosis in leukemia. The Journal of pharmacology and experimental therapeutics *329*, 524-531.

Ibrahim, S.H., Kohli, R., and Gores, G.J. (2011). Mechanisms of Lipotoxicity in NAFLD and Clinical Implications. J Pediatr Gastr Nutr *53*, 131-140.

Imre, G., Heering, J., Takeda, A.N., Husmann, M., Thiede, B., zu Heringdorf, D.M., Green, D.R., van der Goot, F.G., Sinha, B., Dotsch, V., *et al.* (2012). Caspase-2 is an initiator caspase responsible for pore-forming toxin-mediated apoptosis. The EMBO journal *31*, 2615-2628.

Inoue, S., Browne, G., Melino, G., and Cohen, G.M. (2009). Ordering of caspases in cells undergoing apoptosis by the intrinsic pathway. Cell Death Differ *16*, 1053-1061.

Jelinek, M., Balu Ikova, K., Kopperova, D., V, N.M.-F., Ramek, J., Fidlerova, J., Zanardi, I., Ojima, I., and Kova, J. (2013). Caspase-2 is involved in cell death induction by taxanes in breast cancer cells. Cancer cell international *13*, 42.

Jobgen, W., Fu, W.J., Gao, H., Li, P., Meininger, C.J., Smith, S.B., Spencer, T.E., and Wu, G. (2009). High fat feeding and dietary L-arginine supplementation differentially regulate gene expression in rat white adipose tissue. Amino acids *37*, 187-198.

Kakisaka, K., Cazanave, S.C., Fingas, C.D., Guicciardi, M.E., Bronk, S.F., Werneburg, N.W., Mott, J.L., and Gores, G.J. (2012). Mechanisms of lysophosphatidylcholine-

induced hepatocyte lipoapoptosis. American journal of physiology. Gastrointestinal and liver physiology *302*, G77-84.

Kim, I.R., Murakami, K., Chen, N.J., Saibil, S.D., Matysiak-Zablocki, E., Elford, A.R., Bonnard, M., Benchimol, S., Jurisicova, A., Yeh, W.C., *et al.* (2009). DNA damage- and stress-induced apoptosis occurs independently of PIDD. Apoptosis : an international journal on programmed cell death *14*, 1039-1049.

Kim, J.E., Ahn, M.W., Baek, S.H., Lee, I.K., Kim, Y.W., Kim, J.Y., Dan, J.M., and Park, S.Y. (2008). AMPK activator, AICAR, inhibits palmitate-induced apoptosis in osteoblast. Bone *43*, 394-404.

Kischkel, F.C., Hellbardt, S., Behrmann, I., Germer, M., Pawlita, M., Krammer, P.H., and Peter, M.E. (1995). Cytotoxicity-dependent APO-1 (Fas/CD95)-associated proteins form a death-inducing signaling complex (DISC) with the receptor. EMBO J *14*, 5579-5588.

Kluck, R.M., Martin, S.J., Hoffman, B.M., Zhou, J.S., Green, D.R., and Newmeyer, D.D. (1997). Cytochrome c activation of CPP32-like proteolysis plays a critical role in a Xenopus cell-free apoptosis system. The EMBO journal *16*, 4639-4649.

Kong, J.Y., and Rabkin, S.W. (2002). Palmitate-induced cardiac apoptosis is mediated through CPT-1 but not influenced by glucose and insulin. American journal of physiology. Heart and circulatory physiology *282*, H717-725.

Kotarsky, H., Keller, M., Davoudi, M., Leveen, P., Karikoski, R., Enot, D.P., and Fellman, V. (2012). Metabolite Profiles Reveal Energy Failure and Impaired Beta-Oxidation in Liver of Mice with Complex III Deficiency Due to a BCS1L Mutation. PloS one *7*, e41156.

Kumar, S., Kinoshita, M., and Noda, M. (1997). Characterization of a mammalian cell death gene Nedd2. Leukemia *11 Suppl 3*, 385-386.

Kumar, S., Kinoshita, M., Noda, M., Copeland, N.G., and Jenkins, N.A. (1994). Induction of apoptosis by the mouse Nedd2 gene, which encodes a protein similar to the product of the Caenorhabditis elegans cell death gene ced-3 and the mammalian IL-1 beta-converting enzyme. Genes Dev *8*, 1613-1626.

Kumar, S., Tomooka, Y., and Noda, M. (1992). Identification of a set of genes with developmentally down-regulated expression in the mouse brain. Biochemical and biophysical research communications *185*, 1155-1161.

Kusminski, C.M., Shetty, S., Orci, L., Unger, R.H., and Scherer, P.E. (2009). Diabetes and apoptosis: lipotoxicity. Apoptosis : an international journal on programmed cell death *14*, 1484-1495.

Lamkanfi, M., D'Hondt, K., Vande Walle, L., van Gurp, M., Denecker, G., Demeulemeester, J., Kalai, M., Declercq, W., Saelens, X., and Vandenabeele, P. (2005). A novel caspase-2 complex containing TRAF2 and RIP1. The Journal of biological chemistry *280*, 6923-6932.

Larter, C.Z., and Yeh, M.M. (2008). Animal models of NASH: getting both pathology and metabolic context right. Journal of gastroenterology and hepatology *23*, 1635-1648.

Larter, C.Z., Yeh, M.M., Williams, J., Bell-Anderson, K.S., and Farrell, G.C. (2008). MCD-induced steatohepatitis is associated with hepatic adiponectin resistance and adipogenic transformation of hepatocytes. J Hepatol *49*, 407-416.

Lassus, P., Opitz-Araya, X., and Lazebnik, Y. (2002). Requirement for caspase-2 in stress-induced apoptosis before mitochondrial permeabilization. Science *297*, 1352-1354.

Lavrik, I.N., Golks, A., Baumann, S., and Krammer, P.H. (2006). Caspase-2 is activated at the CD95 death-inducing signaling complex in the course of CD95-induced apoptosis. Blood *108*, 559-565.

Leclercq, I.A., Lebrun, V.A., Starkel, P., and Horsmans, Y.J. (2007). Intrahepatic insulin resistance in a murine model of steatohepatitis: effect of PPARgamma agonist pioglitazone. Laboratory investigation; a journal of technical methods and pathology *87*, 56-65.

Lewis, G.F., Carpentier, A., Adeli, K., and Giacca, A. (2002). Disordered Fat Storage and Mobilization in the Pathogenesis of Insulin Resistance and Type 2 Diabetes. Endocrine Reviews *23*, 201-229.

Li, H., Bergeron, L., Cryns, V., Pasternack, M.S., Zhu, H., Shi, L., Greenberg, A., and Yuan, J. (1997a). Activation of Caspase-2 in Apoptosis. Journal of Biological Chemistry *272*, 21010-21017.

Li, H., Zhu, H., Xu, C.J., and Yuan, J. (1998). Cleavage of BID by caspase 8 mediates the mitochondrial damage in the Fas pathway of apoptosis. Cell *94*, 491-501.

Li, P., Nijhawan, D., Budihardjo, I., Srinivasula, S.M., Ahmad, M., Alnemri, E.S., and Wang, X. (1997b). Cytochrome c and dATP-dependent formation of Apaf-1/caspase-9 complex initiates an apoptotic protease cascade. Cell *91*, 479-489.

Lin, Y., Ma, W., and Benchimol, S. (2000). Pidd, a new death-domain-containing protein, is induced by p53 and promotes apoptosis. Nat Genet *26*, 122-127.

Lindblom, K.R., and Kornbluth, S. (2014). The Complex Interplay Between Metabolism and Apoptosis. In Cell Death, Mechanism and Disease, H. Wu, ed. (Springer), p. 272.

Listenberger, L.L., Han, X., Lewis, S.E., Cases, S., Farese, R.V., Jr., Ory, D.S., and Schaffer, J.E. (2003). Triglyceride accumulation protects against fatty acid-induced lipotoxicity. Proceedings of the National Academy of Sciences of the United States of America *100*, 3077-3082.

Listenberger, L.L., Ory, D.S., and Schaffer, J.E. (2001). Palmitate-induced apoptosis can occur through a ceramide-independent pathway. The Journal of biological chemistry *276*, 14890-14895.

Listenberger, L.L., and Schaffer, J.E. (2002). Mechanisms of lipoapoptosis: implications for human heart disease. Trends in cardiovascular medicine *12*, 134-138.

Liu, X., Kim, C.N., Yang, J., Jemmerson, R., and Wang, X. (1996). Induction of apoptotic program in cell-free extracts: requirement for dATP and cytochrome c. Cell *86*, 147-157.

Luo, X., Budihardjo, I., Zou, H., Slaughter, C., and Wang, X. (1998). Bid, a Bcl2 interacting protein, mediates cytochrome c release from mitochondria in response to activation of cell surface death receptors. Cell *94*, 481-490.

Lupi, R., Dotta, F., Marselli, L., Del Guerra, S., Masini, M., Santangelo, C., Patane, G., Boggi, U., Piro, S., Anello, M., *et al.* (2002). Prolonged exposure to free fatty acids has cytostatic and pro-apoptotic effects on human pancreatic islets: evidence that beta-cell death is caspase mediated, partially dependent on ceramide pathway, and Bcl-2 regulated. Diabetes *51*, 1437-1442.

Malhi, H., Bronk, S.F., Werneburg, N.W., and Gores, G.J. (2006). Free fatty acids induce JNK-dependent hepatocyte lipoapoptosis. The Journal of biological chemistry *281*, 12093-12101.

Malhi, H., Guicciardi, M.E., and Gores, G.J. (2010). Hepatocyte Death: A Clear and Present Danger. Physiological Reviews *90*, 1165-1194.

Mancini, M., Machamer, C.E., Roy, S., Nicholson, D.W., Thornberry, N.A., Casciola-Rosen, L.A., and Rosen, A. (2000). Caspase-2 is localized at the Golgi complex and cleaves golgin-160 during apoptosis. J Cell Biol *149*, 603-612.

Manzl, C., Krumschnabel, G., Bock, F., Sohm, B., Labi, V., Baumgartner, F., Logette, E., Tschopp, J., and Villunger, A. (2009). Caspase-2 activation in the absence of PIDDosome formation. The Journal of cell biology *185*, 291-303.

Masamune, A., Sakai, Y., Satoh, A., Fujita, M., Yoshida, M., and Shimosegawa, T. (2001). Lysophosphatidylcholine induces apoptosis in AR42J cells. Pancreas *22*, 75-83.

McCoy, F., Darbandi, R., Lee, Hoi C., Bharatham, K., Moldoveanu, T., Grace, C.R., Dodd, K., Lin, W., Chen, S.-I., Tangallapally, Rajendra P., *et al.* (2013). Metabolic Activation of CaMKII by Coenzyme A. Molecular cell *52*, 325-339.

McStay, G.P., Salvesen, G.S., and Green, D.R. (2008). Overlapping cleavage motif selectivity of caspases: implications for analysis of apoptotic pathways. Cell death and differentiation *15*, 322-331.

Mei, S., Ni, H.M., Manley, S., Bockus, A., Kassel, K.M., Luyendyk, J.P., Copple, B.L., and Ding, W.X. (2011). Differential roles of unsaturated and saturated fatty acids on autophagy and apoptosis in hepatocytes. The Journal of pharmacology and experimental therapeutics *339*, 487-498.

Miller, C.N., Morton, H.P., Cooney, P.T., Winters, T.G., Ramseur, K.R., Rayalam, S., Della-Fera, M.A., Baile, C.A., and Brown, L.M. (2014). Acute exposure to high-fat diets increases hepatic expression of genes related to cell repair and remodeling in female rats. Nutrition research (New York, N.Y.) *34*, 85-93.

Miller, T.A., LeBrasseur, N.K., Cote, G.M., Trucillo, M.P., Pimentel, D.R., Ido, Y., Ruderman, N.B., and Sawyer, D.B. (2005). Oleate prevents palmitate-induced cytotoxic stress in cardiac myocytes. Biochemical and biophysical research communications *336*, 309-315.

Murray, A.W. (1991). Cell cycle extracts. Methods Cell Biol *36*, 581-605.

Murray, A.W., and Kirschner, M.W. (1989). Cyclin synthesis drives the early embryonic cell cycle. Nature *339*, 275-280.

Mutomba, M.C., Yuan, H., Konyavko, M., Adachi, S., Yokoyama, C.B., Esser, V., McGarry, J.D., Babior, B.M., and Gottlieb, R.A. (2000). Regulation of the activity of caspases by L-carnitine and palmitoylcarnitine. FEBS letters *478*, 19-25.

Muzio, M., Chinnaiyan, A.M., Kischkel, F.C., O'Rourke, K., Shevchenko, A., Ni, J., Scaffidi, C., Bretz, J.D., Zhang, M., Gentz, R., *et al.* (1996). FLICE, a novel FADD-homologous ICE/CED-3-like protease, is recruited to the CD95 (Fas/APO-1) death--inducing signaling complex. Cell *85*, 817-827.

Nagasawa, T., Inada, Y., Nakano, S., Tamura, T., Takahashi, T., Maruyama, K., Yamazaki, Y., Kuroda, J., and Shibata, N. (2006). Effects of bezafibrate, PPAR pan-agonist, and GW501516, PPARdelta agonist, on development of steatohepatitis in mice fed a methionine- and choline-deficient diet. European journal of pharmacology *536*, 182-191.

Nakagawa, T., Tsuruma, K., Uehara, T., and Nomura, Y. (2008). GMEB1, a novel endogenous caspase inhibitor, prevents hypoxia- and oxidative stress-induced neuronal apoptosis. Neuroscience letters *438*, 34-37.

Nemcova-Furstova, V., Balusikova, K., Sramek, J., James, R.F., and Kovar, J. (2013). Caspase-2 and JNK activated by saturated fatty acids are not involved in apoptosis induction but modulate ER stress in human pancreatic beta-cells. Cellular physiology and biochemistry : international journal of experimental cellular physiology, biochemistry, and pharmacology *31*, 277-289.

Neuschwander-Tetri, B.A. (2010). Nontriglyceride hepatic lipotoxicity: the new paradigm for the pathogenesis of NASH. Current gastroenterology reports *12*, 49-56.

Newmeyer, D.D., Farschon, D.M., and Reed, J.C. (1994). Cell-free apoptosis in Xenopus egg extracts: inhibition by Bcl-2 and requirement for an organelle fraction enriched in mitochondria. Cell *79*, 353-364.

Newport, J.W., and Forbes, D.J. (1987). The nucleus: structure, function, and dynamics. Annu Rev Biochem *56*, 535-565.

Niizuma, K., Endo, H., Nito, C., Myer, D.J., Kim, G.S., and Chan, P.H. (2008). The PIDDosome mediates delayed death of hippocampal CA1 neurons after transient global cerebral ischemia in rats. Proceedings of the National Academy of Sciences of the United States of America *105*, 16368-16373.

Nutt, L.K., Buchakjian, M.R., Gan, E., Darbandi, R., Yoon, S.Y., Wu, J.Q., Miyamoto, Y.J., Gibbons, J.A., Andersen, J.L., Freel, C.D., *et al.* (2009). Metabolic control of oocyte apoptosis mediated by 14-3-3zeta-regulated dephosphorylation of caspase-2. Developmental cell *16*, 856-866.

Nutt, L.K., Margolis, S.S., Jensen, M., Herman, C.E., Dunphy, W.G., Rathmell, J.C., and Kornbluth, S. (2005). Metabolic regulation of oocyte cell death through the CaMKII-mediated phosphorylation of caspase-2. Cell *123*, 89-103.

O'Reilly, L.A., Ekert, P., Harvey, N., Marsden, V., Cullen, L., Vaux, D.L., Hacker, G., Magnusson, C., Pakusch, M., Cecconi, F., *et al.* (2002). Caspase-2 is not required for thymocyte or neuronal apoptosis even though cleavage of caspase-2 is dependent on both Apaf-1 and caspase-9. Cell Death Differ *9*, 832-841.

Ogasawara, J., Watanabe-Fukunaga, R., Adachi, M., Matsuzawa, A., Kasugai, T., Kitamura, Y., Itoh, N., Suda, T., and Nagata, S. (1993). Lethal effect of the anti-Fas antibody in mice. Nature *364*, 806-809.

Olsson, M., Vakifahmetoglu, H., Abruzzo, P.M., Hogstrand, K., Grandien, A., and Zhivotovsky, B. (2009). DISC-mediated activation of caspase-2 in DNA damage-induced apoptosis. Oncogene *28*, 1949-1959.

Ow, Y.P., Green, D.R., Hao, Z., and Mak, T.W. (2008). Cytochrome c: functions beyond respiration. Nat Rev Mol Cell Biol *9*, 532-542.

Park, H.H., Logette, E., Raunser, S., Cuenin, S., Walz, T., Tschopp, J., and Wu, H. (2007a). Death domain assembly mechanism revealed by crystal structure of the oligomeric PIDDosome core complex. Cell *128*, 533-546.

Park, M.S., Kim, B.S., and Devarajan, P. (2007b). Hypoxia/re-oxygenation injury induces apoptosis of LLC-PK1 cells by activation of caspase-2. Pediatric nephrology (Berlin, Germany) *22*, 202-208.

Paroni, G., Mizzau, M., Henderson, C., Del Sal, G., Schneider, C., and Brancolini, C. (2004). Caspase-dependent regulation of histone deacetylase 4 nuclear-cytoplasmic shuttling promotes apoptosis. Molecular biology of the cell *15*, 2804-2818.

Peart, M.J., Tainton, K.M., Ruefli, A.A., Dear, A.E., Sedelies, K.A., O'Reilly, L.A., Waterhouse, N.J., Trapani, J.A., and Johnstone, R.W. (2003). Novel mechanisms of apoptosis induced by histone deacetylase inhibitors. Cancer research *63*, 4460-4471.

Penna, F., Pin, F., Costamagna, D., Reffo, P., Baccino, F.M., Bonelli, G., and Costelli, P. (2012). Caspase 2 activation and ER stress drive rapid Jurkat cell apoptosis by clofibrate. PloS one *7*, e45327.

Piro, S., Anello, M., Di Pietro, C., Lizzio, M.N., Patane, G., Rabuazzo, A.M., Vigneri, R., Purrello, M., and Purrello, F. (2002). Chronic exposure to free fatty acids or high glucose induces apoptosis in rat pancreatic islets: possible role of oxidative stress. Metabolism: clinical and experimental *51*, 1340-1347.

Puccini, J., Shalini, S., Voss, A.K., Gatei, M., Wilson, C.H., Hiwase, D.K., Lavin, M.F., Dorstyn, L., and Kumar, S. (2013). Loss of caspase-2 augments lymphomagenesis and enhances genomic instability in Atm-deficient mice. Proceedings of the National Academy of Sciences of the United States of America *110*, 19920-19925.

Puri, P., Mirshahi, F., Cheung, O., Natarajan, R., Maher, J.W., Kellum, J.M., and Sanyal, A.J. (2008). Activation and dysregulation of the unfolded protein response in nonalcoholic fatty liver disease. Gastroenterology *134*, 568-576.

Rahmani, M., Davis, E.M., Crabtree, T.R., Habibi, J.R., Nguyen, T.K., Dent, P., and Grant, S. (2007). The kinase inhibitor sorafenib induces cell death through a process involving induction of endoplasmic reticulum stress. Molecular and cellular biology *27*, 5499-5513.

Ratts, V.S., Flaws, J.A., Kolp, R., Sorenson, C.M., and Tilly, J.L. (1995). Ablation of bcl-2 gene expression decreases the numbers of oocytes and primordial follicles established in the post-natal female mouse gonad. Endocrinology *136*, 3665-3668.

Ratziu, V., Sheikh, M.Y., Sanyal, A.J., Lim, J.K., Conjeevaram, H., Chalasani, N., Abdelmalek, M., Bakken, A., Renou, C., Palmer, M., *et al.* (2012). A phase 2, randomized, double-blind, placebo-controlled study of GS-9450 in subjects with nonalcoholic steatohepatitis. Hepatology *55*, 419-428.

Read, S.H., Baliga, B.C., Ekert, P.G., Vaux, D.L., and Kumar, S. (2002). A novel Apaf-1-independent putative caspase-2 activation complex. The Journal of cell biology *159*, 739-745.

Renatus, M., Stennicke, H.R., Scott, F.L., Liddington, R.C., and Salvesen, G.S. (2001). Dimer formation drives the activation of the cell death protease caspase 9. Proc Natl Acad Sci U S A *98*, 14250-14255.

Ribe, E.M., Jean, Y.Y., Goldstein, R.L., Manzl, C., Stefanis, L., Villunger, A., and Troy, C.M. (2012). Neuronal caspase 2 activity and function requires RAIDD, but not PIDD. Biochem J *444*, 591-599.

Rinella, M.E., and Green, R.M. (2004). The methionine-choline deficient dietary model of steatohepatitis does not exhibit insulin resistance. J Hepatol *40*, 47-51.

Robertson, J.D., Enoksson, M., Suomela, M., Zhivotovsky, B., and Orrenius, S. (2002). Caspase-2 acts upstream of mitochondria to promote cytochrome c release during etoposide-induced apoptosis. The Journal of biological chemistry *277*, 29803-29809.

Rosato, R.R., Almenara, J.A., Maggio, S.C., Coe, S., Atadja, P., Dent, P., and Grant, S. (2008). Role of histone deacetylase inhibitor-induced reactive oxygen species and DNA damage in LAQ-824/fludarabine antileukemic interactions. Molecular cancer therapeutics *7*, 3285-3297.

Rotter, B., Kroviarski, Y., Nicolas, G., Dhermy, D., and Lecomte, M.C. (2004). AlphaII-spectrin is an in vitro target for caspase-2, and its cleavage is regulated by calmodulin binding. Biochem J *378*, 161-168.

Sadagopan, N., Li, W.L., Roberds, S.L., Major, T., Preston, G.M., Yu, Y., and Tones, M.A. (2007). Circulating succinate is elevated in rodent models of hypertension and metabolic disease. Am J Hypertens *20*, 1209-1215.

Sakahira, H., Enari, M., and Nagata, S. (1998). Cleavage of CAD inhibitor in CAD activation and DNA degradation during apoptosis. Nature *391*, 96-99.

Scaffidi, C., Fulda, S., Srinivasan, A., Friesen, C., Li, F., Tomaselli, K.J., Debatin, K.M., Krammer, P.H., and Peter, M.E. (1998). Two CD95 (APO-1/Fas) signaling pathways. EMBO J *17*, 1675-1687.

Schaffer, J.E. (2003). Lipotoxicity: when tissues overeat. Current opinion in lipidology *14*, 281-287.

Schweizer, A., Briand, C., and Grutter, M.G. (2003). Crystal structure of caspase-2, apical initiator of the intrinsic apoptotic pathway. J Biol Chem *278*, 42441-42447.

Selak, M.A., Armour, S.M., MacKenzie, E.D., Boulahbel, H., Watson, D.G., Mansfield, K.D., Pan, Y., Simon, M.C., Thompson, C.B., and Gottlieb, E. (2005). Succinate links TCA cycle dysfunction to oncogenesis by inhibiting HIF-alpha prolyl hydroxylase. Cancer cell *7*, 77-85.

Seth, R., Yang, C., Kaushal, V., Shah, S.V., and Kaushal, G.P. (2005). p53-dependent caspase-2 activation in mitochondrial release of apoptosis-inducing factor and its role in renal tubular epithelial cell injury. The Journal of biological chemistry *280*, 31230-31239.

Shi, M., Vivian, C.J., Lee, K.J., Ge, C., Morotomi-Yano, K., Manzl, C., Bock, F., Sato, S., Tomomori-Sato, C., Zhu, R., *et al.* (2009). DNA-PKcs-PIDDosome: a nuclear caspase-2-activating complex with role in G2/M checkpoint maintenance. Cell *136*, 508-520.

Shikama, Y., U, M., Miyashita, T., and Yamada, M. (2001). Comprehensive studies on subcellular localizations and cell death-inducing activities of eight GFP-tagged apoptosis-related caspases. Exp Cell Res *264*, 315-325.

Shimabukuro, M., Ohneda, M., Lee, Y., and Unger, R.H. (1997). Role of nitric oxide in obesity-induced beta cell disease. The Journal of clinical investigation *100*, 290-295.

Shin, S., Lee, Y., Kim, W., Ko, H., Choi, H., and Kim, K. (2005). Caspase-2 primes cancer cells for TRAIL-mediated apoptosis by processing procaspase-8. EMBO J *24*, 3532-3542.

Shiokawa, K., Tashiro, K., Atsuchi, Y., and Kawazoe, Y. (1986). Alteration of the Pool of Free Amino-Acids during Oogenesis, Oocyte Maturation and Embryogenesis of Xenopus-Laevis and Xenopus-Borealis. Zool Sci *3*, 793-799.

Smythe, C., and Newport, J.W. (1991). Systems for the study of nuclear assembly, DNA replication, and nuclear breakdown in Xenopus laevis egg extracts. Methods in cell biology *35*, 449-468.

Staiger, K., Staiger, H., Weigert, C., Haas, C., Häring, H.-U., and Kellerer, M. (2006). Saturated, but Not Unsaturated, Fatty Acids Induce Apoptosis of Human Coronary Artery Endothelial Cells via Nuclear Factor-κB Activation. Diabetes *55*, 3121-3126.

Stefanis, L., Troy, C.M., Qi, H., Shelanski, M.L., and Greene, L.A. (1998). Caspase-2 (Nedd-2) processing and death of trophic factor-deprived PC12 cells and sympathetic neurons occur independently of caspase-3 (CPP32)-like activity. The Journal of neuroscience : the official journal of the Society for Neuroscience *18*, 9204-9215.

Suda, T., Takahashi, T., Golstein, P., and Nagata, S. (1993). Molecular cloning and expression of the Fas ligand, a novel member of the tumor necrosis factor family. Cell *75*, 1169-1178.

Susin, S.A., Lorenzo, H.K., Zamzami, N., Marzo, I., Brenner, C., Larochette, N., Prevost, M.C., Alzari, P.M., and Kroemer, G. (1999). Mitochondrial release of caspase-2 and -9 during the apoptotic process. J Exp Med *189*, 381-394.

Swanton, E., Savory, P., Cosulich, S., Clarke, P., and Woodman, P. (1999). Bcl-2 regulates a caspase-3/caspase-2 apoptotic cascade in cytosolic extracts. Oncogene *18*, 1781-1787.

Taegtmeyer, H. (1978). Metabolic responses to cardiac hypoxia. Increased production of succinate by rabbit papillary muscles. Circulation research *43*, 808-815.

Takahashi, Y., Soejima, Y., and Fukusato, T. (2012). Animal models of nonalcoholic fatty liver disease/nonalcoholic steatohepatitis. World journal of gastroenterology : WJG *18*, 2300-2308.

Talanian, R.V., Dang, L.C., Ferenz, C.R., Hackett, M.C., Mankovich, J.A., Welch, J.P., Wong, W.W., and Brady, K.D. (1996). Stability and oligomeric equilibria of refolded interleukin-1beta converting enzyme. J Biol Chem *271*, 21853-21858.

Talanian, R.V., Quinlan, C., Trautz, S., Hackett, M.C., Mankovich, J.A., Banach, D., Ghayur, T., Brady, K.D., and Wong, W.W. (1997). Substrate Specificities of Caspase Family Proteases. Journal of Biological Chemistry *272*, 9677-9682.

Tamm, C., Zhivotovsky, B., and Ceccatelli, S. (2008). Caspase-2 activation in neural stem cells undergoing oxidative stress-induced apoptosis. Apoptosis : an international journal on programmed cell death *13*, 354-363.

Tartaglia, L.A., Ayres, T.M., Wong, G.H., and Goeddel, D.V. (1993). A novel domain within the 55 kd TNF receptor signals cell death. Cell *74*, 845-853.

Tilly, J.L., Tilly, K.I., and Perez, G.I. (1997). The genes of cell death and cellular susceptibility to apoptosis in the ovary: a hypothesis. Cell death and differentiation *4*, 180-187.

Tinel, A., and Tschopp, J. (2004). The PIDDosome, a protein complex implicated in activation of caspase-2 in response to genotoxic stress. Science *304*, 843-846.

Trauth, B.C., Klas, C., Peters, A.M., Matzku, S., Moller, P., Falk, W., Debatin, K.M., and Krammer, P.H. (1989). Monoclonal antibody-mediated tumor regression by induction of apoptosis. Science *245*, 301-305.

Troy, C.M., Rabacchi, S.A., Friedman, W.J., Frappier, T.F., Brown, K., and Shelanski, M.L. (2000). Caspase-2 mediates neuronal cell death induced by beta-amyloid. The Journal of neuroscience : the official journal of the Society for Neuroscience *20*, 1386-1392.

Troy, C.M., Stefanis, L., Greene, L.A., and Shelanski, M.L. (1997). Nedd2 is required for apoptosis after trophic factor withdrawal, but not superoxide dismutase (SOD1) downregulation, in sympathetic neurons and PC12 cells. The Journal of neuroscience : the official journal of the Society for Neuroscience *17*, 1911-1918.

Tu, S., McStay, G.P., Boucher, L.-M., Mak, T., Beere, H.M., and Green, D.R. (2006a). In situ trapping of activated initiator caspases reveals a role for caspase-2 in heat shock-induced apoptosis. Nat Cell Biol *8*, 72-77.

Tu, S., McStay, G.P., Boucher, L.M., Mak, T., Beere, H.M., and Green, D.R. (2006b). In situ trapping of activated initiator caspases reveals a role for caspase-2 in heat shock-induced apoptosis. Nat Cell Biol *8*, 72-77.

Uchibayashi, R., Tsuruma, K., Inokuchi, Y., Shimazawa, M., and Hara, H. (2011). Involvement of Bid and caspase-2 in endoplasmic reticulum stress- and oxidative stress-induced retinal ganglion cell death. Journal of neuroscience research *89*, 1783-1794.

Unger, R.H., Clark, G.O., Scherer, P.E., and Orci, L. (2010). Lipid homeostasis, lipotoxicity and the metabolic syndrome. Biochimica et biophysica acta *1801*, 209-214.

Unger, R.H., and Orci, L. (2002). Lipoapoptosis: its mechanism and its diseases. Biochimica et Biophysica Acta (BBA) - Molecular and Cell Biology of Lipids *1585*, 202-212.

Upton, J.P., Austgen, K., Nishino, M., Coakley, K.M., Hagen, A., Han, D., Papa, F.R., and Oakes, S.A. (2008). Caspase-2 cleavage of BID is a critical apoptotic signal downstream of endoplasmic reticulum stress. Molecular and cellular biology *28*, 3943-3951.

Upton, J.P., Wang, L., Han, D., Wang, E.S., Huskey, N.E., Lim, L., Truitt, M., McManus, M.T., Ruggero, D., Goga, A., *et al.* (2012). IRE1alpha cleaves select microRNAs

during ER stress to derepress translation of proapoptotic Caspase-2. Science *338*, 818-822.

Vakifahmetoglu-Norberg, H., Norberg, E., Perdomo, A.B., Olsson, M., Ciccosanti, F., Orrenius, S., Fimia, G.M., Piacentini, M., and Zhivotovsky, B. (2013). Caspase-2 promotes cytoskeleton protein degradation during apoptotic cell death. Cell death & disease *4*, e940.

Vakifahmetoglu, H., Olsson, M., Orrenius, S., and Zhivotovsky, B. (2006). Functional connection between p53 and caspase-2 is essential for apoptosis induced by DNA damage. Oncogene *25*, 5683-5692.

Vakifahmetoglu, H., Olsson, M., Tamm, C., Heidari, N., Orrenius, S., and Zhivotovsky, B. (2008). DNA damage induces two distinct modes of cell death in ovarian carcinomas. Cell death and differentiation *15*, 555-566.

van Loo, G., Saelens, X., Matthijssens, F., Schotte, P., Beyaert, R., Declercq, W., and Vandenabeele, P. (2002). Caspases are not localized in mitochondria during life or death. Cell Death Differ *9*, 1207-1211.

Vastag, L., Jorgensen, P., Peshkin, L., Wei, R., Rabinowitz, J.D., and Kirschner, M.W. (2011). Remodeling of the Metabolome during Early Frog Development. PloS one *6*, e16881.

von Ahsen, O., and Newmeyer, D.D. (2000). Cell-free apoptosis in Xenopus laevis egg extracts. Methods Enzymol *322*, 183-198.

Wagner, K.W., Engels, I.H., and Deveraux, Q.L. (2004). Caspase-2 can function upstream of bid cleavage in the TRAIL apoptosis pathway. The Journal of biological chemistry *279*, 35047-35052.

Wang, L., Miura, M., Bergeron, L., Zhu, H., and Yuan, J. (1994). Ich-1, an Ice/ced-3-related gene, encodes both positive and negative regulators of programmed cell death. Cell *78*, 739-750.

Waterhouse, N.J., and Green, D.R. (1999). Mitochondria and apoptosis: HQ or high-security prison? J Clin Immunol *19*, 378-387.

Wejda, M., Impens, F., Takahashi, N., Van Damme, P., Gevaert, K., and Vandenabeele, P. (2012). Degradomics Reveals That Cleavage Specificity Profiles of Caspase-2 and Effector Caspases Are Alike. Journal of Biological Chemistry *287*, 33983-33995.

Wieckowska, A., and Feldstein, A.E. (2005). Nonalcoholic fatty liver disease in the pediatric population: a review. Current opinion in pediatrics *17*, 636-641.

Wiesner, R.J., Deussen, A., Borst, M., Schrader, J., and Grieshaber, M.K. (1989). Glutamate degradation in the ischemic dog heart: contribution to anaerobic energy production. Journal of molecular and cellular cardiology *21*, 49-59.

Witek, R.P., Stone, W.C., Karaca, F.G., Syn, W.K., Pereira, T.A., Agboola, K.M., Omenetti, A., Jung, Y., Teaberry, V., Choi, S.S., *et al.* (2009). Pan-caspase inhibitor VX-166 reduces fibrosis in an animal model of nonalcoholic steatohepatitis. Hepatology *50*, 1421-1430.

Wu, J.Y., Kao, H.J., Li, S.C., Stevens, R., Hillman, S., Millington, D., and Chen, Y.T. (2004). ENU mutagenesis identifies mice with mitochondrial branched-chain aminotransferase deficiency resembling human maple syrup urine disease. The Journal of clinical investigation *113*, 434-440.

Yi, C.H., Pan, H., Seebacher, J., Jang, I.H., Hyberts, S.G., Heffron, G.J., Vander Heiden, M.G., Yang, R., Li, F., Locasale, J.W., *et al.* (2011). Metabolic regulation of protein N-alpha-acetylation by Bcl-xL promotes cell survival. Cell *146*, 607-620.

Yuan, J., Shaham, S., Ledoux, S., Ellis, H.M., and Horvitz, H.R. (1993). The C. elegans cell death gene ced-3 encodes a protein similar to mammalian interleukin-1 beta-converting enzyme. Cell *75*, 641-652.

Yuzefovych, L., Wilson, G., and Rachek, L. (2010). Different effects of oleate vs. palmitate on mitochondrial function, apoptosis, and insulin signaling in L6 skeletal muscle cells: role of oxidative stress. American Journal of Physiology - Endocrinology And Metabolism *299*, E1096-E1105.

Zhang, Y., Padalecki, S.S., Chaudhuri, A.R., De Waal, E., Goins, B.A., Grubbs, B., Ikeno, Y., Richardson, A., Mundy, G.R., and Herman, B. (2007). Caspase-2 deficiency enhances aging-related traits in mice. Mechanisms of Ageing and Development *128*, 213-221.

Zhivotovsky, B., Samali, A., Gahm, A., and Orrenius, S. (1999). Caspases: their intracellular localization and translocation during apoptosis. Cell Death Differ *6*, 644-651.

Biography

Erika Lee Segear Johnson

Born to Edward and Betty Jeanne Segear on October 18, 1985 in Kingston, PA.

Married to Timothy Jan Johnson on November 27, 2009 in Pocono Manor, PA.

Had her first child, Porter Lee Johnson, on April 5, 2013 in Durham, NC.

Education

Doctor of Philosophy, Molecular Cancer Biology
Certificate in Cell and Molecular Biology
Duke University Medical Center, Durham, NC, May 2014

Bachelor of Science in Biology; Summa cum laude
The Pennsylvania State University, The Behrend College, Erie, PA, May 2008

Publications

Machado MV, Michelotti GA, Pereira de Almeida T, Kruger L, Swiderska-Syn M, Karaca G, Xie G, Lindblom K, **Johnson ES**, Kornbluth S, Diehl AM. (2014) Reduced lipoapoptosis, hedgehog pathway activation, and fibrosis in caspase-2 deficient mice with nonalcoholic steatohepatitis. Submitted to Gastroenterology.

Batchvarov J, Bustamante X, Czerwinski M, **Johnson ES**, Kornbluth S, Capel B. (2013) A grafted ovarian fragment rescues host fertility after chemotherapy. Submitted to *JCI*.

Johnson ES, Lindblom KR, Alexander Robeson, Robert D. Stevens, Olga R. Ilkayeva, Christopher B. Newgard, Kornbluth S, Andersen JL. (2013) Metabolomic profiling reveals a role for caspase-2 in lipoapoptosis. *J Biol Chem*. 288(20):14463-75.

Johnson ES, Kornbluth S. (2012) Life, death, and the metabolically-controlled protein acetylome. *Curr Opin Cell Biol*. 24(6):876-80.

Johnson ES, Kornbluth S. (2012) Phosphatases driving mitosis: pushing the gas and lifting the brakes. *Prog Mol Biol Transl Sci*. 106:327-41.

Andersen JL, Thompson JW, Lindblom KR, **Johnson ES**, Yang CS, Lilley LR, Freel CD, Moseley MA, and Kornbluth S.(2011) A biotin switch-based proteomics approach

identifies 14-3-3ζ as a target of Sirt1 in the metabolic regulation of Caspase-2. *Mol Cell*. 43(5): 834 – 842.

Horn SR, Thomenius MJ, **Johnson ES**, Freel CD, Wu JQ, Coloff JL, Yang CS, Tang W, An J, Ilkayeva OR, Rathmell JC, Newgard CB, Kornbluth S (2011) Regulation of mitochondrial morphology by APC/CCdh1-mediated control of Drp1 stability. *Mol Biol Cell*. 22(8):1207-16.

Zou S, Chang J, LaFever L, Tang W, **Segear Johnson EL**, Hu J, Wilk R, Krause HM, Drummond-Barbosa D, Irusta PM (2011) Identification of dAven, a *Drosophila melanogaster* ortholog of the cell cycle regulator Aven. *Cell Cycle* 10(6): 989-998.

Esmaili AM, **Segear Johnson EL**, Thaivalappil SS, Kuhn HM, Kornbluth S, Irusta PM. (2010) Regulation of the ATM activator protein Aven by CRM1-dependent nuclear export. *Cell Cycle* 9(19): 3913-3920.

Campbell M, **Segear E**, Beers L, Knauber D, Suttle J (2008) Dormancy in potato tuber meristems: chemically induced cessation in dormancy matches the natural process based on transcript profiles. *Funct Integr Genomics* 8(4):317-328.

Honors and Awards

2008-20010: **Cell and Molecular Biology NIH Training Grant:** Duke University Graduate School

2008-2014: **Cell and Molecular Biology Training Program:** Duke University Graduate School

2012: **Outstanding Poster Presentation:** Department of Pharmacology and Cancer Biology Symposium

2012-2014: **F31 Pre-doctoral Fellowship: Ruth L. Kirschstein National Research Service Award (NRSA):** National Institutes of Health, National Cancer Institute

2012: **Fitzgerald Academic Achievement Award:** Department of Pharmacology and Cancer Biology, Duke University Graduate School

2013: **Robert J. Fitzgerald Scholar:** Department of Pharmacology and Cancer Biology, Duke University Graduate School

2013-2014: **Duke Scholar in Molecular Medicine, Endocrinology and Metabolism:** Duke University School of Medicine